

FEASIBILITY AND DESIGN REQUIREMENTS OF FISSION POWERED  
MAGNETIC FUSION PROPULSION SYSTEMS FOR A MANNED MARS  
MISSION

A Thesis

Submitted to the Faculty

of

Purdue University

by

Paul W. Stockett

In Partial Fulfillment of the

Requirements for the Degree

of

Master of Science in Nuclear Engineering

August 2019

Purdue University

West Lafayette, Indiana

**THE PURDUE UNIVERSITY GRADUATE SCHOOL  
STATEMENT OF THESIS APPROVAL**

Dr.Chan K. Choi, Co-Chair

School of Nuclear Engineering

Dr. Robert S. Bean, Co-Chair

School of Nuclear Engineering

Dr. Lefteri H. Tsoukalas

School of Nuclear Engineering

Dr. David s. Koltick

Department of Physics and Astronomy

**Approved by:**

Dr. Shripad Revankar

Graduate Program Chairman

For my family, particularly my parents who have instilled the importance of life-long learning and self growth in me from a young age. None of this would have been possible without your love, support, and sacrifices. For this I am eternally grateful.

## ACKNOWLEDGMENTS

It takes a village to raise a child.”-African Proverb

This quote accurately portrays my masters journey as I received much support and guidance along the way. Without this, I would not have not been able to complete my project. This list is in no way comprehensive but I would like to acknowledge those crucial to my village.

First and foremost I would like to thank my parents for always encouraging me to follow my dreams and to finish what I start. I can't imagine having gone down this path without your unconditional love and support.

Secondly, I would like to thank my teachers at Malvern Prep. They not only nurtured my quest for knowledge but also helped ignite my passion for learning. It was there that I learned to challenge myself academically and to take the road less traveled in pursuit of my goals. Without the experiences and guidance they provided me, I would have never double majored as an undergraduate at Purdue or been introduced to the field of nuclear engineering which ultimately led me to pursue my masters in nuclear space propulsion.

At Purdue, my passion for research was ignited by Dr. Sally Bane. Dr. Bane provided me with my first research position in her cold plasma group within the AAE Department. It was thanks to the guidance of Dr. Sally Bane and Dr. Ravichandra Jagannath that I was able to assist and conduct experimental research as an undergraduate. It was this introduction to the entire research process and how publishing worked that helped cement the idea of pursuing further education to continue performing cutting edge research. A special thank you to Dr. Bane for encouraging me to learn Latex which has made writing research papers and this thesis significantly easier.

As my passion for research continued to grow, it became clear that graduate school was in my future. The mentorship, friendship, and advice I received from those already in graduate school as i finished my undergraduate studies and began my graduate studies was invaluable in assisting me in my journey. Specifically, I wanted to recognize Mark Brown, Andrew Fairbanks and Russel Brayfield for their support and guidance. They not only provided me with technical knowledge and assisted with my project but also in navigating through graduate school and research effectively. Thank you for teaching me the ropes.

I would like to thank my committee members, Dr. Lefteri Tsoukalas and Dr. David Koltick, for serving on my committee. They provided fresh eyes and an outside perspective to the decades old problem of fusion propulsion. Their guidance and support were greatly appreciated.

Finally I would like to thank my Co-Chairs, Dr. Chan Choi and Dr. Robert Bean. Not only did they provide the financial support to allow me to pursue this project. Their guidance has been invaluable. I would particularly like to thank Dr. Choi for introducing me to the field of nuclear fusion and nuclear space propulsion along with his tireless efforts to assist me over the years in studying fusion technology as it relates to space propulsion. His eye for detail has shaped me into the engineer I am today. I would like to thank Dr. Bean for introducing me to the field of non-proliferation thanks to a conversation during lab one day that sparked a significant portion of this work along with the advice both academic and professionally throughout this journey. I could not have asked for a better set of advisors as you have cared for me as a student and as a person. Words cannot describe how much it means to me that you both took me under your wings and mentored me and it is something I will forever be grateful for.

## TABLE OF CONTENTS

	Page
LIST OF TABLES . . . . .	viii
LIST OF FIGURES . . . . .	x
NOMENCLATURE . . . . .	xii
ABSTRACT . . . . .	xiv
1 INTRODUCTION . . . . .	1
1.1 Problem Description . . . . .	1
1.2 Motivation . . . . .	5
1.3 Constraints and Assumptions . . . . .	7
1.4 Project Overview . . . . .	8
2 CONSTRAINTS AND PARAMETERS . . . . .	10
2.1 Mission Constraints . . . . .	10
2.1.1 Rocket Parameters . . . . .	10
2.1.2 Mission Parameters and Constraints . . . . .	12
2.2 Health Constraints . . . . .	15
3 LITERATURE REVIEW AND ALTERNATIVE ROCKETRY METHODS . . . . .	17
3.1 Nuclear Power Sources in Space . . . . .	17
3.1.1 History of Nuclear Power Sources in Space . . . . .	17
3.1.2 Potential Power Sources for Spacecraft Power and Propulsion . . . . .	19
3.1.3 Previous Space Reactor Programs and Studies . . . . .	23
3.2 Overview of Rocketry Methods and Comparison . . . . .	27
3.2.1 Nuclear Electric Propulsion . . . . .	30
3.2.2 Comparison of Fission and Fusion Rocketry . . . . .	31
4 MAGNETIC CONFINEMENT FUSION PROPULSION SYSTEMS . . . . .	36
4.1 Overview . . . . .	36
4.2 Dense Plasma Focus . . . . .	37
4.2.1 Physical Basis . . . . .	38
4.2.2 Evaluation Methodology . . . . .	42
4.3 Gasdynamic Mirror . . . . .	47
4.3.1 Physical Basis . . . . .	48
4.3.2 Evaluation Methodology . . . . .	49
5 EVALUATION OF FISSION POWERED MAGNETIC FUSION THRUSTERS	52

	Page
5.1 Evaluation Overview . . . . .	52
5.2 Case 1: Self Sustaining Fusion Thruster . . . . .	55
5.3 Case 2: Fission Powered Fusion Thruster . . . . .	59
5.4 Case 3: Fission assisted Fusion Thruster . . . . .	62
5.5 Comparison of Ppropulsion Power Systems . . . . .	65
6 NON-PERFORMANCE DESIGN CONSIDERATIONS . . . . .	68
6.1 International Legal Considerations . . . . .	68
6.2 Non-Proliferation Considerations . . . . .	69
6.2.1 Current Status of Safeguards in Space . . . . .	69
6.2.2 The Need for a New Approach to Safeguards in Space . . . . .	70
6.2.3 Proposed Solution . . . . .	71
6.3 Safety Considerations-Radiological and Environmental . . . . .	72
7 CONCLUSION . . . . .	76
7.1 Conclusions . . . . .	76
7.2 Future Work . . . . .	78
REFERENCES . . . . .	82
APPENDICES	
A Computer Codes . . . . .	88
A.1 GDM-script . . . . .	88
A.1.1 Sample Output . . . . .	92
A.2 DPF Propulsion Code . . . . .	92
A.2.1 Sample Output . . . . .	117

## LIST OF TABLES

Table	Page
1.1 Comparison of the current major propulsion systems . . . . .	2
2.1 Number of Predicted Safe Days in Space using Various Models . . . . .	16
3.1 Comparison of the four main power conversion methods for spaceborne nuclear systems . . . . .	21
3.2 Power Conversion and Output Capabilities of tested nuclear reactors for space. *Denotes reactors that have been flown in space, while the other reactors have undergone ground testing. . . . .	23
3.3 Comparison of fission vs fusion rocket engines. * denotes the reactor mass plus shielding and adapter. . . . .	32
4.1 DPF Parameters from the Livermore-I Experiment [15]. * Denotes assumed values. . . . .	39
4.2 Original Reaction Rate Coefficients [65] . . . . .	43
4.3 Updated Reaction Rate Coefficients from Bosch-Hale [69] . . . . .	44
4.4 $p - B^{11}$ Reaction Rate Coefficients from Nevins and Swain [70] . . . . .	45
4.5 Fusion only powered DT Fueled GDM parameters with $\eta_{DEC}=0.9$ [61,62] .	50
5.1 Fuel Evaluation based on DPF Fusion Performance. *Denotes that charged particle power is less than the power loss. . . . .	56
5.2 Comparison of fusion powered DPF and GDM. Note the TEC mass for the DPF is assumed to be included in the payload mass of 100 metric tons.	58
5.3 Comparison of fission powered DPF and GDM . . . . .	60
5.4 Comparison of fission assisted DPF and GDM (with $\eta_{DEC} = 0.5$ ). . . . .	62
5.5 Summary of Results . . . . .	67
A.1 GDM Code Sample output for a fission powered Gasdynamic Mirror . . . .	92
A.2 Sample Output of DPF Propulsion Code. For 4 thrusters with a $\Delta V$ of 20 km/s for all three cases as established for both DT and $D - He^3$ fuel types (2 and 3 respectively). No direct energy conversion was used in this sample run. . . . .	118

A.3	Sample Output of the mass calculations from the DPF Propulsion code. For 4 thrusters with a $\Delta V$ of 20 km/s for all three cases as established for both DT and $D - He^3$ fuel types (2 and 3 respectively). No direct energy conversion was used in this sample run. . . . .	119
-----	---	-----

## LIST OF FIGURES

Figure	Page
2.1 Desired Mission Parameters based on the thrust to weight ratio requirements for a Mars mission. . . . .	11
2.2 Range of arrival and departure $\Delta V$ 's over a 10 year span to achieve various times of flight for a Mars Mission for flight times ranging from 30-500 days. Generated using the EasyPorkchop-Porkchop Plot Generator by Juan Luis Gonzalo, Universidad Politecnica de Madrid (Technical University of Madrid).12	12
2.3 Range of arrival and departure $\Delta V$ 's over a 10 year span to achieve various times of flight for a Mars Mission for flight times ranging from 10-100 days. Generated using the EasyPorkchop-Porkchop Plot Generator by Juan Luis Gonzalo, Universidad Politecnica de Madrid (Technical University of Madrid).13	13
2.4 Desired Mission Parameters for a Mars Mission From <i>Fission Reactor Options and Scaling for Powering Magnetic Fusion Thrusters for a Manned Mars Mission</i> [24] by Stockett et al.; reprinted by permission of the American Institute of Aeronautics and Astronautics, Inc . . . . .	14
3.1 Comparison of four main methods of rocket propulsion and their capabilities for a Mars mission [49]. Original image from <i>Human Mars Mission Definition: Requirements &amp; Issues</i> by B.G. Drake for the Human 2 Mars Summit, May 2013 . . . . .	29
4.1 Schematic of the differences between the Mather and Phillipov Type [64] . .	37
4.2 Schematic of the DPF Propulsion System [65] . . . . .	40
4.3 Description of the four operational phases of the Dense Plasma Focus Pulse [65] . . . . .	41
4.4 Basic schematic of a mirror fusion device [56]. . . . .	48
5.1 Schematic of self-sustaining fusion thruster in which all power generated from the fusion reaction is used for either thrust or recirculated to ship controls and to power the fusion reactor. This case is has not yet been achieved due to not enough power being generated overcome the losses to be self-sustaining. . . . .	53
5.2 Schematic of fission powered fusion thruster. . . . .	54
5.3 Schematic of fission assisted fusion thruster. . . . .	55

Figure	Page
5.4 Evaluation of Case 1 against the desired Mission Parameters. . . . .	57
5.5 Evaluation of Case 2 against the desired mission parameters From <i>Fission Reactor Options and Scaling for Powering Magnetic Fusion Thrusters for a Manned Mars Mission</i> [24] by Stockett et al.; reprinted by permission of the American Institute of Aeronautics and Astronautics, Inc . . . . .	61
5.6 Effect of DEC efficiency on thrust to weight ratio for a fission assisted DPF.	63
5.7 Evaluation of Case 3 against the desired Mission Parameters From <i>Fission Reactor Options and Scaling for Powering Magnetic Fusion Thrusters for a Manned Mars Mission</i> [24] by Stockett et al.; reprinted by permission of the American Institute of Aeronautics and Astronautics, Inc . . . . .	65
5.8 Comparison of all three cases for $DHe^3$ fueled DPF against the desired Mission Parameters. . . . .	66

## NOMENCLATURE

ALARA	As Low As Reasonably Achievable
C/S	Containment and Surveillance
DPF	Dense Plasma Focus
DUFF	Demonstration using Flattop Fission
GDM	Gas Dynamic Mirror
$I_{SP}$	Specific Impulse
IAEA	International Atomic Energy Agency
ICF	Inertial Confinement Fusion
KRUSTY	Kolopower Reactor Using Stirling Technology
LEO	Low-Earth Orbit
MCF	Magnetic Confinement Fusion
NASA	National Aeronautics and Space Administration
NCSR	NASA Space Cancer Risk
NEP	Nuclear Electric Propulsion
NERVA	Nuclear Engine for Rocket Vehicle Application
NNWS	Non-Nuclear Weapons State
NPT	Non-proliferation Treaty
NTP	Nuclear Thermal Propulsion
NWS	Nuclear Weapons State
PRPP	Proliferation Resistance and Physical Protection
REID	Radiation Exposure Induced Death
ROSCOSMOS	Roscosmos State Corporation for Space Activities
RTG	Radioisotope Thermal Generator
SEP	Solar Electric Propulsion

SMR	Small Modular Reactors
SNM	Special Nuclear Material
$\frac{T}{W}$	Thrust to Weight Ratio
$t_{flight}$	Time of flight
UNARM	Unattended and Remote Monitoring
VASIMR	Variable Specific Impulse Magnetoplasma Rocket
$\Delta V$	Velocity Increment

## ABSTRACT

Stockett, Paul W M.S., Purdue University, August 2019. Feasibility and Design Requirements of Fission Powered Magnetic Fusion Propulsion Systems for a Manned Mars Mission. Major Professors: Dr. Chan K. Choi & Dr. Robert S. Bean.

For decades nuclear fusion space propulsion has been studied but due to technological set backs for self-sustaining fusion, it has been repeatedly abandoned in favor of more near-term or present day solutions. While these present day solutions of chemical and electric propulsion have been able to accomplish their missions, as the human race looks to explore Mars, a near term solution utilizing nuclear fusion propulsion must be sought as the fusion powered thruster case currently does not meet the minimum 0.2 thrust-to-weight ratio requirement. The current work seeks to investigate the use of a fission powered magnetic fusion thruster for a manned Mars mission with an emphasis on creating a very near-term propulsion system. This will be accomplished by utilizing present day readily available technology and adapting methods of nuclear electric and nuclear fusion propulsion to build this fission assisted propulsion system. Near term solutions have been demonstrated utilizing both DT and  $D-He^3$  fuels for a fission powered and fission assisted Dense Plasma Focus fusion device capable of achieving thrust-to-weight ratios greater than 0.2 for  $\Delta V$ 's of 20 km/s. The Dense Plasma Focus can achieve thrust-to-weight ratios of 0.34 and 0.4 for fission assisted and fission powered cases, respectively, however, the Gasdynamic Mirror device proved to be an infeasible design as a fission powered thruster due to the increased weight of a fission reactor.

# 1. INTRODUCTION

## 1.1 Problem Description

In the current state of human space exploration, there is no mission more desired than that of a manned flight to Mars which is beginning to reach levels of anticipation that have not been observed since the days of the Space Race and placing a man on the moon around 1969. Placing Neil Armstrong on the moon was the greatest engineering feat ever accomplished at that time using less computing power than what is found in a typical cell phone or calculator nowadays. While achieving a manned flight to Mars will be exponentially more difficult than that of the moon landing, seeing how far computing power has come since then, it is reasonable to suspect that with current technology that Mars is within the realm of possibility.

The combination of technology and desire to reach Mars makes it not a question whether if humans will ever step foot on Mars but a question whether when will humans step foot on Mars whether that will be in five years or twenty years. Society craves for a near term solution to this problem, not one that will be seen in twenty years. It is possible that this solution already exists but has not been pieced together for this application. Nuclear fusion propulsion provides the highest degrees of thrust, specific impulse, and variability amongst those parameters as can be seen in Table 1.1 against the other five common types of propulsion system being investigated currently; Nuclear Thermal Propulsion(NTP), Nuclear Electric Propulsion(NEP), Solar Electric Propulsion (SEP), and Chemical Rockets.

Unfortunately the only two technologies that are currently ready to fly are nuclear electric propulsion and chemical propulsion which has reached close to its limit in terms of performance but, like the computing power to get men to the moon, is outdated. Nuclear electric on the other hand is a newer technology that features

Table 1.1.  
Comparison of the current major propulsion systems

Propulsion Type	Thrust (kN)	Specific Impulse (s)
Chemical [1, 2]	384-2094	266-462
NTP (Solid Core) [3, 4]	333	825- 900
NTP (Vapor Core) [5]	120	3275
Fusion (DPF) [6, 7]	449-1000	1311-2000
Fusion (GDM) [8]	$2.512-4468 * 10^3$	$1110-3.106 * 10^5$
NEP [9]	$2 * 10^{-5} - 0.015$	1300-8000
SEP [10]	$6 * 10^{-3}$	5000-7000

incredibly high specific impulse but minute values of thrust as demonstrated in Table 1.1 due to the low thrust produced by ion thrusters powered by the nuclear power sources(NPS). A seemingly simple solution would be to switch out the ion thrusters for a device more powerful, a device such as a fusion thruster. The fusion thruster is not currently capable of powering itself hence the coupling of a nuclear power system while being able to supply 5-8 orders of magnitude more thrust than that of ion thrusters.

Magnetic fusion propulsion systems require an immense amount of energy to operate, unfortunately, capacitors with energy densities of 1-10MJ/Kg are not technologically available yet. Recently, super capacitors built for secondary power sources in electric vehicles have reached power and energy densities as high as 1.838 kW/kg [11], while other super capacitors have obtained power densities as high as 43.3.3 kW/kg [12], 53.1 Wh/kg [13], and 0.01-0.02 MJ/kg [14]. There is still much room for improvement in the field of super capacitors, as they are over a 100x away from the proposed theoretical maximum of 2 MJ/kg [15].

The power requirements do not end there, the ship will also need to be habitable for humans for the duration of the trip, while the bimodal rocket will require 16.7kWe [16].

That estimate is without the amount of power needed for the number of passengers or living space necessary for the crew while the Mars Base Camp, designed by Lockheed Martin, would be an additional 150kW of power on Mars [17]. Therefore, it is probable that the spacecraft will need more than 150kW of power for the operation of both the propulsion system and the life support system. Many current designs, including Elon Musks BFR design, include the use of a solar array for powering the life support while the rocketry is traditional chemical propulsion design. The size of a solar array needed to power a fusion propulsion device would be impractically large for a spacecraft, as the International Space Station uses 110kW generated by  $405.8m^2$  of solar panels [18], so extrapolating the area for a required power of 150kW would mean that a spacecraft would require  $553.36m^2$  of solar panels; assuming there would be no loss in the panel's efficiency in generating energy as the spacecraft moves away from the sun in its journey from Earth to Mars. Therefore, an additional means of power generation is needed. A viable candidate for this is nuclear power generation from a fission reactor, since a radioisotope generator would not produce enough power for the vehicle. Fission reactors have historically demonstrated their ability to provide a safe and reliable means of energy, with recent work being conducted to reduce the size and cost of said nuclear fission reactors.

Nuclear rocketry has been around almost as long as modern chemical rocketry, both having major advances in the 50s and 60s. However, further advancement of nuclear rocketry was stalled due to legislation, i.e., the Nuclear Test Ban Treaty, which limited testing due to the release of fission fragments from the rockets. The release of fragments remains an issue to this day, even with modern nuclear thermal rockets. Fortunately, nuclear thermal rockets are no longer the only type of nuclear rocketry being investigated, nuclear fusion and nuclear electric propulsion are also currently being investigated for manned missions to Mars. While nuclear electric propulsion would only require a low amount of power to produce a high specific impulse ( $I_{SP}>6000s$ ), the amount of thrust produced would be meager at about 2.26N, meaning this option would lengthen travel time between planets despite its power

efficiency [19]. The supposed benefit of efficiency and simplicity of design of nuclear electric propulsion is quickly outweighed by the benefits presented by fusion propulsion. Fusion propulsion has two main sub-types, inertial confinement fusion (ICF) and magnetic confinement fusion (MCF). ICF not only produces a higher specific impulse, but it also has higher specific power than that of MCF propulsion systems [20]. The length of the MCF devices makes up for its efficiency with a range of lengths from 40.3-113m [20] recorded from the early days of the technology. Due to the vast difference in size and methodology of confinement, ICF systems require an input power of roughly  $10^5$ MW, while MCF systems require approximately  $10^4$ MW or less [19]. Compared to ICF, MCF systems have been more diligently investigated for use in space, as well as terrestrial power applications.

For the reasons stated above, this work will focus on the use of magnetic confinement propulsion systems for a manned mission to Mars. These propulsion systems will be evaluated with a fission reactor as their power supply when tested for calculations of weight and power production. Within MCF propulsion systems, several designs have been suggested such as the GasDynamic Mirror (GDM), Tandem Mirror, Dense Plasma Focus(DPF), Field Reversed Configuration, Spherical Torus, and more. This work will focus on the DPF and GDM devices, by analyzing the power requirements necessary for a fission reactor to produce the necessary power for both the life support system and the propulsion system, as well as mission parameters pertinent to a manned Mars mission. For a manned Mars mission, the relevant mission parameters are as follows:

1. Thrust
2. Specific Impulse
3. Travel Duration
4. Mass Ratio
5. Specific Power

6. Input Power
7.  $\Delta V$
8. Payload Mass
9. Propellant Mass
10. Thrust to Weight Ratio

For the non-propulsion electric power, a constant value of 200kWe has been chosen as the target value for electric power needed for the life support system.

## 1.2 Motivation

When Neil Armstrong landed on the moon, it no longer became a question if mankind would make it to Mars but instead became the question when will mankind reach Mars. It was inevitable due to the unquenchable thirst for exploration and innovation. The 50 years following the moon landing, that thirst had subsided as the moon and deep space were being studied and probed as technology was constantly being improved upon. However, the human population has once again grown restless as another generation seeks to make their mark on history with the next great feat of human achievement. This has resulted in increased discussions and plans of manned missions to Mars by both government entities such as NASA and ROSCOSMOS along with private industry leaders including SpaceX, Boeing, and Lockheed Martin.

The previous half century has provided mankind with an unprecedented level of knowledge on how humans react in space physically and mentally for periods up to six months at a time. Stays in space longer than six months have rarely been completed and poses multiple unknowns to future missions that require stays in space longer than six months specifically in regard to an astronaut's health. Five major health hazards have been identified for space missions by Moses et al. [21] which are being researched by NASA's Human Research Program including:

- Altered Gravity
- Radiation
- Distance from Earth
- Isolation
- Hostile/Closed Environment-Spacecraft Design

with altered gravity and radiation being the two biggest unknowns standing in the way of manned missions to Mars. The six month stays at the ISS have provided information on weighs for astronauts to combat weightlessness and the effects of micro-gravity which Moses, et al. propose can be mitigated for Mars missions in a similar fashion to the ISS but point out that the longer an astronaut is in space the more significant the effects [21]. This leaves radiation effects as the sole major unknown for interplanetary travel which arises from the fact that very few astronauts have ever ventured outside of Low-Earth Orbit (LEO), where they are only subjected to 45% of the cosmic radiation in deep space, even for a couple of days not months [21]. This provides a very limited sample to which radiation effects can be studied and used as a basis for the safe limits.

While each organization has their own unique plan to reach Mars, it has long been proposed that the fastest and most efficient way to reach Mars is to do so with nuclear propulsion. Nuclear propulsion is one of the few methods that can achieve both high specific impulse and high thrust which is seen as requirements to drastically reduce the trip duration to ensure astronaut safety from radiation [21]. This makes nuclear propulsion the ideal candidate for the first manned mission to Mars.

In what is quickly becoming a second space race between not only the United States and Russia, but other private industry competitors as well, the focus should be not on what technology will reach Mars as there are multiple technologies that within the next century if not the next couple decades will prove feasible. Instead the question of which technology or combination of technology will allow humans to

reach Mars the soonest. A near term solution for a manned Mars mission is crucial in determining the future of space exploration as technological advancements are happening at an unprecedented rate throughout society such that space exploration can not be seen to lag too far beyond or be too slow with advancements to keep the public's interest and funding.

The easiest near term solutions would stem from analyzing and overcoming limitations of the currently available technologies. One recently proposed method to develop a near term solution was to incorporate a nuclear power source, particularly that of a fission reactor, as the power supply for the Variable Specific Impulse Magnetoplasma Rocket (VASIMR®) engine [22]. This is a modification to that of a typical nuclear electric propulsion system but opens the door for even more modifications to potentially further enhance the propulsion system characteristics. One such idea involves coupling a fission reactor with fusion propulsion system only in terms of providing power. Fusion propulsion as previously discussed have theoretically the best flight performance characteristics but have been limited on not self sustaining. Therefore, if the nuclear electric concept is modified by replacing an electric thruster such as the VASIMR® with that of a fusion engine like a dense plasma focus device or a gasdynamic mirror, a potential near term solution with highly desirable rocket performance is created.

### 1.3 Constraints and Assumptions

Two major sets of constraints have been identified for the current work. The first set of constraints are the mission constraints particularly as they relate to rocket performance. This includes rocket parameters such as specific impulse, thrust to weight ratio and mass fraction as these numbers are crucial in determining the trajectory and time of flight of the mission.

Time of flight of the mission in turn is used in the second set of constraints as it relates to the health constraints of the mission. As with any type of travel, space

travel is not without its risks which must be acknowledged and minimized. These two sets of constraints will be elaborated on in Chapter 2.

## 1.4 Project Overview

Chapter one will discuss the motivation behind the project along with a brief overview of any limiting factors and assumptions. This will allow a thorough discussion of the problem to set up the investigation of design requirements and feasibility of utilizing a fission powered magnetic fusion thruster for a manned mars mission.

Chapter two will provide a more in-depth look at the constraints and assumptions made for the current work. In the process of describing the mission constraints, this chapter will provide a fundamental basis on the important parameters of rocketry. Following the mission constraints, the health constraints faced by astronauts in space will be discussed.

In chapter three, a brief history of nuclear power sources in space will be given. This will be followed with a discussion on potential nuclear power sources for the powering of a magnetic fusion thruster focusing on the power conversion methods available and weighing the advantages and disadvantages to them. This chapter will end with a discussion that provides a comparison between the four main types of propulsion currently being studied; i.e., NEP, NTP, fusion, and chemical, will be presented. Following the comparison, an in depth discussion of nuclear electric propulsion and the comparison of fission versus fusion rockets will be given.

Chapter four will discuss the magnetic fusion propulsion systems that have been studied. This will narrow the project to focus on two devices in particular, the DPF and GDM devices. Accordingly the second half of this chapter will focus on the physics of the DPF and GDM devices.

Chapter five will be the bulk of the current work as it will present the methodology for comparison of the magnetic fusion thrusters against each other coupled with the fission reactors for the various parameters laid out in Section 1.1.

In chapter six, consideration will be given to the design aspects not directly related to the operation of the problem system. This section will expand upon safety considerations of a nuclear reactor in space as well as any shielding necessary to mitigate radiation from not just the reactor but interplanetary travel as well. As previously mentioned, interplanetary travel and specifically the radiation of one is subjected to during it is a major concern for this mission and therefore will be revisited in this chapter. The general requirements of the proposed propulsion system would not be complete without discussing any non-proliferation concerns that arise with the design.

In conclusion, chapter seven will summarize the work that has been done along with all relevant results. Chapter seven will also make recommendations on this technology along with the proposing any future work that needs to be done for this technology.

## 2. CONSTRAINTS AND PARAMETERS

### 2.1 Mission Constraints

#### 2.1.1 Rocket Parameters

The essential principles of rocketry dates back to Issac Newton and his three laws of motion, most specifically his third law which states that for every action there is an equal and opposite reaction. This is the defining principle for propulsion in that as propellant is exhausted out of the rocket nozzle, the force it exerts backwards causes an equal and opposite force that must be exerted on the rocket. This is the force that moved the rocket forward and is popularly known as thrust. The thrust of a rocket engine can be calculated using the following equation which can be derived from the Newton's second law and is one of the defining characteristics of a rocket [23]:

$$F = F_{propellant} + F_{pressure} = \dot{m}_{propellant} * v_{exhaust} + A_{exit}(p_{exit} - p_{atmosphere}) \quad (2.1)$$

where the thrust is made up of two terms, the first being the force created when the propellant is exhausted and the second being the thrust created by a pressure differential between the nozzle and the atmosphere the rocket is in. However, it is generally more common for the thrust of the rocket to appear in the form of thrust to weight ratio ( $\frac{T}{W}$ ). This essentially normalizes the thrust value which then allows for easy comparison between different engines and engine types. For a Mars mission, a thrust to weight ratio greater than 0.2 is desired [15] regardless of the total velocity increment for the mission (discussed in Section 2.1.2). This creates a desired mission parameter space as seen in Figure 2.1.

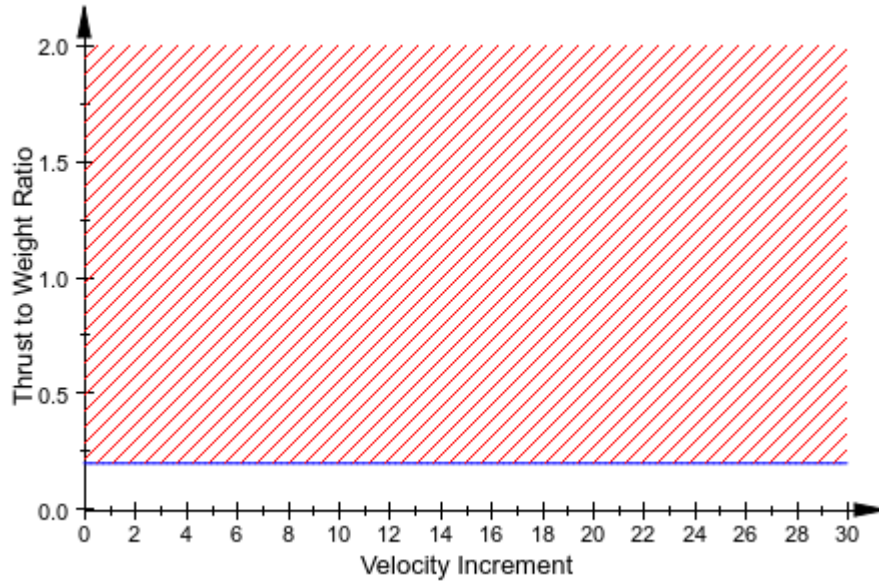


Figure 2.1. Desired Mission Parameters based on the thrust to weight ratio requirements for a Mars mission.

Along with the thrust to weight ratio, rockets are also classed based on their specific impulse. The specific impulse ( $I_{SP}$ ) is measure of the rockets efficiency and can be defined utilizing the following equation:

$$I_{SP} = \frac{F}{\dot{m}_{propellant} * g_{earth}} = \frac{v_{exhaust}}{g_{earth}} \quad (2.2)$$

where it is important to note that the gravity term is always the gravity term for Earth to again keep things normalized regardless of where the rocket engine is operating. The ambient pressure term is small and thus ignored.

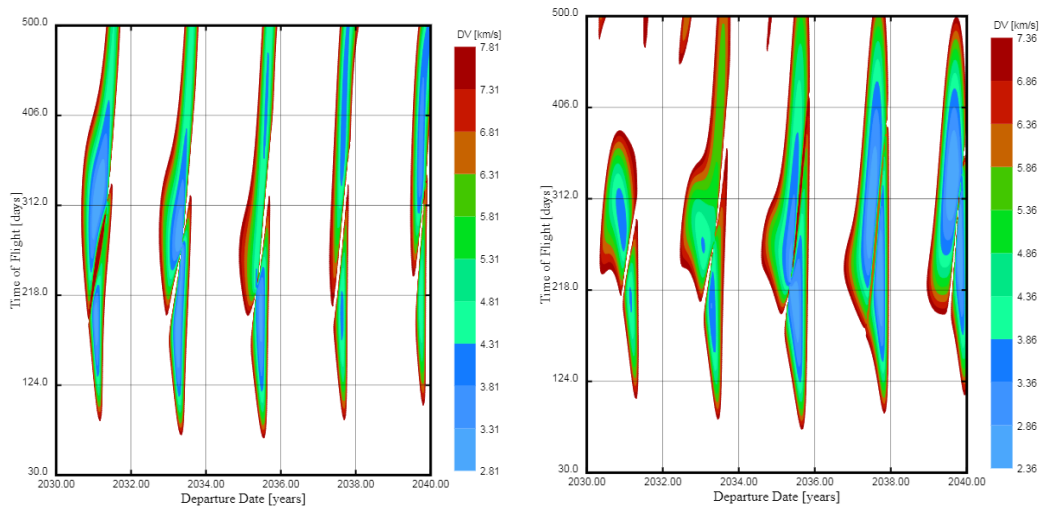
The final rocket parameter of interest is partially dependent on the mission the system is being used for as it is a function of the propellant mass as it is the ratio or rocket mass fraction seen in the following equation:

$$f_m = \frac{m_f}{m_0} \quad (2.3)$$

where  $m_f$  is the final dry weight of the rocket without propellant and  $m_0$  is the initial mass of the rocket including the propellant.

### 2.1.2 Mission Parameters and Constraints

Space missions have two main constraints in the desired time of flight,  $t_{flight}$ , and in the change of velocity that was needed from the propellant or velocity increment,  $\Delta V$ . As is typical with almost any mission, there are multiple burns of the propellant that are required for the various maneuvers required for the trajectory of the mission. All of these burns produce a  $\Delta V$ . The mission  $\Delta V$  is the sum of these smaller velocity increments. These smaller velocity increments are calculated using a method known as patched conics for Kepler Orbits [23] which will be discussed in Section 4.2.2.



(a) Departure  $\Delta V$

(b) Arrival  $\Delta V$

Figure 2.2. Range of arrival and departure  $\Delta V$ 's over a 10 year span to achieve various times of flight for a Mars Mission for flight times ranging from 30-500 days. Generated using the EasyPorkchop-Porkchop Plot Generator by Juan Luis Gonzalo, Universidad Politécnica de Madrid (Technical University of Madrid).

As will be discussed in Section 2.2, the time of flight for a manned mission is critical to mission success due to the health risks associated with long term exposure to space radiation. When analyzing a new mission, a porkchop plot such as the ones in Figures 2.2 and 2.3 is created. By solving the Lambert problem, the porkchop plot depicts the various  $\Delta V$ 's necessary to complete the mission in a set period of time.

Figure 2.2 shows the range of  $\Delta V$ 's for missions spanning up to 500 days which is approaching the limit of safe days in space as seen in Table 2.1. However, as we can see in Figure 2.3 when that upper limit is shrunk down to 100 days, the maximum  $\Delta V$  is actually higher than initially predicted by the first figure.

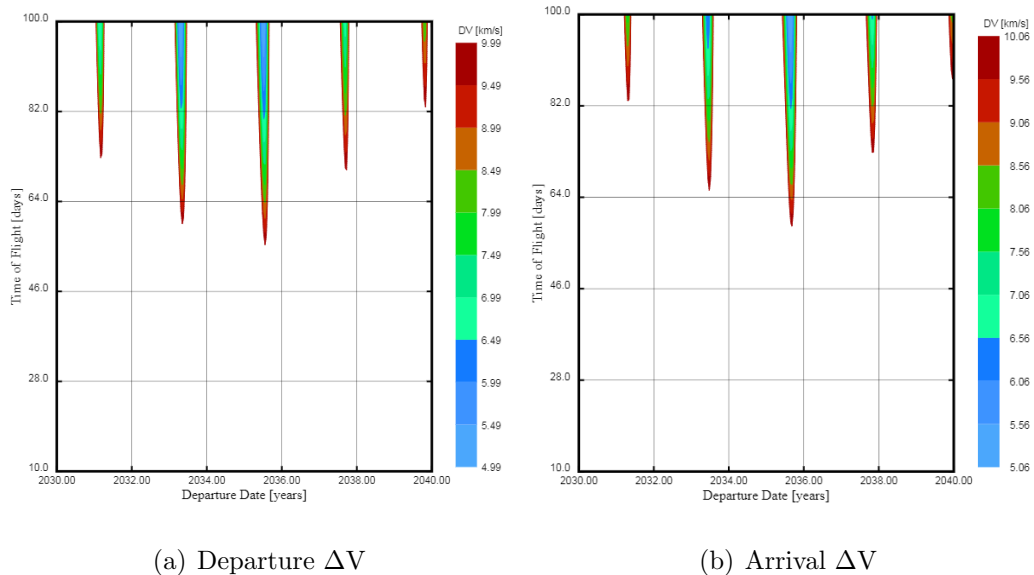


Figure 2.3. Range of arrival and departure  $\Delta V$ 's over a 10 year span to achieve various times of flight for a Mars Mission for flight times ranging from 10-100 days. Generated using the EasyPorkchop-Porkchop Plot Generator by Juan Luis Gonzalo, Universidad Politécnica de Madrid (Technical University of Madrid).

Utilizing these porkchop plots will provide a range of  $\Delta V$ 's to use in this work from approximately 5 km/s to 20 km/s with the higher  $\Delta V$ 's being characteristic of missions with approximately 50 day flight times. When the  $\Delta V$  range is restricted to 5 to 20 km/s, the desired mission parameter space can be seen in Figure 2.4. A rocket engine must perform with this parameter space to be utilized for a successful manned Mars mission.

While lower  $\Delta V$ 's represent the more energy efficient trajectories such as a Hohmann transfer which is the trajectory between two planets that requires the least amount of fuel. Hohmann transfers, however, come at the cost of increased trip time due to

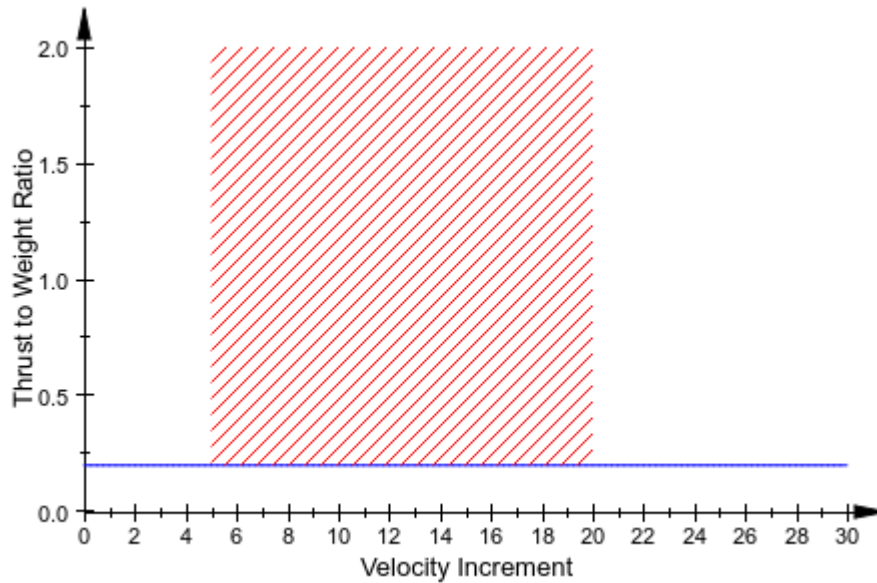


Figure 2.4. Desired Mission Parameters for a Mars Mission From *Fission Reactor Options and Scaling for Powering Magnetic Fusion Thrusters for a Manned Mars Mission* [24] by Stockett et al.; reprinted by permission of the American Institute of Aeronautics and Astronautics, Inc

the low propellant mass and low energy needed. Each rocket, however, is limited in its maximum velocity increment and is a function of its specific impulse and its mass fraction as can be seen below in what is known as the rocket equation [23]:

$$\Delta V_{max} = I_{SP} * g_{earth} * \ln\left(\frac{m_f}{m_0}\right) = v_{exhaust} * \ln(f_m) \quad (2.4)$$

It is important to note that these mission total  $\Delta V$ 's and therefore trip times are highly dependent on the spacecraft angle of departure relative to the orbital velocity of the departure planet [23]. This creates an optimization problem which must be addressed when calculating minimum time of flight.

## 2.2 Health Constraints

As previously discussed in Section 1.2, one of the major assumptions that needs to be made when analyzing a manned interplanetary mission is to address the following health concerns [21]:

1. Mars Dust
2. Pathogens
3. Microgravity
4. Space Radiation
5. Psychological Effects
6. Toxic Chemicals
7. Life Support System Failure

These concerns addressed through technological and medical advances are outside the scope of this project with the exception of radiation exposure which is in part addressed by this project due to the reduction in travel time for the trip from Earth to Mars when compared with that of chemical propulsion. This provides the first major limiting constraint for an interplanetary trip to Mars as the number of safe days in space due to the full effects of cosmic radiation outside of the Earth's magnetic field. Table 2.1 shows the number of safe days predicted in space using several different models notably the NASA Space Cancer Risk (NCSR) tool [21, 25]. The NCSR was developed specifically to evaluate the space cancer risk in astronauts for deep space missions and is continuously being refined as more research becomes available. The number of predicted safe days in space is estimated from estimations on the upper 95% confidence of the 3% Radiation Exposure Induced Death (REID) from fatal cancers. These limits are not a one size fits all and vary as age and gender of the astronaut dose [26]. The 3% REID is used by NASA while other agencies use their

own limits based off the International Commission on Radiological Protection [26]. The variations in models is due in large part to the fact that the effects of full cos-

Table 2.1.  
Number of Predicted Safe Days in Space using Various Models

Model	Number of Safe Days
NCSR-2012 [21]	277-500 Days
NCSR-2014 [25]	300 Days(Women) & 400 Days(Men)

mic radiation including galactic cosmic rays is not yet fully understood despite the fact that astronauts routinely perform six month missions on the International Space Station. These astronauts are only exposed to approximately 45% of the radiation they would be in deep space with the only astronauts ever experience deep space were those on the Apollo missions which had a a very small window of exposure compared to an interplanetary trip [21]. The National Council on Radiation Protection and Measurement has established a 2.0 Gy dose limit for space missions [27] while other studies have shown that the 3-4 Gy is enough radiation to cause fatalities to 50% of the population ( $LD_{50/30}$ ). NASA abides by the ALARA (As Low as Reasonably Achievable) Principle which is commonly taught in undergraduate programs for nuclear engineering that states that radiation exposure should be as limited as possible without placing the recipient at any unnecessary risk [26]. As noted by Cucinotta, ALARA serves to show that the dose limits are set maximums that should not be approached if possible [26].

Another major health factor that was not mentioned in previous studies is whether or not the astronauts will be able to survive the g-forces that they are subjected if higher  $\Delta V$  missions are chosen as the optimum mission. These forces can be significant when an impulsive burn of a high thruster propulsion system is utilized.

## 3. LITERATURE REVIEW AND ALTERNATIVE ROCKETRY METHODS

### 3.1 Nuclear Power Sources in Space

#### 3.1.1 History of Nuclear Power Sources in Space

Rocket and nuclear technologies both began garnering great interest during the Second World War, which has led to an intertwined history of the two technologies as they continued to grow and become more mainstream instead of sole government and military applications. The first major collaboration of the two technologies was when nuclear propulsion was actively investigated during the 1960s as a means of reaching Mars by both the United States (USA) and the former Soviet Union (USSR) through their well-known Project Orion (USA) [9], the NERVA project (USA) [28] and the RD-0140 project (USSR) [5]. Unfortunately due to the signing of the Limited Test Ban Treaty, these projects came to a premature end due to lack of safe ground testing available at the time.

After their shutdown the focus shifted to supporting current near Earth missions as well as deep space probes which corresponded to a shift away from advanced propulsion and towards power generation, creating the new class of nuclear power sources in space. This class initially started with the use of a nuclear reactor with the SNAP-10A demonstration flight by the United States as a proof of concept that a nuclear reactor could be flown on a satellite and only operated for 43 days [29]. After the flight of the SNAP-10A, nuclear power source in space expanded to include the use of radioisotope thermal generators (RTGs) as the United States switched to using these in lieu of nuclear reactors due to their simplicity and high specific power. Meanwhile, across the Pacific, the USSR began and continued to launch satellites

with nuclear reactors on-board totalling 35 soviet reactors launched between 1967 and 1988 [30] before making the switch to RTGs. These reactors ranged from less than a full day of operation to approximately 100 days of operation [30].

Unfortunately these reactor flights have not been without incident as two of the USSRs space reactors experienced accidental reentries of Cosmos 954 and Cosmos 1402 [30] over Canada and the South Pacific, respectively. It was after the reentry of Cosmos 954 that the United Nations decided to discuss and create policy surrounding the use of the Nuclear Power Sources in Space. It was during these talks in 1983 that Cosmos 1402 reentered furthering the need for these discussions and policies. Out of these talks the *Principles Relevant to the use of Nuclear Power Sources in Outer Space* was created as a non-binding resolution of the United Nations. These principles will be discussed in further detail in Section 6.1.

After the switch from nuclear reactors to RTGs, RTGs became commonplace for space missions ranging from the Mars Rovers to a number of deep space probes. These were seen as a safer and more simpler option particularly for missions that did not require high levels of power. There are two main drawbacks to the use of RTGs as nuclear power sources. The first drawback is the low energy conversion rates of approximately 7% but have the potential through improving Stirling conversion technologies to increase these efficiencies up to 22-32% [31]. The second drawback is the low power output of these devices that generally does not exceed a few kilowatts of power. The power limitation has not been a major issue yet in space missions due to the low power requirement on deep space probes such as Voyager 1 and 2 without humans on-board. The major advantages of RTGs besides being safer and simpler is the low mass and long lifetime of these systems. Current systems feature a power density of  $5.2W_e kg^{-1}$  while featuring a power lifetime ranging from 3 to 30+ years [31]. It should be noted that the lifetime of these devices does vary depending on which radioisotope is used as the different half lives will determine how much power is still being produced as time goes on. It should also be noted, that there have been concerns over the use of Pu-238 which is the most common fuel for RTGs

in terms of supply of this material particularly in the United States as the US does not produce its own Pu-238 but has instead relied on other countries such as Russia for it [31,32].

As missions begin to become more complex and longer duration human missions are being discussed, renewed interest in reactors for space generation has been created. Leading to the development of three mission classes [33]:

1. Rovers and Robotic Science Missions which require approximately  $1 - 10kW_e$
2. Surface Outposts and Bases Missions which require approximately  $10 - 100kW_e$
3. Spacecraft Power and Propulsion Missions which require  $100+ kW_e$

Since the early 2000's NASA technological development focus began to shift from the first mission class of rovers and robotic science missions to that of the second class with surface outposts and bases. In addition to the life support challenges involved with these missions, NASA has begun to investigate power sources for such missions including the use of nuclear power. This renewed look at nuclear power in space also sparked renewed interest in the use of small nuclear reactors for propulsion systems with Project Prometheus [34]. This interest then evolved into the development and testing of the Kilopower Reactor Using Stirling Technology (KRUSTY) project which featured a  $1kW_e$  reactor with plans to scale to  $10kW_e$ . This project marks a major step forward in the development and testing of surface fission reactors and begins to pave the pathway forward for future testing and research for the second and third classes listed above.

### 3.1.2 Potential Power Sources for Spacecraft Power and Propulsion

As previously discussed, there has been two main nuclear power sources used in space and a third one will be discussed later when discussing thermionic conversion. RTGs while reliable for years to come have very low efficiencies and low power outputs which makes them suitable and preferable for rovers and robotic science missions.

This aligns with their current uses, however, once the power level begins to reach the surface outposts and base missions class, the RTGs are at or past their current limit in terms of power [33]. With the elimination of RTGs as a possibility, nuclear reactors and nuclear batteries are the two remaining options. Nuclear batteries are continuing to gain momentum as they can be created with specific masses below that of traditional reactors utilizing Brayton cycles but are yet to be proven in flight tests as nuclear reactors have.

## **Power Conversion Methods**

One of the biggest challenges in space is the power conversion method of the reactor. This is due to the reactors remoteness and unique environment including little to no gravity, that presents challenges not faced by terrestrial systems and requires designs that do not include single point failures [35]. As discussed by El-Genk, one of the main systems to avoid single point failures is the power conversion systems which can be accomplished by utilizing multiple energy conversion methods and loops [35]. While utilizing multiple loops and systems for power conversion eliminates the possibility of single point failures, it has a negative effect on rocket performance as it will increase the mass and, hence, lower the thrust to weight ratio [35].

Presently there are five main power conversion methods being utilized or investigated for use by nuclear power sources: Rankine, Brayton, Stirling, thermoelectric, and thermionic. Each one of these systems has its own advantages and disadvantages based on its level complexity and whether or not the conversion system is dynamic or static. For the purposes of this work, thermoelectric will not be considered due to its high specific mass and low efficiencies [36]. One of the main focuses with the power conversion is to determine the specific mass of the system aiming to achieve as low of a specific mass as possible for the reactor. As can be seen in Table 3.1, the choice of power conversion system can have a major implication on the mass of the system

since the specific mass can vary by over an order of magnitude depending on which system is chosen especially when analyzing these systems for Spacecraft Power and Propulsion.

Table 3.1.  
Comparison of the four main power conversion methods for spaceborne nuclear systems

Mission Type	System Specific Mass $\frac{kg}{kW_e}$			
	Brayton	Rankine	Stirling	Thermionic
Rovers and Robotic Science	76.4-304 [33]	N/A	59.8-96.1 [33]	N/A
Surface Outposts and Bases	19-341 [33]	N/A	43.9-295 [33]	N/A
Spacecraft Power and Propulsion	2-26.4 [33]	6.06-34.20 [37]	20.7-31.0 [33]	1 [21]

Of the three dynamic conversion systems being considered, the Rankine cycle is the most complicated of the four power conversion methods due to its liquid metal working fluid [36]. Despite its complexity, liquid Rankine conversion systems feature efficiencies of approximately 25% which is quite high particularly compared with the least complicated conversion methods which routinely have efficiencies of 10% or less [36]. It can be observed in Table 3.1 that despite being capable of low specific masses, for the spacecraft power and propulsion missions of which this report focuses on, the Rankine conversion system also can have the largest specific mass.

The Brayton cycle as shown in Table 3.1 is the favorite conversion method for space reactors due to its current specific mass capability of 2 kg per  $kW_e$  which would scale a 10 MW reactor to weight approximately 20,000 kg. Similar to the Rankine

cycle, the Brayton cycle also has efficiencies of approximately 25% but unlike the Rankine cycle, the Brayton cycle features more mature technology as it is commonly used [37]. Brayton cycles have also been shown to have lower system masses than Rankine cycles and Stirling systems when a reflector is used for the core [36,37]. A Brayton system is comparable to a Stirling system when a bare reactor is utilized. Mason notes that the type of mission has an effect on which power conversion system should be used. For low power missions, such as robotic missions, Stirling is far superior in terms of mass savings than Brayton system. However, when the other two mission classes are observed, the specific mass cross over point occurs between 15-20 and 30-40,  $kW_e$  respectively [33].

As previously mentioned, Stirling conversion systems provide superior specific masses for lower power missions but do not fare as well for higher power missions such as spacecraft power and propulsion as seen in Table 3.1. Stirling converters are capable of reaching efficiencies between 25-30% [38]. Of the three dynamic conversion systems discussed, Stirling converters are by far the simplest but also generate power at the lowest frequency at approximately 60hz [38].

Thermionic conversion systems differ from its fellow static conversion system, thermoelectric, in that despite having relatively low conversion efficiencies of approximately 10%, they are capable of achieving lower specific masses [38] as evidenced in Table 3.1. Recent breakthroughs at NASA have led to the creation of a nuclear power source known as the Nuclear Thermionic Avalanche Cell (NTAC). While the NTAC is not a nuclear reactor, it is a nuclear power source capable of working in space that is scalable to 10 MW at a specific mass of 1 kg per  $kW_e$  [21]. As shown in Table 3.1 is the lowest of the all current conversion methods. Similar to thermoelectric, thermionic also possess the advantage of having no moving parts.

### 3.1.3 Previous Space Reactor Programs and Studies

Since the inception of nuclear power sources in space with the SNAP-10A in the 1960's, humanity has investigated the use of nuclear reactors in space on multiple occasions. In the US alone, these projects include but are not limited to the SNAP-10A, SAFE-400, SP-100, Project Prometheus, DUFF, and Krusty. Meanwhile across the Pacific, the Soviets investigated nuclear reactors in space with the Romashka, Topaz, and Rorsat Reactors. A comparison of the basics of these reactors can be seen in Table 3.2 which shows how similar these designs were in the early stages. It is interesting to note that with exception of the two newest projects, DUFF and KRUSTY, the reactors exclusively used thermoelectric or thermionic conversion two methods which are not commonly considered now for spacecraft power and propulsion type missions.

Table 3.2.

Power Conversion and Output Capabilities of tested nuclear reactors for space. \*Denotes reactors that have been flown in space, while the other reactors have undergone ground testing.

Reactor	Power Conversion Method	Power Output	Weight
SNAP 10A* [39, 40]	Thermoelectric	34-45.5 $kW_t$	435 kg (Core)
SP-100 [39, 41]	Thermoelectric	2.4 $MW_t$	4600 kg
DUFF [42, 43]	Stirling	700 $W_t$	>1000 kg
KRUSTY [44, 45]	Stirling	5 $kW_t$	339-1293 kg
Romashka* [40]	Thermoelectric	40 $kW_t$	455 kg (Core)
Topaz* [40]	Thermionic	130-150 $kW_t$	1000 kg (Reactor)
Rorsat* [40]	Thermoelectric	< 100 $kW_t$	<390 kg (Reactor)

## American Studies

While research on the use of nuclear reactors in space dates back to 1955 in the US with the ROVER/NERVA Project [39], it wasn't until the 1960's that the United States launched their first and only nuclear reactor into Space. The first reactor was the SNAP-10A which as shown in Table 3.2 is on the low end of power output for the reactors that have flown in space, but that it is consistent with the others in using thermoelectric power conversion. The SNAP-10A was operated for 43 days in space before shutting down and remaining in orbit [39]. After the success of SNAP-10A, work continued with the SNAP-8 and SNAP-50 reactors which both underwent varying levels of ground testing but were never flight tested [39] with the SNAP-50 differing from the other SNAP models in that it was a fast reactor instead of a thermal reactor.

Other designs that received attention in the 1950, '60, and '70's included gaseous core reactors, metal cooled reactors and in core thermionic reactors. These designs also reached varying stages of testing ranging from successful criticality tests of the gaseous core reactors to simply testing the conversion system associated with them [39]. Whereas the SNAP designs were more geared towards low power such as  $0.5 kW_e$  for the SNAP-10A, these designs were more focused on higher power such as  $1000 MW_t$  for the gaseous core reactor [39].

As these projects were discontinued, work began on the SP-100 reactor which was largely regarded as the next step after the SNAP-10A as its power level was set to scale from 10-1000  $kW_e$  [46]. This range of power levels was to provide flexibility in mission selection for use of the SP-100 reactor and was facilitated by the separation of the power conversion system from the reactor itself as a second assembly [46]. This provided a major advantage over the SNAP-10A as different power conversion systems such as those discussed previously that could be interchanged more readily according to the mission without necessarily changing the reactor design [46].

As funding changed so did the projects within NASA, which led to a hiatus in the development of nuclear reactors in space between the late 90's and the early 2000's when the draught was ended with the creation of the Jupiter Ice Moons Orbiter Mission (JIMO) which did not come to fruition prior to being cancelled. Despite cancellation of the JIMO's missions and lack of its success, it did succeed in the sparking renewed interest in the use of nuclear reactors in space, notably by shifting the attention back to fission surface power for either the Moon or Mars [36]. This inevitably led to the investigation of the three most promising methods of power conversion: Brayton, Stirling, and thermoelectric as recommended by the Department of Energy and NASA.

One of the first steps in this was demonstrating successful use of the thermoelectric converters with heat pipe cooling for what would now be considered the rover and robotic science mission class. This was accomplished in an incredibly quick fashion with the Demonstration Using Flattop Fissions (DUFF) lasted under 6 months and cost under one million dollars [44]. Besides demonstrating the technology, this was also pivotal in that it showed that rapid prototyping and testing of these systems for low cost was possible. This was a break in tradition in that all previous projects were large undertakings. Poston et al. state that this was one of the main reasons that all previous projects had failed and that smaller steps like DUFF were needed [44]. Following the success of DUFF, the Kilopower Reactor Using Stirling Technology (KRUSTY) reactor project was created with this goal in mind of making incremental advancements in technology and demonstrations. The KRUSTY reactor was also designed to operate at the lower power output of  $5kW_t$  placing it at the low end of the rover and robotic science mission class, although scalable up to  $10 kW_e$  [44]. Lessons learned from these kilopower reactors will not only be used to enhance these designs and future reactors for the rover and robotic science mission class but also will aid in laying out a path to success in developing reactors for the spacecraft power and propulsion class leading into the megapower range.

## Soviet/Russian Studies

As stated by Bennett, not as much is known about the Soviet nuclear space program outside of what is known about the 35 reactors that have been flown between 1967 and 1988 by them [40]. Similar to that of the SNAP-10A, many of these reactors remain in orbit now that they have been shut down. Whereas the SNAP-10A only operated for 43 days, the Soviet reactors operated from less than 3 hours with the Cosmos 367, 402, and 785 to approximately one year with the Cosmos 1867 [40]. The 35 reactors launched by Russia fall into three reactor classes: ROMASHKA, (Thermionic experimental conversion in the active zone) TOPAZ, and RORSAT [40]. It should be noted that there are conflicting numbers of launches and classes as Zakirov et al. claim the launch of only 34 reactors and a class of reactors called BOUK, which constituted the majority of the launches by the Soviets [47].

The ROMASHKA reactors were very similar to that of the SNAP-10A in terms of power output and conversion method with both reactors using the thermoelectric power conversion method to convert the roughly  $40 kW_t$  being produced [40]. It is notable that the ROMASHKA reactor was a fast reactor differing from the thermal reactor utilized in the SNAP-10A design.

Following the ROMASHKA project, at least three different TOPAZ Reactors were tested with the goal of increased power over the ROMASHKA [40]. As previously mentioned there are conflicting reports regarding the Soviet space reactor program, where Zakirov et al. propose that there were only two classes of TOPAZ reactors [47]. The power level increased by an order of magnitude to reach a thermal power output of between 130 and 150  $kW_t$  which along with an increased efficiency of approximately 5% led to a maximum electric output of 10  $kW_e$  [40]. A notable design change between the two designs is that TOPAZ utilizes a thermionic conversion system instead of a thermoelectric conversion system and is a thermal reactor instead of a fast reactor.

Finally, the third reactor class utilized by the Soviets was the RORSAT class. The RORSAT class marked a return to the use of fast reactors utilizing a thermo-

electric conversion system which is what was originally flown in the ROMASHKA class. Despite being of the same type and utilizing the same conversion system, it is important to note that the reactor designs were different in that the RORSAT class generated roughly double the thermal output of the ROMASHKA class yielding an electric power level between the ROMASHKA and TOPAZ classes at  $5 kW_e$  [40]. Based on the design characteristics provided by Zakirov et al., the BOUK reactors appear to be the same reactors referred to as RORSAT by Bennett as both authors provide nearly identical thermal power but slightly different electrical output with the BOUK reactors producing  $2.5 kW_e$  [47].

As with the US, there has also been renewed interest in Russia for the use of nuclear reactors in space. The main difference is that unlike the US, Russia is more heavily leaning towards using it for propulsion with nuclear electric propulsion (NEP). The NEP designs seek to build off of the TOPAZ and BOUK designs to couple them with new high powered electric thrusters [47]. The goal of the renewed interest in space reactors is to develop a MW-class reactor for new NEP systems [47].

### 3.2 Overview of Rocketry Methods and Comparison

There have primarily been four types of rocketry investigated and tested: nuclear thermal propulsion, solar electric propulsion, nuclear electric propulsion and chemical propulsion. Nuclear fusion propulsion is notably missing from this list as it has not been as extensively tested or flown as of yet while the other methods have all featured full engine tests.

Chemical has been the most common form of propulsion to date, particularly for any manned missions. This is due in large part to its simplicity and thrust levels. As can be seen in both Table 1.1 and Figure 3.1 that the thrust levels are among some of the highest currently available making it ideal for missions that require large vehicle masses and lift off from the ground such as all human missions to date. The downside to chemical propulsion is that due to its simplicity the technology has

now reached close to its maturity limit. Since it is a combustion driven process where a fuel mixture is ignited, it is limited in regards to the speed of the propellant and efficiency of the rocket which is noted by the lowest specific impulse of any of the propulsion types. More exotic fuels such as solid propellants embedded with nano-particles [48] are currently being studied in an attempt to further increase the performance characteristics of chemical propulsion. These efforts are still quite far from achieving the specific impulses that can be achieved with other propulsion types. This low specific impulse and moderately high thrust has resulted in predicted longer travel times from Earth to Mars as shown in Figure 3.1. These predicted travel times not only are longer than desired but also being to push the limits of acceptable safe days in space as discussed in Table 2.1.

Electric Propulsion is typically used in the form of ion thrusters such as Hall thrusters. Unlike chemical propulsion where performance characteristics are limited by the combustion of the propellant, electric propulsion does not actually combust the propellant. Instead, it either provides heating which through expansion can accelerate the propellant or directly accelerates the propellant through the use of electric or magnetic fields. This has led to the classification of three main types of electric propulsion systems: Electrothermal, Electrostatic, and Electromagnetic. Electrothermal propulsion works through the first mechanism mentioned above where the propellant is heated through the conversion of electrical energy. This heated propellant then expands and can be accelerated to incredible speeds which provides the high specific impulse numbers seen in Figure 3.1. Electrostatic thrusters on the other hand does not rely on heating the propellant but instead uses electric fields to accelerate ions, or charged particles, to high speeds. Lastly, electromagnetic propulsion systems operate similar to the electrostatic ones but instead of electric fields, magnetic fields are utilized with plasma propellant as opposed to ion-gas propellant. The electric energy used by these thrusters is typically generated through the use of either solar panels or a nuclear power source, the latter of which will be discussed further in Section 3.2.1. Since nuclear power sources have the potential to produce higher power levels than

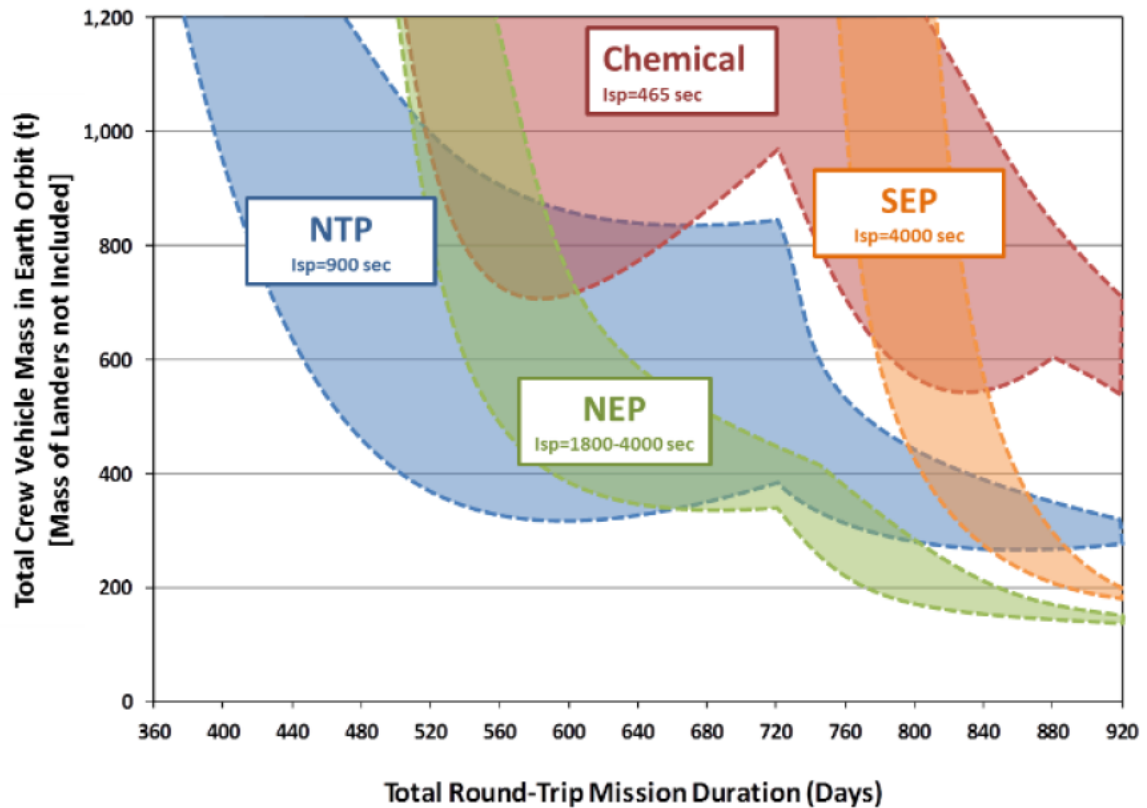


Figure 3.1. Comparison of four main methods of rocket propulsion and their capabilities for a Mars mission [49]. Original image from *Human Mars Mission Definition: Requirements & Issues* by B.G. Drake for the Human 2 Mars Summit, May 2013

solar panels without having enormous arrays, nuclear electric propulsion as shown in Figure 3.1 does provide for faster trip times to Mars than solar electric. Despite the high specific impulse featured with electric propulsion, the thrust levels shown in Table 1.1 are on the lower end of the spectrum. Although as electric propulsion is utilized for more missions, more advances in the technology will begin to yield higher thrust value such as those obtained by using the VASIMR Engine® [21,22].

Nuclear thermal propulsion and to an extent nuclear fusion propulsion, operating in high thrust mode, both function similar to that of electrothermal thrusters in that the reactions heat excess propellant. The main difference between these methods and

an electrothermal thruster is the amount of energy and heat transfer that occurs with nuclear thermal and fusion propulsion systems. This allows for more propellant to be heated up and expelled through what are typically magnetic nozzles. By expelling more propellant, this results in the highest thrust values in Table 1.1 while also maintaining relatively high specific impulse values that are in between chemical and electric propulsion. The combination of high thrust along with high specific impulse allows for the shortest travel times from Earth to Mars as seen in Figure 3.1. The downside to nuclear thermal and nuclear fusion propulsion is that no mission has been flown to date that utilizes either propulsion system. These systems are far more complex than those of chemical and electric propulsion and as such carry more risk due to the relative lack of maturity of the technology for propulsion purposes.

### **3.2.1 Nuclear Electric Propulsion**

Operating similarly to solar electric propulsion, nuclear electric propulsion increases the range of missions that can utilize electric propulsion since solar power capabilities decrease the further from the sun. Another major advantage to using nuclear instead of solar is that the power levels can be varied quite drastically while scaling the mass while solar not only scales mass but also includes large solar panel arrays.

Electric propulsion to date has primarily been utilized for low power and low thrust systems for satellite use. However, as rocket technology continues to evolve and Mars missions become more feasible, higher powered electric propulsion systems such as the Variable Specific Impulse Magnetoplasma Rocket (VASIMR) have been designed and are currently undergoing tests. The VASIMR engine operates similarly to that of a magnetic mirror fusion reactor without the fusion reactions. Instead simply uses heating of the plasma through electromagnetic waves and the expansion and acceleration of the plasma through magnetic fields to exhaust the plasma out of a magnetic nozzle to produce thrust [50]. One of the major benefits to the VASIMR

design is that it operates under constant power but can scale the specific impulse and the thrust level of the rocket itself [22, 50]. THE VASIMR design can be scaled for input powers ranging between 200 kW and 2 MW which when coupled with a nuclear reactor using MHD converters can achieve a specific mass of approximately 2 kg/kW which is quite low when compared to just power conversion system specific masses as shown in Table 3.1. The VASIMR has been shown to have an  $I_{SP}$  of approximately 5000 sec or higher and is capable of a round trip Mars mission in 149 days [21, 22].

Seeing as NEP is becoming more viable as an interplanetary propulsion method is in part what motivated the current work. Low specific masses achievable by improved power conversion techniques and the resemblance of high power electric thrusters to fusion devices provided a solid bases on which to formally study the effects of adding an auxiliary fission power system to power a fusion thruster, a concept that has been briefly mentioned by long deemed too heavy to be worthwhile [51].

### 3.2.2 Comparison of Fission and Fusion Rocketry

#### Fission

In the early days of rocketry, it was proposed to use controlled detonation of nuclear bombs to propel a spaceship to Mars. This concept was investigated in Project Orion before being abandoned for more controlled nuclear propulsion concepts. This led to the creation of the Nuclear Engine for Rocket Vehicle Application (NERVA) Project between NASA and the Atomic Energy Commission (AEC), of which most nuclear thermal rocket designs have been derived since then. The main concept for NERVA was to use a fission reactor to heat up and energize a gaseous propellant which would then be expelled through a nozzle. This was seen as a way to boost rocket performance since nuclear fission reactions release a significant amount more of energy than that of a standard chemical combustion reaction.

NERVA reached the ground testing phase yielding results found in Table 3.3 prior to its cancellation in 1972 due to no viable missions and changing international laws

surrounding nuclear ground testing [52]. These changing conditions, however, did not cancel their nuclear thermal rocket program continuing with the development of the RD-0140 rocket engine until the collapse of the Soviet Union [53]. The Soviet program never reached the same testing stage as NERVA but was designed to achieve a similar performance as NERVA just on a smaller scale as shown in Table 3.3.

Table 3.3.  
Comparison of fission vs fusion rocket engines. \* denotes the reactor mass plus shielding and adapter.

Engine	Type	Thrust (kN)	$I_{SP}$ (s)	Power Output	Weight (kg)
NERVA [52]	Fission	333.6	825	1000 $MW_t$	11113
BNTR [54]	Fission	66.7	863.7	313.2 $MW_t$	3059
RD-0140* [53]	Fission	35.3	900	196 $MW_t$	2000
NPPS [53]	Fission	68	925	340 $MW_t$	1800
GDM [55, 56]	Fusion	491-3700	1.29-2.07* $10^5$	4130-38664 MW	1.99 * $10^6$
DPF [6]	Fusion	449-1000	1311-2000	3674 $MW_t$	14515-43545

Despite their apparent advantages of chemical rockets, NTRs have several distinct disadvantages which have slowed their progress over time including but not limited to reactor safety, public perception, and testing limitations. The rocket performance is directly related to the performance of reactor including the temperature of the reactor which means to increase performance, pushing the materials selected to close to their limits would be desirable which would necessitate additional safety precautions. An additional concern surrounding reactor safety is the release of fission particles as the propellant is fed through the core before being exhausted out the nozzle [57]. Although this can be scrubbed clean through the use of scrubbers as demonstrated by NERVA, it was also shown to be very expensive to have a facility capable of it during testing from both a facility and equipment standpoint [57]. Any reactor safety

systems must be capable of operation under both gravity and zero gravity conditions with ideally passive safety systems.

The second being that while it can easily be seen and argued that nuclear thermal propulsion for a manned Mars mission is a peaceful use due to other international treaties dictating the peaceful use of space, however, all nuclear testing especially where fission products may be released in the propellant will require substantial testing protocols that could place additional limits on the system based on what can be tested. Instead of the previous above ground nuclear testing that was performed in accordance with the NERVA Project, another concept based on the testing of nuclear devices was published in the early 2000's by Howe et al. [57]. This concept takes advantage of what was formerly the Nevada Test Site but is now the Nevada National Security Site which has not only extensive nuclear testing experience but also a unique geology to handle these tests [57]. The method of testing the nuclear rocket engine similar to nuclear devices would involve boring a hole to a depth of 1200 ft into which the nuclear engine mounted to the surface and entrapped in a steel shell would expel its propellant [57]. This method is believed to be a significantly cheaper alternative to above ground engine testing facilities.

Finally, there is the issue of public perception as both rocket and nuclear technologies have had several accidents such as the Space Shuttle Challenger explosion, Space Shuttle Columbia accident, Chernobyl and Fukushima. Despite the many years without accidents and the low risk of an accident occurring, these past accidents are ingrained in the mind of the public. Unlike the reactors that were launched on satellites, a nuclear thermal rocket would be critical at take-off which adds additional risk if something were to happen at take-off on what would happen to the nuclear material on board. A safer alternative to this would be for the nuclear thermal rocket to be built and utilized for interplanetary travel only, not take-off and landing. A concept known as a Mars Cycler which was proposed by astronaut Buzz Aldrin [58]. This concept is of a spaceship that routinely makes journeys between the orbits of both Earth and Mars similar to that of a shuttle bus on a college campus. This would

mean that further space infrastructure would need to be created in order to get humans from the surface of the planets to the rendezvous point of the cyclor and vice versa but would alleviate many of the safety and public concerns with launching and landing a nuclear thermal rocket.

## **Fusion**

Fusion rocketry has not enjoyed the same amount of investigation as nuclear thermal propulsion although as seen in Table 3.3 fusion propulsion, such as the Dense Plasma Focus and Gasdynamic Mirror, the fusion rocketry offers comparable if not increased rocket performance to Fission device. Part of the reason that fission propulsion has generated more investigation is because fission is a proven concept that is used on a regular basis in nuclear power plants around the world. Fusion, however, is still attempting to prove itself an economical and feasible option by outputting more power than what is currently put in to make the reaction possible which to date has not happened yet. Therefore, much of the fusion research taking place around the world is focused on trying to achieve breakeven for a fusion reactor led by the ITER and Wendelstein-7X Projects.

This is problematic when the fusion rocket ideas that have previously been studied have all assumed that a self sustaining fusion reactor which can create thrust is possible. This is seen in literature by these rockets having the energy multiplication value,  $Q$ , larger than 1, which will be explained in further detail in Section 4.1. If the fusion reactor cannot produce enough energy to power itself it renders the thruster useless. This has resulted in many of the previous studies being numerical or analytical studies with only a few experimental studies having been conducted with no flight qualification testing having been conducted.

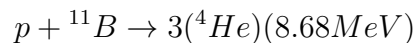
Besides the theoretical better performance than fission propulsion, fusion rocket engines also address some of the concerns mentioned above with regards to fission propulsion. The fusion reactor won't have the fission particles to deal with and there-

fore will not have the same testing restrictions seen with nuclear thermal propulsion unless the fuel type selected is a deuterium-tritium mixture which would then require additional testing protocols and restrictions. Fusion reactors are also inherently safer on lift off than that of a nuclear thermal rocket. Finally while fusion is still nuclear technology, it does not carry the same negative stigma with it by the public as fission technology does.

## 4. MAGNETIC CONFINEMENT FUSION PROPULSION SYSTEMS

### 4.1 Overview

Magnetic confinement fusion operates by generating and confining a hot fusion plasma where it interacts in the form of fusion reactions. Potential fuels and their reactions are listed below:



The plasma is confined either between the magnetic fields in an open magnetic field configuration such as a Gasdynamic mirror or within a pinch such as Z-pinch device like the Dense Plasma Focus. Despite this concept having been around for decades, it has yet to demonstrate itself as a viable option for power generation due to high input power needed to confine the plasma as well as plasma instabilities such as the flute, sausage, and kink instabilities which will be discussed in later sections as they relate to each device. This has led to several of the abandoned power generation concepts such as the spheromak [59, 60], magnetic mirror [8, 51, 55, 56, 61–63] and dense plasma focus [6, 7, 15, 64, 65] devices to be investigated for other uses such as space propulsion. For the purposes of this work, the Gasdynamic Mirror and Dense Plasma Focus devices will be investigated for use as fission assisted devices for space propulsion in the very near term for a manned Mars mission.

## 4.2 Dense Plasma Focus

A Dense Plasma Focus device is a type of pulsed Z-pinch magnetic fusion device that was invented independently by Mather [66] and Fillipov [67]. The Mather and Fillipov types of DPF differ in terms of their electrode aspect ratio with the Mather type having an aspect ratio below 1 and Fillipov type above 1. The difference in geometries can be visualized with Figure 4.1. The Mather-type is the device typically investigated for space propulsion purposes and as such will be the subject of the investigation of the current work.

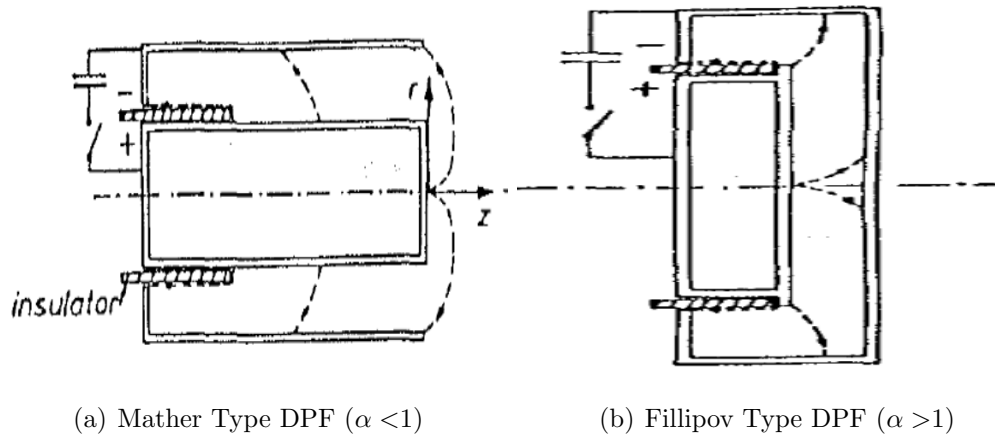


Figure 4.1. Schematic of the differences between the Mather and Fillipov Type [64]

When the DPF is used for space propulsion, the propulsion system can be depicted as shown in Figure 4.2. In this example the chosen fuel is a  $D - He^3$  for the fusion reaction which is fed directly into the plasma focus device prior to being expelled after the fusion reaction through a magnetic nozzle. Additionally there exists a hydrogen tank which provides cooling for the nozzle as well as extra thrust by absorbing waste heat and then being expelled through the nozzle. The mass flow rate of the hydrogen propellant can be varied as was done in previous work [15] but for the purposes of current work is held constant at 30 kilograms per second to be consistent with work from previous studies [15,65]. Additionally this work utilized a  $\Delta V$  of 20 km/s unless noted otherwise and four DPF thrusters for consistency with previous work [15,65].

Previous work by Leakeas showed that the DPF can be operated in one of three propulsion modes [65]:

1. **Low Thrust Mode** where the plasma from the fusion pinch is the only propellant being utilized along with a magnetic nozzle. In this mode the DPF is fired for approximately the entire trip. Without a direct energy converter this mode does not produce any electricity.
2. **Moderate Thrust Mode** where a moderate amount of hydrogen is flowed along the DPF to absorb waste heat and is used as propellant. The hydrogen propellant first passes over the nozzle to cool it before entering a turbine where it deposits some of the energy it has absorbed in order to produce electricity. Similar to the low thrust mode, the DPF is operated for the majority of the trip time in this mode.
3. **High Thrust Mode** where the thrust amount is prioritized to simulate an impulsive burn. The DPF expels a large amount of hydrogen which cools the nozzle and generates electricity through the turbine prior to being expelled to reach high levels of thrust. By reaching such high levels of thrust the DPF only needs to be fired for short periods of time.

This work will only consider the high thrust mode for its analysis as demonstrated by a mass flow rate of 30 kilograms per second of hydrogen.

The DPF device on which the code is based is from the Livermore-I Plasma Focus Experiment which features the characteristics and assumed characteristic found in Table 4.1.

#### 4.2.1 Physical Basis

The operation of the dense plasma focus can essentially be broken down into four phases: Breakdown, Rundown, Focus(Pinch), Re-breakdown [65]. These phases are shown in Figure 4.3. First the gap between the anode and cathode is filled with a fill

Table 4.1.  
DPF Parameters from the Livermore-I Experiment [15]. \* Denotes assumed values.

Geometry	
Anode Radius, cm	5.08
Cathode Radius, cm	8.0
Anode Length, cm	38.2
Pinch Length*, cm	2.54
Pinch Radius*, cm	0.15
Electrical Parameters	
Input Voltage, V	27000
Initial Inductance, H	$2.5 * 10^{-8}$
Capacitance, F	$3.55 * 10^{-4}$
Max Current, MA	20

gas. After which a high current pulse is sent to the DPF which in turn breaks down the fill gas into a plasma state for the breakdown phase. Next the DPF enters into the rundown phase where the azimuthal magnetic field generated by the high current pulse in the anode causes the plasma sheath to move down the length of the device. As the plasma reaches the end of the device, the instabilities in the device become more dominant forcing the plasma to collapse down on itself in the direction of the current [65]. This focus creates a pinch with a very dense hot plasma that is confined on the order of microseconds by the magnetic field. The fusion reactions occur when the plasma is confined releasing an enormous amount of energy in a small fraction of time.

As with many fusion devices, the DPF has to contend with multiple plasma instabilities that affect its performance. In the case of the DPF specifically, two Magnetohydrodynamic (MHD) instabilities known as the sausage and kink instabilities.

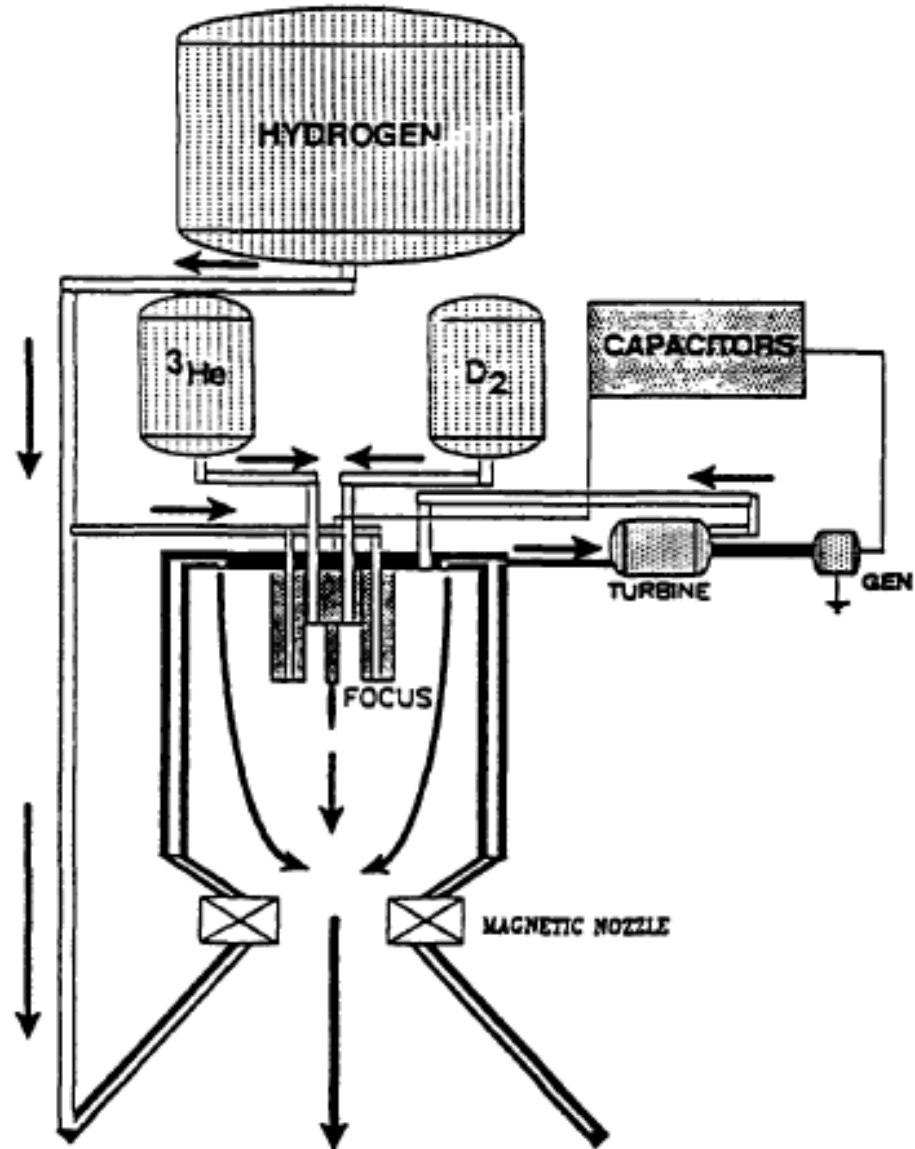


Figure 4.2. Schematic of the DPF Propulsion System [65]

The sausage instability occurs when the poloidal mode number equals zero ( $m=0$ ) whereas the kink instability occurs at  $m=1$ . The poloidal mode number corresponds to shape of deformation the plasma experiences in the poloidal direction [65]. While it is possible to stabilize these instabilities which could yield longer pinch confinement

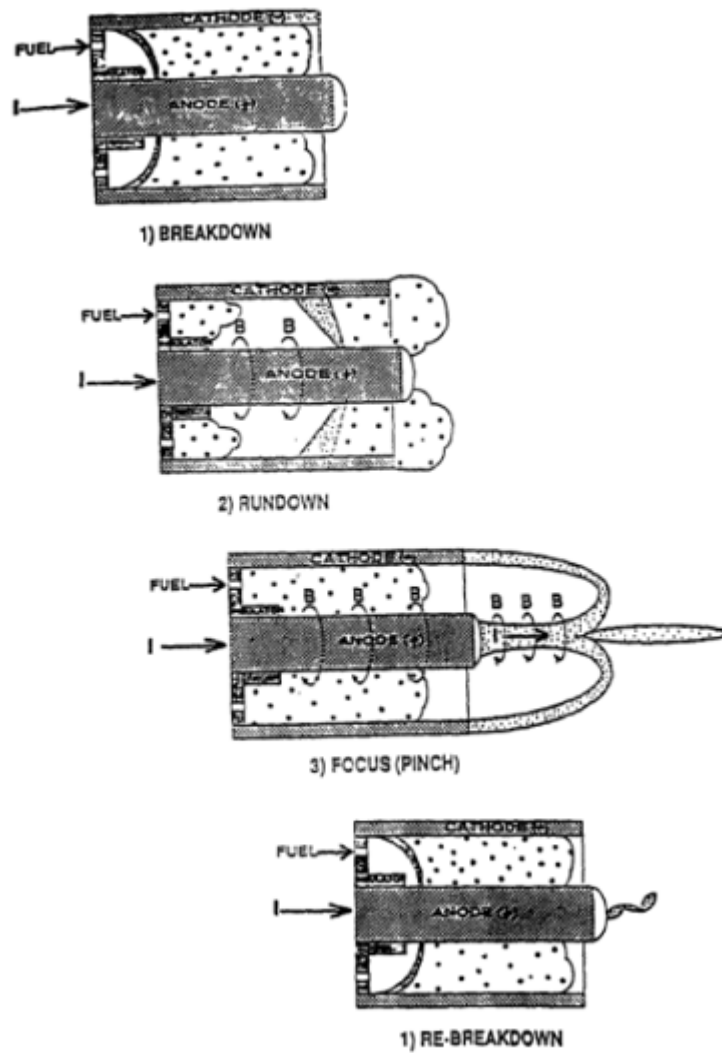


Figure 4.3. Description of the four operational phases of the Dense Plasma Focus Pulse [65]

times, the effect on stabilizing these instabilities in a DPF device requires further study. A strong axial magnetic field can be used to stabilize the sausage instability but the kink instability requires a discussion on the Kruskal-Shafranov Limit which is described by the following equation [68].

$$I(a) < \frac{2\pi a^2 B_t}{\mu_0 R_0} \quad (4.2)$$

where  $I$  is the toroidal plasma current,  $B_t$  is the toroidal magnetic field,  $a$  is the plasma minor radius, and  $R_0$  is the plasma major radius. This limit defines the maximum current that can be used in order to achieve a safety factor of  $q > 1$  at the plasma surface.

A more complete description of the physics and the mathematical basis for the original code can be found in *Parametric Studies of Dense Plasma Focus for Fusion Space Propulsion with D-He<sup>3</sup>* by C.L. Leakeas [65].

#### 4.2.2 Evaluation Methodology

In the early 1990's, researchers at Purdue led by Dr. Chan Choi developed a Dense Plasma Focus propulsion code in Fortran which was used for several reports for the US Air Force and thesis projects [15, 65]. For this project, the code was converted into MATLAB® where it was then checked against the original Fortran code.

#### Code Updates

After the MATLAB® code had been verified, several updates and additions needed to be made. Several of the system parameters utilized in the original code including most significantly the specific energy had become outdated due to improvements in the technology. The original code used an assumed value of 2kJ/kg for the specific energy which was an order of magnitude higher than technology available at the time which is three orders of magnitude below the proposed theoretical maximum from the reports of 2 MJ/kg [15]. Current technology and cutting edge research has managed to increase capacitor specific energy to approximately 800 kJ/kg [13]. This update alone will result in major mass savings for the DPF system.

The next major update was in regards to the fuel. This update is a two part update. As the original code was only written to account for the  $D - He^3$  fuel and was later modified to be capable of using spin-polarized  $D - He^3$  fuel. While  $D - He^3$  fuel is still the preferred fuel, other fuels, such as DT and  $p - B^{11}$ , have

been investigated with other magnetic confinement propulsion systems and therefore should be investigated with the DPF for better comparisons between MCF systems. The code was updated to be capable of utilizing DD, DT, spin-polarized DT,  $p - B^{11}$ , and spin-polarized  $p - B^{11}$ . In the process of updating the number of fuels that the code could be used for, it was discovered that the fusion reaction rates being utilized were not the most updated reaction rates available and therefore needed to be updated. The original code calculated the reaction rate for both the primary  $D - He^3$  using the following equations [65]:

$$X = \log_{10}(KT_{optimum}) \quad (4.3a)$$

$$\langle \sigma v \rangle = 10^{(A*X^3+B*X^2+C*X+D)} \quad (4.3b)$$

where the coefficients for the various reactions can be seen in Table 4.2

Table 4.2.  
Original Reaction Rate Coefficients [65]

Reaction	A	B	C	D
$D - He^3$	0.35715	-3.32451	10.11363	-26.66533
$DD_n$	0.29811	-2.08296	5.70135	-22.0878
$DD_p$	0.30795	-2.12009	5.68718	-22.03746

These reaction rates along with the reaction rate for DT reactions were updated using the following equation from Bosch-Hale [69]:

$$\langle \sigma v \rangle = C_1 * \theta \sqrt{\frac{\xi}{m_r c^2 T^3}} e^{-3\xi} \quad (4.4a)$$

$$\text{where } \theta = \frac{T}{1 - \frac{T*(C_2+T*(C_4+T*C_6))}{1+T*(C_3+T*(C_5+T*C_7))}} \quad (4.4b)$$

$$\text{and } \xi = \frac{B_G}{4\theta} \quad (4.4c)$$

which utilizes the coefficients found in Table 4.3.

Table 4.3.  
Updated Reaction Rate Coefficients from Bosch-Hale [69]

Coefficient	$DD_n$ Reaction	$DD_p$ Reaction	DT Reaction	$D - He^3$ Reaction
$B_G(\sqrt{keV})$	31.3970	31.3970	34.3827	68.7508
$m_r c^2(keV)$	937814	937814	1124656	1124572
$C_1$	$5.4336 * 10^{-12}$	$5.65718 * 10^{-12}$	$1.17302 * 10^{-9}$	$5.51036 * 10^{-10}$
$C_2$	$5.58778 * 10^{-3}$	$3.41267 * 10^{-3}$	$1.15361 * 10^{-2}$	$6.41918 * 10^{-3}$
$C_3$	$7.68222 * 10^{-3}$	$1.99167 * 10^{-3}$	$7.51886 * 10^{-2}$	$-2.02896 * 10^{-3}$
$C_4$	0	0	$4.60643 * 10^{-3}$	$-1.9108 * 10^{-5}$
$C_5$	$-2.964 * 10^{-6}$	$1.05060 * 10^{-5}$	$1.35 * 10^{-2}$	$1.35776 * 10^{-4}$
$C_6$	0	0	$-1.0675 * 10^{-4}$	0
$C_7$	0	0	$1.366 * 10^{-5}$	0

For the  $p = B^{11}$  reaction, the following equation was used to calculate the reaction rate from Nevins and Swain [70]:

$$\xi = \frac{B_g^{\frac{1}{3}}}{4\theta} \quad (4.5a)$$

$$\theta = \frac{kT_{eff}}{1 - kT_{eff} \left( \frac{P_2 + kT_{eff}(P_4 + kT_{eff}P_6)}{1 + kT_{eff}(P_3 + kT_{eff}(P_5 + kT_{eff}P_7))} \right)} \quad (4.5b)$$

$$\langle \sigma v \rangle_{NR} = P_1 * \theta \sqrt{\frac{\xi}{m_r c^2 (kT_{eff})^3}} e^{-3\xi} \quad (4.5c)$$

however, when the plasma temperature was below 130 keV, an additional resonance term needed to be added for the reaction rate:

$$\langle \sigma v \rangle_R \approx 5.41 * 10^{-21} \left( \frac{1}{kT_{eff}} \right)^{\frac{3}{2}} * \exp\left(-\frac{148}{kT_{eff}}\right) \quad (4.5d)$$

$$\langle \sigma v \rangle = \langle \sigma v \rangle_{NR} + \langle \sigma v \rangle_R \quad (4.5e)$$

The coefficients for the  $p - B^{11}$  equations can be found in Table 4.4. However, it is important to note that the  $p - B^{11}$  fuel combination has a significantly higher ignition temperature than DT or  $D - He^3$ , on the order of 500 keV. With such a

high ignition temperature, any plasma temperature below this is unlikely to produce fission products which significantly contribute to the thrust.

Table 4.4.  
 $p - B^{11}$  Reaction Rate Coefficients from Nevins and Swain [70]

Coefficient	Value	Coefficient	Value
$M_r c^2$	859526	$P_4$	$1.0404 * 10^{-3}$
$P_1$	$4.4467 * 10^{-14}$	$P_5$	$2.7261 * 10^{-3}$
$P_2$	$-5.9357 * 10^{-2}$	$P_6$	$-9.1653 * 10^{-6}$
$P_3$	$2.0165 * 10^{-1}$	$P_7$	$9.8305 * 10^{-7}$

### Code Additions

In order to utilize this code to study the effects of adding a fission reactor to power a DPF for space propulsion additions to the code needed to be made, specifically with regards to the sizing and weight of this fission reactor. A subfunction DPF\_fission.m was created that utilized the power created by the fusion reaction as well as the initial power needed for the DPF, both of which were already calculated in the original code. These numbers were then used to size the fission reactor by multiplying the power required by the specific mass of the reactor such that:

$$m_{fission} = P_{required} * \alpha_{fission} \quad (4.6)$$

The alpha fission depends on which power conversion system was utilized in accordance with Table 3.1. A hypothetical power conversion system with an alpha one order of magnitude greater than any current technology,  $\alpha = 0.1kg/kW_e$ , was also included for testing purposes. The power required varied depending on which of the three cases was being studied which will be discussed in greater detail in Section 5.1.

In addition to the introduction of a fission subfunction, it was also noted that in the previous code, the turbine used to generate electricity from the fusion reaction was not

accounted for in the mass calculations. It can be assumed that the mass of the turbine would be less than the payload and, therefore, could have been included in the payload mass. However, for a more complete understanding and to evaluate different scenarios, it is desirable to calculate the turbine/generator mass. Unfortunately work is needed in the area of thermal electric converters for fusion systems and was not included in the code. However, the code did introduce a Power Distribution and Management system which is necessary to control and distribute the power generated which comes at a specific mass of 1 kg per kilowatt electric inputted,  $kW_{e,in}$ . It was also desired to add in a direct energy converter for the fusion reactor. For this a Travelling Wave Direct Energy Converter (TWDEC) was selected for use. The TWDEC has a stated specific mass of 0.14 kg per  $kW_{e,in}$  and an efficiency of 76% [71, 72]. To determine the electricity by the TWDEC, the charge particle energy generated by the fusion reactions needed to be calculated. This was calculated using the following equation:

$$P_{ch} = P_f \left( \frac{1}{Q} + \Psi_R \right) \quad (4.7)$$

where  $Q$  is the fusion gain ratio and  $\Psi_R$  is the radiation parameter. The fusion gain ratio is simply the ratio of fusion power to input power. The radiation parameter is calculated for each fuel type using the following equation [68]:

$$\Psi_R = \frac{f_c W_f - W_{rad}}{W_f} \quad (4.8)$$

where  $f_c$  is the charged particle fraction of the reaction products,  $W_f$  is the fusion energy released and  $W_{rad}$  is the energy loss due to radiation.

The final addition to code was the introduction of a subfunction, *DPF\_flighttime.m*, to calculate the time of flight for the DPF device. This was based on the patched conic method for Kebler described by Emrich [23]. The patched conic method starts by utilizing Newton's law of gravity to find the angular momentum of the spacecraft. This method is an iterative approach that first calculates the maximum attainable  $\Delta V_{vehicle}$  for the vehicle and attempts to match the  $\Delta V$  of the mission profile [23]. The maximum attainable  $\Delta V$  is found using the following equation [23]:

$$\Delta V_{vehicle} = -0.0098 I_{sp} \ln(f_m) \quad (4.9)$$

where as the mission profile which is done by first assuming a value for the orbital eccentricity which is used to calculate the vehicle orbit radius. The orbital eccentricity will later be adjusted to ensure that the mission profile  $\Delta V$  matches that of the vehicle within 0.1%. The  $\Delta V$  of the mission is the sum of the  $\Delta V$  for the departure from an Earth orbit assumed to be 200km and the  $\Delta V$  for the arrival into a 100km Mars orbit. Once this has been completed, the spacecraft trajectory radius( $a$ ) and orbital eccentricity ( $\epsilon$ ) are used to determine the true anomaly of the spacecraft as it arrives at Mars using the following equation:

$$\theta_{Mars} = \cos^{-1}\left(\frac{a(1 - \epsilon^2) - R_{Mars}}{\epsilon R_{Mars}}\right) \quad (4.10)$$

which can then be utilized to calculate the eccentric anomaly of the spacecraft. The eccentric anomaly of the spacecraft can be calculated with the following equation:

$$E_{Mars} = \cos^{-1}\left(\frac{\epsilon + \cos(\theta_{Mars})}{1 + \epsilon \cos(\theta_{Mars})}\right) \quad (4.11)$$

Finally the time of flight between Earth and Mars can be calculated using the following equation:

$$t_{flight} = \sqrt{\frac{a^3}{\mu_s}}(E_{Mars} - \epsilon \sin(E_{Mars})) \quad (4.12)$$

where  $\mu_s$  is the gravitational constant of the sun in  $km^3$  per second squared. It is important to note that in Equation 4.12 that  $E_{Mars}$  should be in radians as opposed to degrees.

### 4.3 Gasdynamic Mirror

Of all the fusion propulsion devices that have been invented, the most studied device is probably the Gasdynamic Mirror first published by Kammash and Lee [56]. The GDM is essentially a simple mirror device that utilizes one of a mirror devices drawbacks in a positive way. Mirror devices operate by confining the plasma between two large ring magnets as shown in Figure 4.4.

The simple mirror magnetic fusion device has been widely studied for use as a power source due to its simplicity but is has not yet achieve a self-sustained fusion

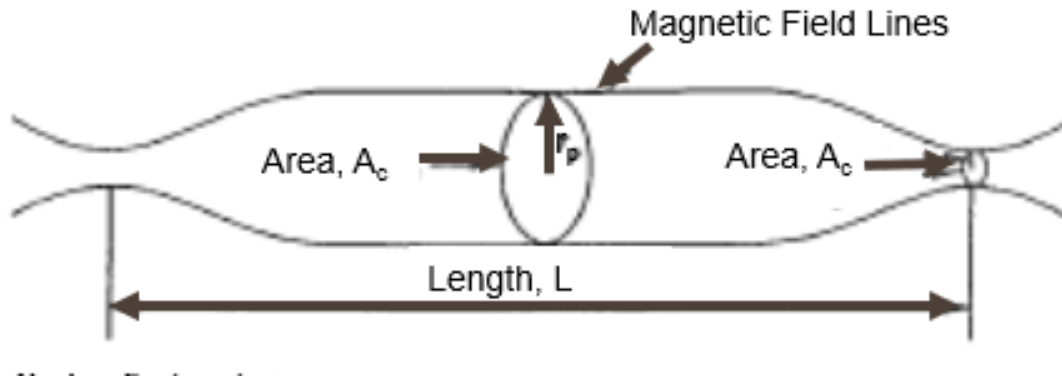


Figure 4.4. Basic schematic of a mirror fusion device [56].

reaction yet. This is in part due to the low  $Q$  value that is achievable due to the significant end losses where particles are lost through the ends of the mirror. Despite this, the magnetic mirror is a steady state reactor in which fusion fuel such as those mentioned in Section 4.1 are constantly ejected into the plasma. This injection process requires a non-trivial amount of power.

For propulsion purposes, the gasdynamic mirror device seeks to capitalize on the shortcomings of the magnetic mirror by using the end losses as a means of propulsion.

### 4.3.1 Physical Basis

As previously stated the GDM seeks to use the end loss of a simple mirror device in a productive fashion by using it as propellant to create thrust. In fact the GDM is designed to mimic a "meridional" nozzle due to it being designed to have a large aspect ratio ( $L \gg r_p$ ) [56]. This is a slightly different derivation of the traditional simple magnetic mirror. In addition, a gasdynamic mirror features a significant increase in plasma density to increase the scattering collisions which will make the end losses more fluid and consistent for its use as a thruster.

The GDM operates by confining the plasma particles between two large ring magnets in an axisymmetric mirror device which features open magnetic field lines. This design confines the particle between two loss boundaries at each one of the magnets where the magnetic fields are strongest. This corresponds to a decrease in electrostatic potential as the plasma gets closer to the magnets where as the peak electrostatic potential occurs in the middle of the device when the magnetic field is weakest inside the device [68]. The plasma confined in the mirror device tends to have a positive potential due to electrons escaping from the system faster than ions initially which then slows the electron losses and increases ion losses until an equilibrium is reached between the two losses [68].

As with the DPF, the GDM is not without instabilities. The GDM suffers from an MHD stability called the flute instability, caused by bad curvature in the magnetic field lines, and a microinstability known as the loss cone instability, caused by depletion of the depletion of particles through the end of the mirror. The flute instability, however, is addressed by mimicking the "meridional" plasma for the aspect ratio [73]. The loss cone can be addressed by reducing the asymmetries in the plasma created by the loss of particles through the end and is accomplished through having a high plasma density [73].

### 4.3.2 Evaluation Methodology

In order to more completely judge the feasibility of a fission powered magnetic fusion thruster, a steady state device needed to be tested alongside the pulsed Dense Plasma Focus. The most studied steady state fusion propulsion system is the Gasdynamic Mirror studied by Kammash et al. [8,55,56,61]. This provided a basis in which a preliminary paper study with some simple updating of results could be performed since an in-house propulsion code for the GDM was not available. The unchanged GDM data from *Performance Optimization of the Gasdynamic Mirror Propulsion System* by Emrich [61] can be found in Table 4.5.

Table 4.5.  
Fusion only powered DT Fueled GDM parameters with  $\eta_{DEC}=0.9$  [61, 62]

Power Parameters		System Masses		Rocket Performance	
$P_f$ , MW	14860	$m_{magnet}$ , Mg	30	Thrust, N	22100
$P_{injector}$ , MW	5064	$m_{radiator}$ , Mg	1077	ISP, s	142200
$P_{brem}$ , MW	317	$m_{injector}$ , Mg	23		
$P_{sync}$ , MW	103	$m_{breeder}$ , Mg	10		
		$m_{shield}$ , Mg	37		
		$m_{cooling}$ , Mg	19		
		$m_{structure}$ , Mg	36		
		$m_{habitat}$ , Mg	65		
		$m_{lander}$ , Mg	60		
		$m_{fuel}$ , Mg	30		

This was accomplished by assuming that updating mass numbers would not affect the performance of the device outside of the thrust to weight ratio. The main mass number to be updated was the capacitor mass as capacitor technology has improved significantly since the original GDM studies. This was accomplished by using the original capacitor specific energy published as 36 kJ per kg and sizing a 1000 MW capacitor bank using this [61]. This number was then subtracted from the the stated fuel cell/capacitor system mass to calculate the fuel cell mass which was held constant for this work. Afterwards the new specific energy of the capacitors of 828 kJ per kilogram, currently achievable energy density with cutting edge technology [13], were used to size the capacitor bank for a 1000 MW pulse and was add to the fuel cell mass to give a new fuel cell/capacitor system mass which will be used for the analysis in this project.

Then by varying the converters utilized with the GDM, additional conclusions on the system mass can be performed. The original work did not include a breakdown of

power generated through the thermal or direct energy converters. The power generated through the direct energy converters was calculated using the method employed above for the DPF device. The thermal energy conversion could not be calculated due to not having an accurate percentage of cyclotron radiation that was placed back into the plasma or other power losses from radiation/equipment as was the case with the DPF. Therefore, it was chosen for the fission powered and fission assisted cases not to include the the thermal energy converter for the mass or fission sizing calculations opting to only use the direct energy converter instead. The input power that will be used for the fission reactor scaling will be the injector power of the reactor. For the fission assisted case, the energy provided by the direct energy conversion case was varied from 10-90% as the it was felt that the stated efficiency of 90% for the direct energy conversion device was optimistic given the TWDEC has a conversion efficiency of 76% [61, 71].

This is a preliminary analysis aimed at demonstrating a proof of concept for the use of a fission powered steady state magnetic confinement propulsion device. Further studies using a GDM propulsion code should follow to further investigate the preliminary analysis made here in a more detailed manner.

## 5. EVALUATION OF FISSION POWERED MAGNETIC FUSION THRUSTERS

### 5.1 Evaluation Overview

To assess the feasibility of a fission powered magnetic fusion thruster three cases will be studied and compared for a steady state Gasdynamic Mirror and a pulsed Dense Plasma Focus:

- **Case 1:** This case will be the base case for comparison. It evaluates the magnetic fusion thrusters as self sustaining power source which generates thrust. This case will also delve into the use of a thermal energy converter, a traveling wave direct energy converter, and the combination of the two in an effort to boost performance.
- **Case 2:** This case will assume that all electric power for the fusion thruster will be generated by a fission reactor. The fission reactor will utilize a thermionic conversion method as described in Section 3.1.2.
- **Case 3:** This case will be used to determine whether a fission powered magnetic fusion thruster can be optimized by using a combination of both the fusion and fission energy produced, however, it will not be presented as a complete optimization.

Case 1 will follow the same methodology as done in previously conducted studies but will be using updated mass numbers based on new technology whereas Case 2 will introduce the concept of the fission reactor being the main power source for the thruster. The thermal efficiency of the turbine was left at 20% from the original

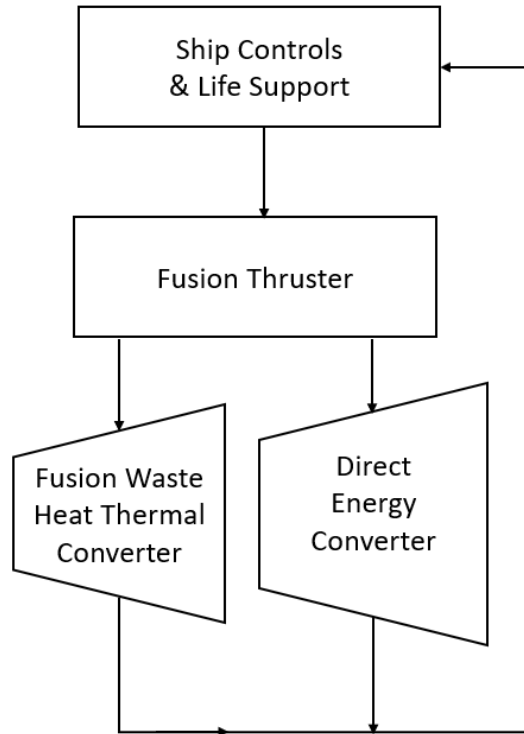


Figure 5.1. Schematic of self-sustaining fusion thruster in which all power generated from the fusion reaction is used for either thrust or recirculated to ship controls and to power the fusion reactor. This case is has not yet been achieved due to not enough power being generated overcome the losses to be self-sustaining.

studies for the DPF as opposed to the 30% features by using a Brayton cycle with the GDM [15,62].

When analyzing Case 3, it became clear that with both direct energy conversion and thermal conversion for the fusion energy that the  $Q$  value was greater than 1 and did not need the fission reactor for the DPF. This could be due in part due to high theoretical conversion efficiency of a travelling wave direct energy converter of 76% [71]. This is perhaps the most likely scenario since fusion reactors have historically struggled to achieve  $Q \geq 1$ . However, with the theory and simulations producing a  $Q$  value greater than 1 for the use of both converters and the direct energy converter alone, Case 3 will use a fission reactor supplying auxiliary power

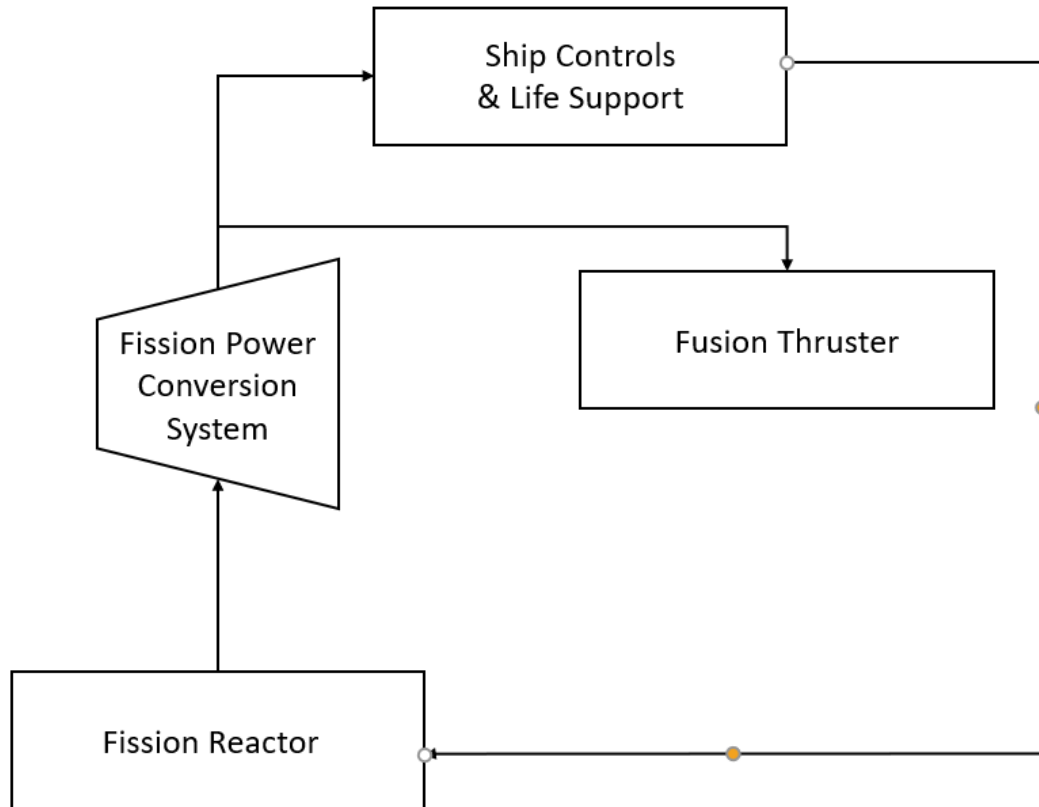


Figure 5.2. Schematic of fission powered fusion thruster.

to supplement that produced by the fusion thermal converter for the DPF. Previous GDM studies cite an efficiency of 90% for the DEC [62]. Hence, for the GDM, the thermal energy converter was neglected for Case 3, and the DEC efficiency was varied from 10%-90%.

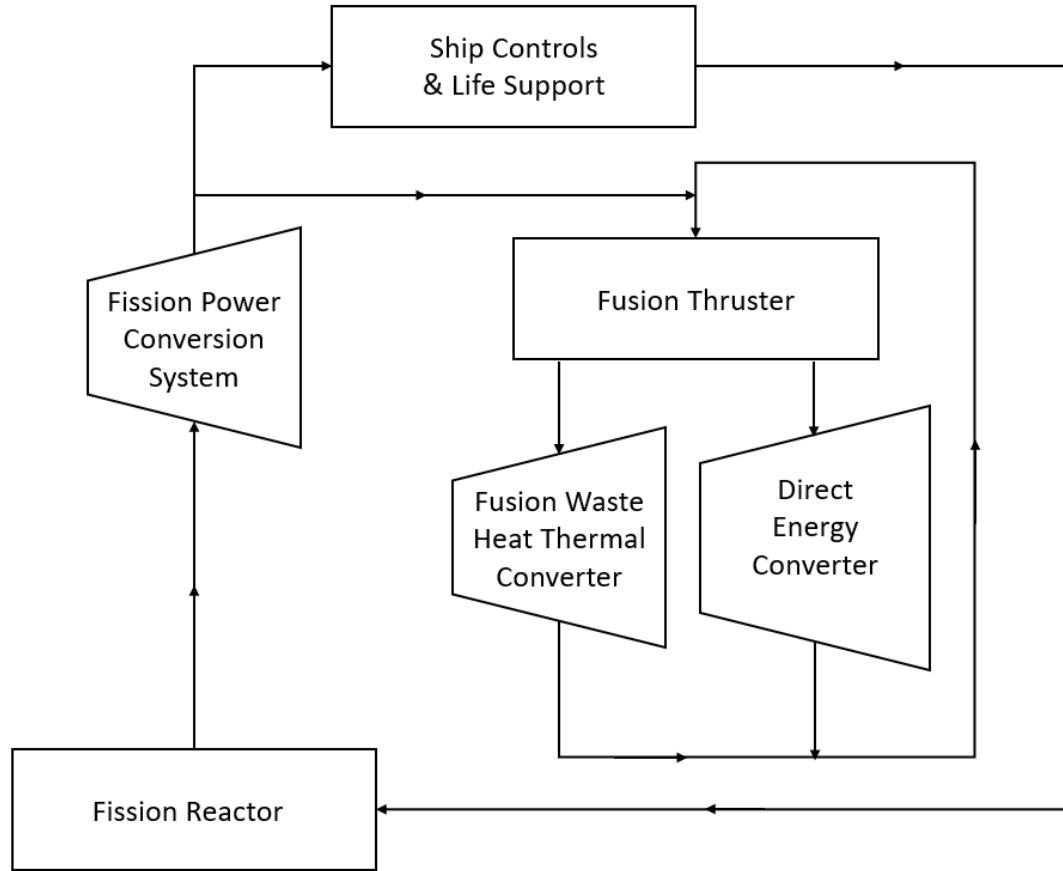


Figure 5.3. Schematic of fission assisted fusion thruster.

## 5.2 Case 1: Self Sustaining Fusion Thruster

As discussed in Section 4.2.2, one of the code updates was to include the capability of utilizing a variety of fusion fuels. The results of the power calculations for these fuels can be seen in Table 5.1. It can be observed that DD and  $p - B^{11}$  fuels are infeasible for use with a DPF. This is due to the low energy from both the DD and  $p - B^{11}$  reactions as well as the extremely high ideal ignition temperature for  $p - B^{11}$ . As can be seen, the two remaining feasible fuel options, DT and  $D - He^3$ , have comparable burn times as well as relatively high charged particle power which can be directly turned into thrust with the use of a magnetic nozzle. Whereas, previous

studies have primarily focused on  $D - He^3$  for DPF devices, this study will include DT as well so it may be compared to the GDM device for the same fuel.

Table 5.1.  
Fuel Evaluation based on DPF Fusion Performance. \*Denotes that charged particle power is less than the power loss.

	DD	DT	$D - He^3$	$p - B^{11}$
DPF Performance-Fusion				
$P_f$ , MW	169.44	5345.91	3381.16	626.41
$P_{charged}$ , MW	0*	1125.96	3295.27	421.33
$P_{brem}$ , MW	43.92	1.21	8.30	5.63
$P_{cyc}$ , MW	446.11	75.97	193.93	328.31
$P_{loss}$ , MW	222.3661	31.20	85.87	136.96
$\dot{m}_{total}$ , $\frac{kg}{s}$	33.21	30.54	31.40	32.63
$t_{burn}$ , sec	9928.40	1896.8	1179.97	2823.30

One of the first tasks of the analysis was establishing a baseline case, which required updates to the previous code with regards to specific energy of the capacitors as technology over approximately the last three decades has led to an increase of three orders of magnitude from 0.2 kJ/kg to 828 kJ/kg. This led to tremendous mass savings of approximately 99% for capacitor mass. Despite this incredible savings, the addition of a power management and distribution device (PMAD) and a direct energy converter reduced the thrust to weight ratio by approximately an order of magnitude from previous studies. As seen in Table 5.2, despite DT having a slightly higher thrust to weight ratio, 0.09, when compared to  $D - He^3$ , 0.06, the trip time for  $D - He^3$  is approximately a day and a half shorter. Figure 5.4 shows that neither DT nor  $D - He^3$  for the fusion power DPF meet the desired mission parameters. A complete sample output of the DPF code can be found in the appendix to supplement the tables found in this chapter.

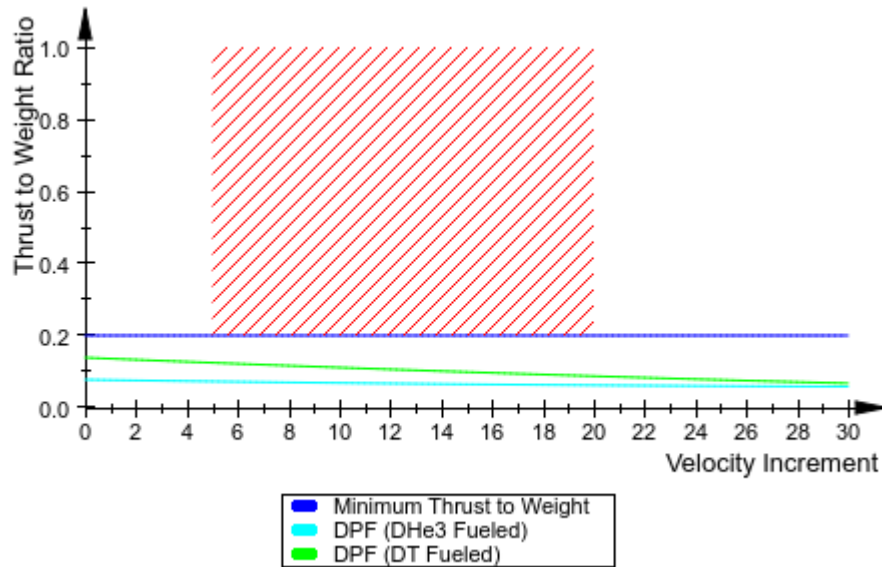


Figure 5.4. Evaluation of Case 1 against the desired Mission Parameters.

One of the shortcomings of previous studies was that it focused primarily on power balance and didn't not go into detail in the electrical circuitry. To better understand the performance of the DPF it was necessary to include a PMAD device which aids in power management and as an associated specific mass of  $1 \text{ kg}/kW_{in}$  [72]. Despite this increase in mass from the PMAD, the decrease in capacitor mass yields a net decrease in mass for the system.

For direct energy conversion, a Travelling Wave Direct Energy Converter was chosen with a specific mass of  $0.14 \text{ kg}/kW_{in}$  which allowed for the weight of the device to be calculated. This is a major improvement in the code as it accounts for converter mass whereas for the turbine, the thermal converter, the mass is assumed to be a portion of the payload. The use of a direct energy converter makes the DPF a more suitable power source as the Q value can be closer to 1 but comes at the steep cost of drastically reducing the thrust to weight ratio to values near or below the threshold for interplanetary travel of 0.2 [15]. Due to the assumption that the direct energy converter mass is a linear relationship to input power, DT appears to perform

better than  $D - He^3$  which is counter what was expected as  $D - He^3$  is the preferred space fuel. If the converter mass was kept constant, then  $D - He^3$  would have the superior thrust to weight ratio.

Table 5.2.

Comparison of fusion powered DPF and GDM. Note the TEC mass for the DPF is assumed to be included in the payload mass of 100 metric tons.

	DPF (DT Fueled)	DPF ( $D - He^3$ Fueled)	GDM (DT Fueled)
System Masses			
$m_{dec}$ , kg	157.63	461.34	$55 * 10^3$
$m_{tec}$ , kg	0*	0*	$53 * 10^3$
$m_{fission}$ , kg	0	0	0
$m_{total}$ , kg	$1.48 * 10^5$	$3.41 * 10^6$	$1.60 * 10^5$
Rocket Performance			
Thrust, N	$1.35 * 10^6$	$2.05 * 10^5$	22100
$\frac{T}{W}$	0.09	0.06	0.0014
$I_{SP}$ , sec	4520.02	6665.60	142200
$t_{flight}$ , days	88.80	87.31	95.15

The GDM analysis uses data published by Emrich [61] with Case 1 only updating the mass of the fuel cell/capacitor system to reflect that of current leading edge technology. This required the assumption the original mass listed to be split into capacitor mass and fuel cell mass, due to the fuel cell being briefly discussed in the original work, the mass of the fuel cells was assumed to be the mass not used in sizing a capacitor bank to produce a 1000MW pulse. In the original study an energy density of 36 kJ/kg was utilized while leading research points to energy densities of 828 kJ/kg resulting in the capacitor mass decreasing from 27.78 Mg to 1.21 Mg. Which meant that the fuel cell was assumed to be the difference between the original stated mass

for the system of 35 Mg and the calculated capacitor mass of 27.78 Mg. Resulting in the fuel cell/capacitor system mass to be reduced from 35 Mg to 8.43 Mg. This small change boosted the thrust to weight ratio to 0.0014 as seen in Table 5.2.

It is particularly notable that despite the high specific impulse values achieved with the GDM, the thrust and thrust to weight ratios are incredibly low and do not meet the 0.2 threshold for interplanetary travel. There have been several previous studies on thrust augmentation for the GDM to increase these values, however, these studies were not included in this analysis due to lack of component specific masses which could be manipulated to perform this analysis. Therefore, it is possible that the GDM could potentially have an increased performance of thrust to weight ratio by utilizing the radiation power to heat hydrogen propellant similar to that of the DPF or by increasing plasma density [63].

### 5.3 Case 2: Fission Powered Fusion Thruster

As previously discussed, Case 2 will only utilize fission reactors for the electric power generation in order to power the ship and the fusion thruster. It was assumed that the thermal and direct energy converters could be removed from both the DPF and GDM. This was done in an effort to reduce mass to offset the additional mass from the fission power system. The removal of the thermal conversion system, however, may not be feasible as the waste heat still needs to be dissipated. In theory, this could potentially be accomplished using radiators but that was not investigated as part of this project. For the DPF, the fission reactor needed to provide approximately 80 MW of power to operate the DPF while the GDM required enough power to operate the injectors at a power of 5064 MW. It should also be noted that while a PMAD had to be added for the fusion only case, it corresponds to 0 kg, for the fission case due to its inclusion in the specific mass parameters from Table 3.1. Therefore any mass from the PMAD is scaled with and included in the fission reactor mass,  $m_{fission}$ .

Table 5.3.  
Comparison of fission powered DPF and GDM

	DPF (DT Fueled)	DPF ( $D - He^3$ Fueled)	GDM (DT Fueled)
System Masses			
$m_{dec}$ , kg	0	0	0
$m_{tec}$ , kg	0	0	0
$m_{fission}$ , kg	268085.92	268085.92	5070000
$m_{total}$ , kg	$6.17 * 10^5$	$5.29 * 10^5$	$6.57 * 10^6$
Rocket Performance			
Thrust, N	$1.35 * 10^6$	$2.05 * 10^6$	22100
$\frac{T}{W}$	0.22	0.40	$3.4313 * 10^{-4}$
$I_{SP}$ , sec	4520.02	6665.60	142200
$t_{flight}$ , days	89.26	88.32	199.50

Table 5.3 demonstrates that the introduction of a fission reactor for power generation increases the thrust to weight ratios for both DPF configurations while decreasing it for the GDM. The DPF now operates within the desired mission parameters over the entire range of  $\Delta V$ s as observed in Figure 5.5. It is important to note that while both fuel configurations meet the necessary requirements, the higher thrust to weight values achievable to by the  $D - He^3$  fueled DPF provides more mission flexibility. This allows for an increase in payload mass for similar performance to DT while still remaining within the desired parameters as well as features a reduced trip time for  $D - He^3$  as seen in Table 5.3. However, the introduction of the fission reactor for the GDM has the opposite effect as it greatly reduced the thrust to weight ratio as well as lengthening the time of flight to more than double that of the DPF.

For the Case 2 study of the GDM, power required to be supplied by the fission reactor was the injector power. It should be noted that compared to the initial power

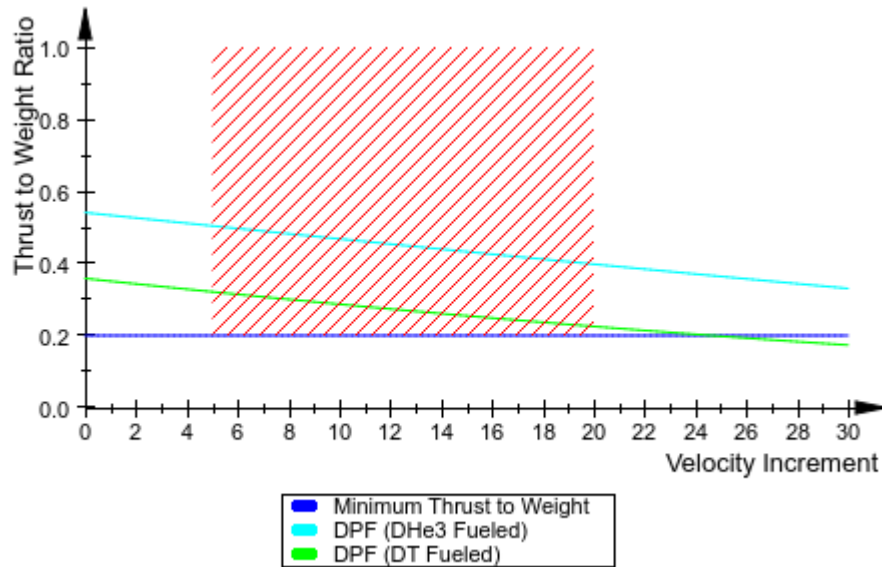


Figure 5.5. Evaluation of Case 2 against the desired mission parameters From *Fission Reactor Options and Scaling for Powering Magnetic Fusion Thrusters for a Manned Mars Mission* [24] by Stockett et al.; reprinted by permission of the American Institute of Aeronautics and Astronautics, Inc

requirement of the DPF of approximately 80 MW, the GDM has a far greater power requirement and operates at steady state. This large increase in power requirement even for low specific masses such as thermionic systems, the mass of the fission reactor as seen in Table 5.3 is quite substantial and larger than the rest of the system combined. Due to this, the thrust to weight ratio drops significantly as a function of specific mass similar to that of the DPF. The major difference between the DPF and the GDM is that while they suffer decreases in thrust to weight ratios as specific mass increases, the DPF is still capable of achieving above the 0.2 threshold. The thrust to weight of the GDM was significantly below that threshold only to be further lowered when adding a fission reactor to provide power. These low thrust to weight ratios coupled with the large masses make this design infeasible from both the financial in terms of launching that much mass would be very expensive, and performance perspectives.

### 5.4 Case 3: Fission assisted Fusion Thruster

The final case for the DPF will seek to utilize the thermal energy conversion turbine as well as a fission reactor to provide the necessary power and improve rocket performance. This will provide insight into whether or not a fission assisted DPF system can be optimized to yield better performance than either the fission only case or the fusion only case. As shown in Table 5.4, the thrust to weight ratios and time of flights are slightly lower than that of the fission only case. It is also noteworthy that while the thrust to weight ratio increased for the GDM from the fission only case, it still does not reach the desired 0.2 threshold.

Table 5.4.  
Comparison of fission assisted DPF and GDM (with  $\eta_{DEC} = 0.5$ ).

	DPF (DT Fueled)	DPF ( $D - He^3$ Fueled)	GDM (DT Fueled)
System Masses			
$m_{dec}$ , kg	157.63	461.34	$55 * 10^3$
$m_{tec}$ , kg	0*	0*	$53 * 10^3$
$m_{fission}$ , kg	0	0	1250000
$m_{total}$ , kg	$7.28 * 10^5$	$6.21 * 10^5$	$2.80 * 10^6$
Rocket Performance			
Thrust, N	$1.35 * 10^6$	$2.05 * 10^6$	22100
$\frac{T}{W}$	0.19	0.34	$6.3131 * 10^{-4}$
$I_{SP}$ , sec	4520.02	6665.60	142200
$t_{flight}$ , days	89.14	88.15	100.76

For the analysis of the fission assisted GDM, it was assumed that no energy was provided from the thermal energy conversion system and that mass was removed. This analysis only considered the power produced by the direct energy converter which in the original work had an efficiency of 90% but did not specify the type of direct

energy converter. For comparison, the Travelling Wave Direct Energy Converter has an efficiency of 70%. Since direct energy converters can have a wide range of efficiencies, the effect of varying on the thrust to weight ratio were of interest as this will change the necessary weight of the fission reactor as now the required power is the difference between the injector power and the power generated from the direct energy converter. The charged particle power was calculated using the method discussed in Section 4.2.2 while the values from the original work were used to make an assumption on the specific mass of the direct energy converter which would then be used for scaling based on charged particle power in.

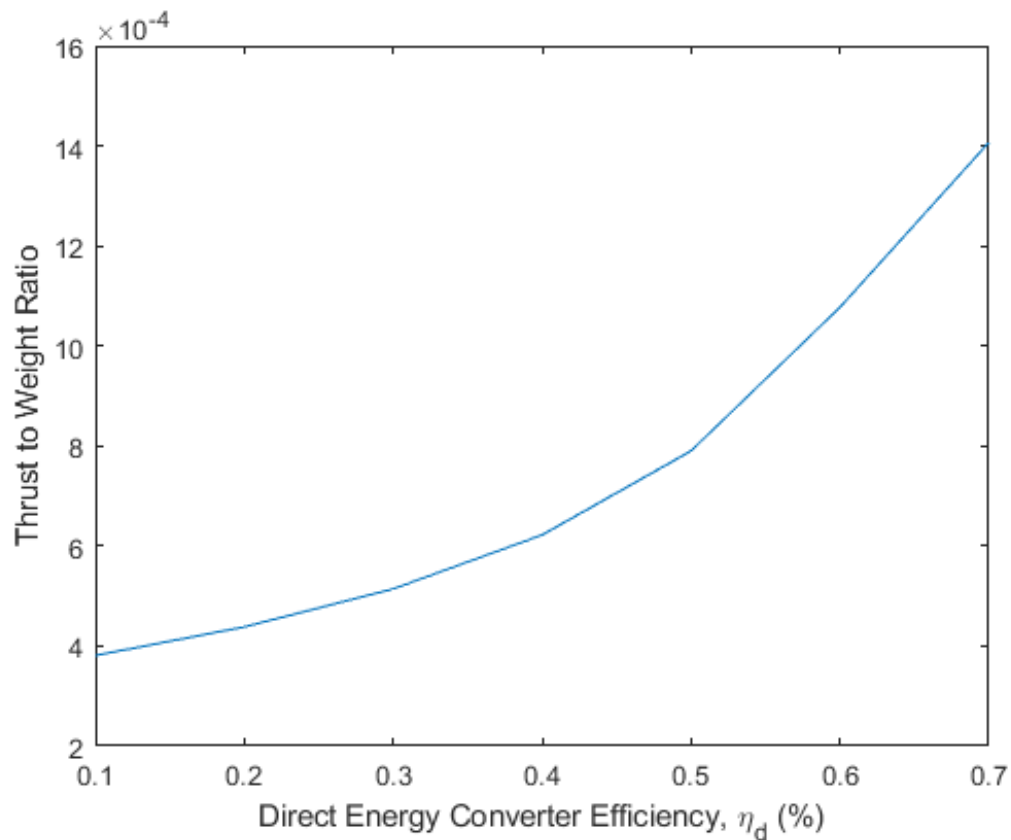


Figure 5.6. Effect of DEC efficiency on thrust to weight ratio for a fission assisted DPF.

As can be seen from Figure 5.6, the thrust to weight ratio does not show significant change for conversion efficiencies between 10-50%. After this 50% threshold the conversion efficiencies contribute enough power to the injector power need that the fission reactor does not need to supply nearly as much and therefore requires a smaller mass. This smaller mass helps to significantly boost the thrust to weight ratios. For a conversion efficiencies of 70% there was no fission mass as the converted charged particle power was greater than the requisite injector power. At 70% efficiency it can be seen that the fission assisted GDM begins to approach the thrust to weight value of 0.0015 from Case 1, the fusion powered GDM. However, despite approaching the thrust to weight ratio achieved by the fusion powered GDM, not using the thermal energy converter may not be feasible due to heat removal constraints or would require large and heavy radiators which would in turn lower the thrust to weight ratios to below the fusion only levels from Case 1. If that were the case, then both Case 2 and the current case would both under perform the original concept of a self-sustaining GDM. This will require more work to be conducted in order to achieve the  $Q \geq 1$  requirement of a self-sustaining device since a fission assisted device appears infeasible as initially predicted by Kammash et al. [51].

Unlike Case 2, where both DT and  $D - He^3$  fuels were viable candidates for the complete range of  $\Delta V$ s, Figure 5.4 reveals that the DT Fueled DPF does not meet the minimum thrust to weight threshold for  $\Delta V$ s greater than approximately 18 km/s. This is significant in that it generally has a lower thrust to weight ratio which restricts the overall mission flexibility as a small increase in mass could potentially cause the thrust to weight ratio to drop below the minimum threshold.

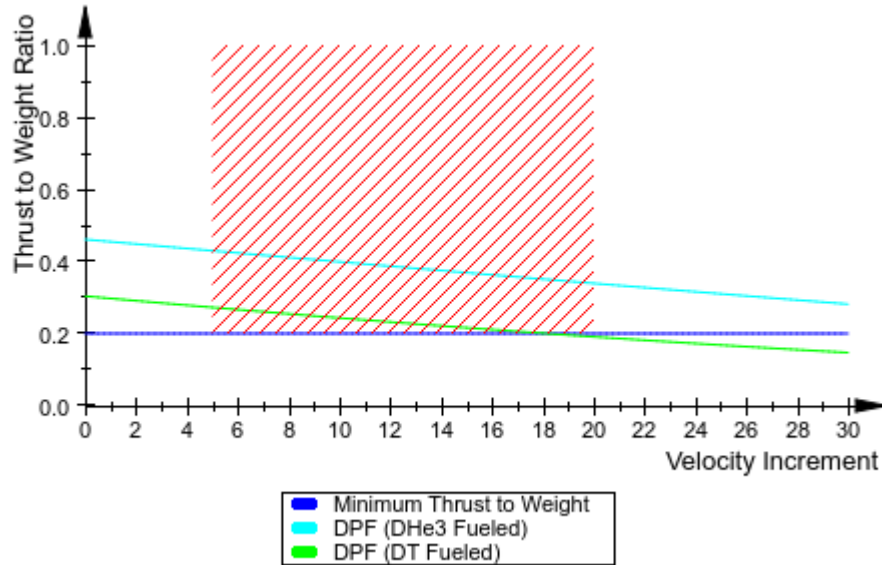


Figure 5.7. Evaluation of Case 3 against the desired Mission Parameters From *Fission Reactor Options and Scaling for Powering Magnetic Fusion Thrusters for a Manned Mars Mission* [24] by Stockett et al.; reprinted by permission of the American Institute of Aeronautics and Astronautics, Inc

## 5.5 Comparison of Propulsion Power Systems

As cases 1,2, and 3 were evaluated it became clear that the GDM device did not meet the minimum thrust to weight ratio threshold of 0.2 regardless of configuration. This can be seen in Table 5.5 where the GDM is outperformed in every category except specific impulse by the DPF. It also became clear when analyzing Table 5.5 that  $D - He^3$  consistently outperforms DT as a fuel for the DPF with the one exception being the DT fueled fusion powered DPF has a slightly higher thrust to weight value than the  $D - He^3$  version. This is due to the increased mass of the included direct energy converter. It is worth noting that while the DPF needs a direct energy converter to operate as self sustaining that its addition has reduced the thrust to weight ratio of the device below the 0.2 threshold when compared to values from previous work [15,65]. This addition renders the fusion only case to be the worst case for the DPF while

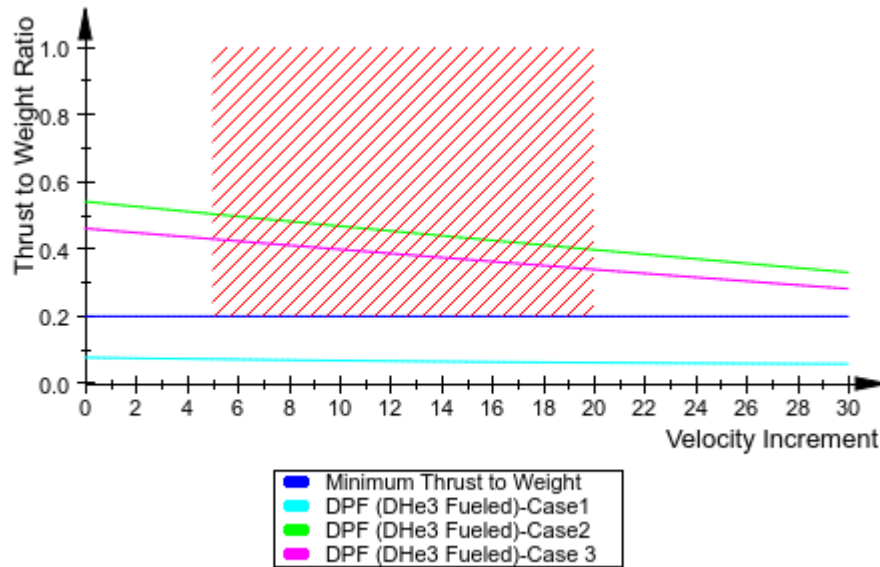


Figure 5.8. Comparison of all three cases for  $DHe^3$  fueled DPF against the desired Mission Parameters.

it was the optimum case for the GDM due to its steady state and enormous power requirement natures.

On the other hand, the optimum case of the DPF occurs with the fission powered DPF. This is largely due to lack of mass from the fusion energy converters, however, as previously discussed it may not be the most realistic scenario to completely remove the thermal electric converters which convert the waste heat. While this will reduce the thrust to weight ratios some, case 3 demonstrates that this would only be a marginal decrease and not severely impact rocket performance. The main effect it would have would be eliminating the use of DT fuel at higher  $\Delta V$  which would most likely not be considered in favor of  $D - He^3$  for the increased thrust to weight ratio anyways. As shown in Figure 5.8, the fusion case fails to meet the desired mission parameters while both fission powered and fission assisted cases achieve the desired thrust to weight ratio for the entire range of  $\Delta V$ 's for the  $D - He^3$  fuel.

Table 5.5.  
Summary of Results

	$m_{total}$ , kg	Thrust, N	$\frac{T}{W}$	$I_{SP}$ , sec	$t_{flight}$ , days
Case 1: Fusion Powered					
DPF (DT Fueled)	$1.48 * 10^5$	$1.35 * 10^6$	0.09	4520.02	88.80
DPF ( $D - He^3$ )	$3.41 * 10^6$	$2.05 * 10^6$	0.06	6665.60	87.31
GDM (DT Fueled)	$1.60 * 10^6$	22100	0.0014	102800	95.15
Case 2: Fission Powered					
DPF (DT Fueled)	$6.17 * 10^5$	$1.35 * 10^6$	0.22	4520.02	89.26
DPF ( $D - He^3$ )	$5.29 * 10^5$	$2.05 * 10^6$	0.40	6665.60	88.32
GDM (DT Fueled)	$6.57 * 10^6$	22100	$3.43 * 10^{-4}$	102800	199.50
Case 3: Fission Assisted					
DPF (DT Fueled)	$7.28 * 10^5$	$1.35 * 10^6$	0.19	4520.02	89.14
DPF ( $D - He^3$ )	$6.21 * 10^5$	$2.05 * 10^6$	0.34	6665.60	88.15
GDM (DT Fueled)	$2.80 * 10^6$	22100	$6.31 * 10^{-4}$	102800	100.76

## 6. NON-PERFORMANCE DESIGN CONSIDERATIONS

### 6.1 International Legal Considerations

Following the accidental reentries of two Soviet nuclear powered satellites, COSMOS 954 and COSMOS 1402 [30], the United Nations published the non-binding agreement, "Principles Relevant to the Use of Nuclear Power Sources in Outer Space". These principles define safety protocols specifically for spaceborne fission nuclear power sources based off the methods already in place by the United States and Soviet Union at the time. However, as previously mentioned this a non-binding agreement between member states and the UN and as such does not carry as much weight or restrictions to it as a formal treaty would. These principles will be discussed further in Section 6.3 as they directly relate the safety of the design. It is interesting to note that the only two nuclear power sources currently included in these principles are fission reactors and RTGs and does not include fusion reactors.

Contrary to the non-binding nature of the previously mention principles, the Treaty on the Non-Proliferation of Nuclear Weapons is a legally binding document which violation of could lead to international sanctions and other repercussions. This treaty dictates how nuclear material must be used and accounted for, for non military purposes, in an effort to prevent the spread of nuclear weapon technology. This treaty; however, is primarily used when addressing terrestrial nuclear power sources and material. The ramifications, challenges and potential solutions to non-proliferation in space will be addressed in Section 6.2.

## 6.2 Non-Proliferation Considerations

The use of nuclear power sources for terrestrial applications was primarily established through the signing of the Treaty on the Nonproliferation of Nuclear Weapons. This led to the establishment of the International Atomic Energy Agency (IAEA) which was charged with monitoring the use of special nuclear material (SNM) and drawing conclusions on whether or not all the material being used was declared and that it was being used for peaceful purposes. This is accomplished through individual agreements with the the individual states. It should be noted that "The Principles Relevant to the Use of Nuclear Power Sources in Outer Space" dictates that the two nuclear power sources to be used are fission reactors fueled with highly enriched Uranium, weapons grade SNM, and radioisotope thermal generators which depending on fuel also can contain SNM [74].

### 6.2.1 Current Status of Safeguards in Space

Despite the use of nuclear power sources in space dating back over half a century, the issue of nonproliferation in space has not previously been investigated. Instead it has been briefly mentioned in a few studies as something that should be considered but not something that would potentially mark an end to its usage [75]. Currently, any accountability of spaceborne SNM is handled by simply marking it as expended in space in the state's inventory log [76]. This has allowed for the United States and Russia, the only two countries to launch SNM in space, to simply boost any reactors to storage orbits after shutdown where they will presumably remain for hundreds of years [30].

This is a newer development in the technology for two reasons. The first being that for a long time, the only two states with easy access to space were the United States and Russia. Two countries that are Nuclear Weapon States (NWS) which by definition cannot proliferate to one another which partially explains why proliferation concerns were not raised earlier in the technology development. Access to space

has not only become possible for other NWS but also Non-Nuclear Weapon States (NNWS) and even private companies such as SpaceX. The second being that as space technology continues to develop it becomes increasingly likely that material sent up in space can no longer be assumed to be expended and irrecoverable which effectively ends the safeguards of that material [77].

### **6.2.2 The Need for a New Approach to Safeguards in Space**

As the Soviets stated in the early 1980's, as access to space increased the amount of orbital debris will increase and potentially jeopardize the future of space missions [78]. This issue was partially addressed by a non-binding agreement through the United Nations but still continues to worsen and will inevitably require clean up either by private companies seeking to improve safety for their own access to space or by government seeking the same [78]. Besides just the improvement of technology allowing spaceborne objects to be recoverable, active debris cleanup poses a threat to the current method of storing defunct nuclear reactors in space.

Then it is important to understand the distinction in what the IAEA is tasked with. The IAEA is tasked with drawing a safeguards conclusion meaning that with a reasonable level of confidence the IAEA inspector feels that all material that is declared is where it is supposed to be, being used for the correct purposes and not diverted for non-peaceful uses. This is crucial in understanding the inspection process. A major aspect of the current process is a physical inspection of any and all civilian facilities that use SNM. Obviously, while the technology exists for in person inspections in space, this is extremely cost and time prohibitive for the IAEA. Therefore new methods must be developed to monitor the material in lieu of physical inspections. Currently the IAEA utilizes a variety of methods that fall into two main categories to monitor the material in between inspections: Containment and surveillance (C/S) and Unattached and Remote Monitoring (UNARM). Modern C/S methods consist of electronic seals, alarms, and cameras which provide data to the

IAEA and are checked by the inspector during physical inspection; however, mission constraints must be taken into account. If mission constraints such as mass, power usage, and bandwidth are not taken into account the burden of nonproliferation practices on nuclear power sources in space could mark an end to their uses which would essentially stall human space exploration and greatly limited the desitnations humans can safely explore in space.

### **6.2.3 Proposed Solution**

As previously stated, the issue of nonproliferation in space is changing more rapidly than the policies set to govern them through the NPT and the state agreements with the IAEA. Stockett and Bean recently proposed a two pronged conceptual solution to the issue of nonproliferation of SNM in spaceborne nuclear systems [79]. The first approach is a proactive design approach by evaluating each potential space reactor against the Proliferation Resistance and Physical Protection (PRPP) that was established for Gen IV reactors [79]. The second is to utilized Continuity of Knowledge (CoK) as one of the primary methods of drawing safeguards conclusions [79].

Due to the uniqueness of each space missions, many components are build specifically for those missions and the power source could easily be seen as one of them even if it is a scaled version of a previously demonstrated power source. With minor modifications made to the PRPP methodology to take into account the nature of the power source being used in space as opposed to terrestrial applications, a suitable and established evaluation method would be created. This evaluation method could then be applied to spaceborne systems to determine whether or not they meet the proliferation resistance standards deemed necessary for a spaceborne nuclear power source.

Continuity of Knowledge is defined by Blair et al. to be "A system of data or information regarding an item that is uninterrupted and authentic and provides the IAEA with adequate insight to draw definitive conclusions that nuclear material is

not being diverted from peaceful purposes” [80]. C/S and UNARM measurements in between inspections are already used along with the initial physical inspection to obtain and maintain a continuity of knowledge that the material is still where and in the same state it was said to be in at the time of physical inspection. As the number of facilities continues to grow the resources of the IAEA will become strained, resulting in the need to more heavily rely on CoK [81]. This is particularly applicable to space as humanity continues to explore and expand through space undoubtedly through the use of nuclear space systems.

This proposed solution aims to not only satisfy the need for accountability in space but also addresses issues such as latency and component failure. For any space mission there are periods of latency between when a signal is initiated and when it is received which can vary from 3 to 22 minutes between Earth and Mars. The latency issue is addressed by through utilization of the Nyquist frequency, which is the optimal rate at which material must be checked to maintain CoK [82]. This means that latency would only become important if it was longer than the Nyquist frequency. Then by designing the power source to meet the Gen IV PPRP requirements and utilizing C/S and UNARM to maintain CoK, it is reasonable to conclude that the failure of one component would not reset the confidence of the system to zero as was discussed by Bean et al. [82]. This conclusion is currently counter to the stance of the IAEA that maintains that if one component fails then the confidence level is reduced to zero and would need to be reestablished which could be potentially difficult to do in space not to mention cost prohibitive.

### **6.3 Safety Considerations-Radiological and Environmental**

The safety of nuclear systems needs to be a paramount part of the design process. As previously discussed in Section 2.2 radiation levels dictate how long an astronaut can safely stay in space. These limits range from approximately 300-500 days depending on multiple factors including gender, age, health history and the model

used. Therefore it is absolute necessity for a manned Mars mission to be capable of round trip transit faster than the maximum number of predicted safe days to ensure a healthy return of the crew. This has been demonstrated to be achievable with either a GDM or DPF device as shown by the current work.

Along with trip time, several other methods can be employed to assist in lowering the radiation dose to astronauts and crew, but come at a steep cost both financially and to the system mass which is a non-trivial issue [21]. Passive safety systems such as normal radiation shielding uses light weight materials can be used as shield around the hull of the spacecraft while active shielding such as the use of magnetic and electric fields can be employed to deflect some of the radiation [21]. By deflecting some or even all of the radiation the number of safe days in space can be increased which while desirable also increases the system mass which could make the system infeasible; however, this warrants further study to fully investigate the effects on system mass of adding a shield around the outside of the hull, using active shielding or a combination of the two methods.

The above mentioned methods of faster trip times and shielding are crucial in ensuring the safety of the crew but the safety of those not on board the ship as well as the safety of the environment also needs to be taken into account. Fortunately for fission reactors, these factors were previously taken into account in the "Principles Relevant to the Use of Nuclear Power Sources in Outer Space" which state the following from Principle 3 [74]:

"2. (b) The sufficiently high orbit is one in which the orbital lifetime is long enough to allow for sufficient decay of the fission products to approximately the activity of the actinides. The sufficiently high orbit must be such that the risks to existing and future outer space missions are kept to a minimum. The necessity for the parts of a destroyed reactor also to attain the required decay time before re-entering the Earth's atmosphere shall be considered in determining the sufficiently high orbit altitude."

2. (d) Nuclear reactors shall not be made critical before they have reached their operating orbit or interplanetary trajectory.
2. (e) The design and construction of the nuclear reactor shall ensure that it can not become critical before reaching the operating orbit during all possible events, including rocket explosion, re-entry, impact on ground or water, submersion in water or water intruding into the core.
2. (f) In order to reduce significantly the possibility of failures in satellites with nuclear reactors on board during operations in an orbit with a lifetime less than in the sufficiently high orbit (including operations for transfer into the sufficiently high orbit), there shall be a highly reliable operational system to ensure an effective and controlled disposal of the reactor.”

where Sections 2. (b) and 2. (f) are based on similar safety protocols that were developed independently in the United States and Soviet Unions that included mechanisms to prevent the accidental reentry of a critical system. The first was if an abnormality was detected or the mission was ended, the reactor would boost to a higher orbit where SNM it would be allowed to sufficiently decay [30]. The second safety mechanism only occurred if the system failed to boost in which case the core could be ejected from the system into space such that it would reenter separately from the system [30]. The goal of doing so was to allow the fuel to burn up in atmosphere and disperse the radiation such that there was less than a 0.5 rem dose from the fallout in the first year [30].

Sections 2. (d) and 2. (e) both dictate how the power sources must be transported into orbit which would limited a design such as the current one from being used as a liftoff engine if it wasn't already deemed infeasible for that purpose due to its thrust to weight ratio. This is still necessary for discussion as it impacts how fuel will be transported to and from the orbiters when refueling is necessary and how the reactor itself will be transported to orbit.

While RTGs were not considered due to their low power output, it is reasonable to assume that the safety principles surrounding RTGs would be relevant to nuclear batteries of which one is considered in the current work. Principle 3 states the following with regard to the use of RTGs in space [74]:

”3. (a) Radioisotope generators may be used for interplanetary missions and other missions leaving the gravity field of the Earth. They may also be used in Earth orbit if, after conclusion of the operational part of their mission, they are stored in a high orbit. In any case ultimate disposal is necessary.

3. (b) Radioisotope generators shall be protected by a containment system that is designed and constructed to withstand the heat and aerodynamic forces of re-entry in the upper atmosphere under foreseeable orbital conditions, including highly elliptical or hyperbolic orbits where relevant. Upon impact, the containment system and the physical form of the isotope shall ensure that no radioactive material is scattered into the environment so that the impact area can be completely cleared of radioactivity by a recovery operation.”

which follows a similar design of the safety protocols for fission reactors in that after operation, these devices must be boosted to a storage orbit for decay. The main difference between the RTGs and fission reactors can be seen in Section 3. (b) in that as opposed to safety protocols for fission reactors which eject the reactor if necessary to ensure burn up in atmosphere and widespread of the radiation which results in lower doses. RTGs on the other hand must be design to stay intact and not leak radiation if it were to reentry. This is a non-trivial challenge as it requires RTGs to withstand a wide array of forces and environments. It is likely the use of a nuclear battery would be subject to these same constraints in order to effectively protect the environment.

## 7. CONCLUSION

### 7.1 Conclusions

Fusion propulsion has been demonstrated to be the ideal propulsion concept for manned interplanetary travel such as a manned Mars mission. This is due to its superior thrust and specific impulse values when compared to other propulsion methods. Despite the advantages of having such great rocket performance, fusion propulsion is not without its drawbacks. The first disadvantage as observed with regards to the Gasdynamic Mirror propulsion system is the massive size of these systems with proportional masses meaning the thrust to weight ratio is relatively low. If the thrust to weight ratio is below 1 than the rocket engine cannot lift off meaning that the only use of it would be for an orbiter such as the one proposed by Buzz Aldrin [83] where it could stay in space and simply travel from orbit to orbit where another ship would transport humans to and from the respective planet. While the second and third disadvantages are both related to the system power, fusion reactors require an immense amount of power to operate regardless of whether the device is pulsed or steady state (but requires even more power if the device is steady state). Unlike chemical rockets where the only energy needed is at ignition and then it burns, fusion rockets need to first generate the plasma for the fusion reaction. The issue of large input power is an issue that has been plaguing fusion from the beginning and is the reason for the third disadvantage which is that a self-sustaining fusion device has yet to be achieved.

Due to these reasons little experimental work has been done as that has previously been seen as a major obstacle to achieving fusion propulsion, resulting in much of the work done being theoretical or simulations like the current work. However, this could change to more experimental work being performed if there was a clear path forward for fusion propulsion as a near term solution as opposed to a theoretical concept for

use in the future. In order for the development of a near term solution, the issue of  $Q$  being less than 1 needs addressed through either self sustaining technology or through the use of an auxiliary power source as investigated the by the current work. The current work investigated three cases for fusion propulsion including the theoretical self sustaining fusion reaction, a fission powered magnetic fusion thruster, and a fission assisted magnetic fusion thruster for a pulsed device, the DPF, and a steady state device, the GDM.

The preliminary paper study of the GDM revealed decreased rocket engine performance for both fission powered and fission assisted GDM systems. This was due to two mainly two reasons. The first being the large mass and moderate thrust of the GDM design already yielded a low thrust to weight ratio that adding a massive fission reactor reduced the thrust to weight ratio even lower. The second is the size of the reactor or number of reactors needed to power the GDM. The GDM requires an injector power greater than many modern commercial fission power plants ( $P_{injector} > 5000MW$ ). These two reasons make the design a fission assisted GDM infeasible for a manned mission to Mars. It is likely that due to the high input power required, that other steady state fusion propulsion devices will arrive at the same conclusion.

A more thorough analysis of the DPF was conducted using an in-house propulsion code that revealed at the designs of a fission powered and fission assisted DPF are feasible designs for a very near term Mars mission. Like the GDM, the fission powered and fission assisted designs did see decreased performance, this performance was still able to meet both the desired thrust to weight ratio and travel time from Earth to Mars. This was possible with both DT and  $D - He^3$  fuels achieving thrust to weight ratios of approximately 0.2-0.5 and trip times of approximately 88-90 days depending on the configuration utilized. These trip times are significantly faster than current proposed chemical methods and are far enough below the the recommended safe days in space that a round trip mission with a stay on Mars is possible. This demonstrates that this design is possible with with current or near term technology and should

actively be considered for inclusion and use for a manned Mars mission in the very near term. It is reasonable that other pulsed fusion propulsion systems would reach the same conclusion given the lower input power than the steady state devices.

As previously discussed, the use of nuclear power sources in space is not without constraints due to international laws and agreements. Most importantly of which is the non-proliferation treaty which as previously discussed needs revisiting as the assumptions made surrounding nuclear material in space begin to become invalid. However, it is believed that non-proliferation concerns can be mitigated enough through design and other means, such as the proposed solution by Stockett and Bean [79] that it will not end the use/advancement of nuclear power sources in space [75].

The current work does not support the concept of a fission powered or fission assisted GDM due to the extra weight and size of the reactor adding an infeasible amount of weight to the design. The concept of a fission assisted or even fission assisted DPF device has been shown in the current work to be a feasible concept for a very near term solution for a manned Mars mission. The achievable thrust to weight ratios, similar to that of the GDM, are below one which means that these devices would not be capable of liftoff from the planets but would make ideal propulsion systems for an orbiter as previously discussed.

## 7.2 Future Work

This project has proven that not only is the concept of fission powered magnetic fusion thrusters possible but also achievable in the near term and warrants future work. The following areas have been identified as areas which will require future work to further develop the concept:

- Power Conversion System, specifically for systems larger than  $10MW_e$
- Coupling a DPF with a direct energy converter
- Capacitor Charging and Discharging

- CFD and Ground Testing of the Fusion Thruster
- Continuity of Knowledge and Nonproliferation Policies Specific to SNM in Space.

Despite being one of the most heavily researched topics as of late for nuclear power sources in space, there is still much work needed to be done for power conversion research. Ideally the specific mass of the power source would be below  $1 kW_e$  per kilogram which is not currently achievable. As previously discussed as the power level increases the specific power regardless of power conversion method. The second aspect of the power conversion method research is the safety of these systems at high power levels in a space environment. Recent developments in thermionic nuclear batteries have shown that it may be possible to obtain low specific mass using a static system [21]. However, if instead a dynamic system is chosen, extra precautions must be taken in regards to utilizing passive safety systems to ensure safe operation of the reactor as well as guaranteed power to the ship. Precautions such as those previously discussed involving multiple energy conversion systems ensure that the crew always has power for the ship. This is critical on manned missions due to the length of the missions and no where close to evacuate or seek refuge/assistance. Secondly, for the fusion system, the power conversion associated with thermal energy should be more thoroughly investigated to fully include the mass of the turbine/conversion system to obtain a more complete understanding of the system masses and rocket performance.

Very little work has been done to assess feasibility and performance of a DPF coupled with a direct energy converter. This is vital for future development of the concept as while it is unlikely its inclusion would raise the  $Q > 1$  which would be the ideal case as self sustaining devices have increased and more desirable performance than fission assisted, the inclusion of a direct energy converter would mean a smaller fission reactor and lower mass required.

One of the major assumptions of this work is that it assumes the capacitors utilized for their higher specific energies can be charged and discharged at the necessary

frequency. The current work does not account for the need for a power supply to supply high current power to the capacitors in order to achieve fast charge times. For a steady state design such as a self sustaining gasdynamic mirror and a fission power fusion thruster, the constant power eases some of the charging concerns as the power is readily available although may need to be increased to achieve certain capacitor charging times. For a pulsed device such as a Dense Plasma Focus, the charging of the capacitors is a major concern. As the DPF pulse would need to be fast enough and generate enough energy to sufficiently charge the capacitors before the next pulse is needed fractions of a second later. This was briefly investigated but ultimately fell outside the scope of this project due to its complexity and therefore should be the focus of future studies.

Particularly with the Dense Plasma Focus, the development and use of computational fluid dynamic (CFD) models could prove a cost efficient way to gain a more complete understanding of the physics involved as was done with the gasdynamic mirror. Studies like these can reveal the effect of instabilities in the plasma device which can be varied with experimental work. In addition to the physics of the pinch, it would also be beneficial to study the effects on the pinch of the excess hydrogen propellant used and their interactions with each other. Then as the KRUSTY and DUFF experiments have shown, it is possible to perform rapid prototyping of nuclear systems for demonstration purposes. Before a system is placed into space, ground testing needs to be conducted on each individual system and in this case due to the critical nature of the system should be conducted for an electrically coupled fission system.

Finally, as previously discussed as more nuclear power sources are used in space, the more necessary it becomes to revisit the current safeguards structure. In order to use Continuity of Knowledge as one of the primary mechanisms from which to draw conclusions more research into the concept and how confidence of the system is affected by component failure. In addition to further research needed for CoK, preliminary analysis of current nuclear power source designs in space should be eval-

uated against the PRPP methodology to determine what modifications to it need to be made for spaceborne systems.

## REFERENCES

## REFERENCES

- [1] Rocketdyne Propulsion and Power. Space shuttle main engine orientation.
- [2] *SpaceX Falcon 9 Data Sheet*. Office of Safety and Mission Assurance-NASA, May 2017.
- [3] W Robbins. An historical perspective of the nerva nuclear rocket engine technology program. In *Conference on Advanced SEI Technologies*, page 3451.
- [4] Stanley Gunn. Nuclear propulsion a historical perspective. *Space Policy*, 17(4):291–298, 2001.
- [5] David I Poston and Terry Kammash. A computational model for an open-cycle gas core nuclear rocket. *Nuclear science and engineering*, 122(1):32–54, 1996.
- [6] Robert Thomas, Yang Yang, GH Miley, and FB Mead. Advancements in dense plasma focus (dpf) for space propulsion. In *AIP Conference Proceedings*, volume 746, pages 536–543. AIP, 2005.
- [7] Sean D Knecht, Robert E Thomas, Franklin B Mead, George H Miley, and David Froning. Propulsion and power generation capabilities of a dense plasma focus (dpf) fusion system for future military aerospace vehicles. In *AIP Conference Proceedings*, volume 813, pages 1232–1239. AIP, 2006.
- [8] Terry Kammash, Myoung-Jae Lee, and David I Poston. High-thrust-high-specific impulse gasdynamic fusion propulsion system. *Journal of propulsion and power*, 13(3):421–427, 1997.
- [9] Vadim Zakirov and Vladimir Pavshook. Feasibility of the recent russian nuclear electric propulsion concept: 2010. *Nuclear Engineering and Design*, 241(5):1529–1537, 2011.
- [10] Franklin Chang Díaz, John Carr, Les Johnson, William Johnson, Giancarlo Genta, and P Federica Maffione. Solar electric propulsion for human mars missions. *Acta Astronautica*, 160:183–194, 2019.
- [11] Vanessa Paladini, Teresa Donateo, Arturo De Risi, and Domenico Laforgia. Super-capacitors fuel-cell hybrid electric vehicle optimization and control strategy development. *Energy conversion and management*, 48(11):3001–3008, 2007.
- [12] Don N Futaba, Kenji Hata, Takeo Yamada, Tatsuki Hiraoka, Yuhei Hayamizu, Yozo Kakudate, Osamu Tanaike, Hiroaki Hatori, Motoo Yumura, and Sumio Iijima. Shape-engineerable and highly densely packed single-walled carbon nanotubes and their application as super-capacitor electrodes. *Nature materials*, 5(12):987, 2006.

- [13] Chenguang Liu, Zhenning Yu, David Neff, Aruna Zhamu, and Bor Z Jang. Graphene-based supercapacitor with an ultrahigh energy density. *Nano letters*, 10(12):4863–4868, 2010.
- [14] Mike F Ashby and James Polyblank. Materials for energy storage systemsa white paper. *University of Cambridge*, 2012.
- [15] Chan K Choi. Engineering considerations for the self-energizing magnetoplasma-dynamic (mpd)-type fusion plasma thruster. Technical report, PURDUE UNIV LAFAYETTE IN SCHOOL OF NUCLEAR ENGINEERING, 1992.
- [16] Joshua Clough. *Integrated propulsion and power modeling for bimodal nuclear thermal rockets*. PhD thesis, University of Maryland, College Park, 2007.
- [17] Timothy Cichan, Stephen A Bailey, Scott D Norris, Robert P Chambers, Steven D Jolly, and Joshua W Ehrlich. Mars base camp: An architecture for sending humans to mars by 2028. In *Aerospace Conference, 2017 IEEE*, pages 1–18. IEEE, 2017.
- [18] Brian Dunbar. Powering the future: Nasa glenn contributions to international space station (iss) electrical power system, Sep 2011.
- [19] Chit Hong Yam, T Troy McConaghy, K Joseph Chen, and James Longuski. Preliminary design of nuclear electric propulsion missions to the outer planets. In *AIAA/AAS Astrodynamics Specialist Conference and Exhibit*, page 5393, 2004.
- [20] Stanley, Craig Williams, and Stanley Borowski. An assessment of fusion space propulsion concepts and desired operating parameters for fast solar system travel. In *33rd Joint Propulsion Conference and Exhibit*, page 3074, 1997.
- [21] Robert W Moses, Dennis Bushnell, David R Komar, Sang Choi, Ronald Litchford, Franklin Chang-Diaz, and Mark Carter. Maintaining human health for humans-mars. In *2018 AIAA SPACE and Astronautics Forum and Exposition*, page 5360, 2018.
- [22] Franklin R Chang Díaz, Mark D Carter, Timothy W Glover, Andrew V Ilin, Christopher S Olsen, Jared P Squire, Ron J Litchford, Nobuhiro Harada, and Steven L Koontz. Fast and robust human missions to mars with advanced nuclear electric power and vasmir® propulsion. *Proceedings of Nuclear and Emerging Technologies for Space*, pages 705–712, 2013.
- [23] William J Emrich Jr. *Principles of Nuclear Rocket Propulsion*. Butterworth-Heinemann, 2016.
- [24] Paul W Stockett, Robert S Bean, and Chan K Choi. 2019 aiaa energy and propulsion forum.
- [25] Francis A Cucinotta, Murat Alp, Blake Rowedder, and Myung-Hee Y Kim. Safe days in space with acceptable uncertainty from space radiation exposure. *Life sciences in space research*, 5:31–38, 2015.
- [26] Francis A Cucinotta. Radiation risk acceptability and limitations. *Space Radiation Program Element, NASA Johnson Space Center, Houston, TX*, 2010.

- [27] Paul Todd, Michael J Pecaut, and Monika Fleshner. Combined effects of space flight factors and radiation on humans. *Mutation Research/Fundamental and Molecular Mechanisms of Mutagenesis*, 430(2):211–219, 1999.
- [28] Zakirov Vadim and Pavshook Vladimir. Russian nuclear rocket engine design for mars exploration. *Tsinghua Science and Technology*, 12(3):256–260, 2007.
- [29] Gary L Bennett, Richard J Hemler, and Alfred Schock. Space nuclear power-an overview. *Journal of propulsion and power*, 12(5):901–910, 1996.
- [30] Gary L Bennett. Soviet space nuclear reactor incidents: perception versus reality. *Space Nuclear Pm./er S)/stems*, 1989.
- [31] RC OBrien, RM Ambrosi, NP Bannister, SD Howe, and Helen V Atkinson. Safe radioisotope thermoelectric generators and heat sources for space applications. *Journal of Nuclear Materials*, 377(3):506–521, 2008.
- [32] John Casani. Space fission power: Nasa’s best bet to continue to explore the outer solar system. 2019.
- [33] Lee S Mason. A comparison of brayton and stirling space nuclear power systems for power levels from 1 kilowatt to 10 megawatts. In *AIP Conference Proceedings*, volume 552, pages 1017–1022. AIP, 2001.
- [34] Steven Oleson. Electric propulsion for project prometheus. In *39th AIAA/ASME/SAE/ASEE Joint Propulsion Conference and Exhibit*, page 5279, 2004.
- [35] Mohamed S El-Genk. Space nuclear reactor power system concepts with static and dynamic energy conversion. *Energy Conversion and Management*, 49(3):402–411, 2008.
- [36] Lee S Mason. A comparison of fission power system options for lunar and mars surface applications. In *AIP Conference Proceedings*, volume 813, pages 270–280. AIP, 2006.
- [37] Glen Reed Longhurst, Edwin Allan Harvego, Bruce Gordon Schnitzler, Gary Dean Seifert, John Phillip Sharpe, Donald Alan Verrill, Kenneth Donald Watts, and Benjamin Travis Parks. Multi megawatt power system analysis report. Technical report, Idaho National Laboratory (INL), 2001.
- [38] Lee S Mason. Power technology options for nuclear electric propulsion. In *IECEC’02. 2002 37th Intersociety Energy Conversion Engineering Conference, 2002.*, pages 114–121. IEEE, 2002.
- [39] David Buden and Gary L Bennett. On the use of nuclear reactors in space. *Physics Bulletin*, 33(12):432, 1982.
- [40] Gary L Bennett. A look at the soviet space nuclear power program. In *Proceedings of the 24th intersociety energy conversion engineering conference*, pages 1187–1194. IEEE, 1989.
- [41] Scott F Demuth. Sp100 space reactor design. *Progress in nuclear energy*, 42(3):323–359, 2003.

- [42] Marc A Gibson, Maxwell H Briggs, James L Sanzi, and Michael H Brace. Heat pipe powered stirling conversion for the demonstration using flattop fission (duff) test. 2013.
- [43] David I Poston, Patrick R McClure, David D Dixon, Marc A Gibson, and Lee S Mason. Experimental demonstration of a heat pipe–stirling engine nuclear reactor. *Nuclear Technology*, 188(3):229–237, 2014.
- [44] David I Poston, Marc Gibson, and Patrick McClure. Design of the krusty reactor. *Proceedings NETS-2018, ANS*, 2018.
- [45] David I Poston, Marc Gibson, and Patrick McClure. Kilopower reactors for potential space exploration missions. In *Nuclear and Emerging Technologies for Space, American Nuclear Society Topical Meeting*. ANS, 2019.
- [46] Gary L Bennett, Richard J Hemler, and Alfred Schock. Status report on the us space nuclear program. *Acta astronautica*, 38(4-8):551–560, 1996.
- [47] Vadim Zakirov and Vladimir Pavshook. Feasibility of the recent russian nuclear electric propulsion concept: 2010. *Nuclear Engineering and Design*, 241(5):1529–1537, 2011.
- [48] Ilyes Ghedjatti, Yuan Shiwei, and Wang Haixing. A review on the application and usefulness of metal nanosized particles in solid rocket propellants. In *2018 3rd International Conference on Smart and Sustainable Technologies (SpliTech)*, pages 1–6. IEEE, 2018.
- [49] Mike Houts and Sonny Mitchell. Development and utilization of nuclear thermal propulsion. 2016.
- [50] Franklin R Chang Diaz. The vasmir rocket. *Scientific American*, 283(5):90–97, 2000.
- [51] T Kammash and M-J Lee. Fission-assisted or self-sustaining gasdynamic mirror propulsion system. In *32nd Joint Propulsion Conference and Exhibit*, page 3066, 1996.
- [52] JH Altseimer, GF Mader, and JJ Stewart. Operating characteristics and requirements for the nerva flight engine. *Journal of Spacecraft and Rockets*, 8(7):766–773, 1971.
- [53] Zakirov Vadim and Pavshook Vladimir. Russian nuclear rocket engine design for mars exploration. *Tsinghua Science And Technology*, 12(3):256–260, 2007.
- [54] Steven P Fusselman, Stanley K Borowski, Patrick E Frye, Stanley V Gunn, and Calvin Q Morrison. Nerva-derived concept for a bimodal nuclear thermal rocket. In *AIP Conference Proceedings*, volume 746, pages 512–519. AIP, 2005.
- [55] Ricky Tang. Study of the gasdynamic mirror (gdm) propulsion system. 2011.
- [56] Terry Kammash and Myoung-Jae Lee. Gasdynamic fusion propulsion system for space exploration. *Journal of Propulsion and Power*, 11(3):544–553, 1995.
- [57] Steven D Howe, Bryan Travis, and David K Zerkle. Safe testing of nuclear rockets. *Journal of Propulsion and Power*, 17(3):534–539, 2001.

- [58] Buzz Aldrin. Cyclic trajectory concepts. In *SAIC presentation to the Interplanetary Rapid Transit Study Meeting, Jet Propulsion Laboratory*, volume 28, 1985.
- [59] Craig Williams, Stanley Borowski, Leonard Dudzinski, and Albert Juhasz. A spherical torus nuclear fusion reactor space propulsion vehicle concept for fast interplanetary piloted and robotic missions. In *35th Joint Propulsion Conference and Exhibit*, page 2704, 1999.
- [60] Craig Williams, Stanley Borowski, Leonard Dudzinski, and Albert Juhasz. Fast interplanetary propulsion using a spherical torus nuclear fusion reactor propulsion system. In *Space Technology Conference and Exposition*, page 4520, 1999.
- [61] William J Emrich Jr and Terry Kammash. Performance optimization of the gasdynamic mirror propulsion system. In *AIP Conference Proceedings*, volume 504, pages 1420–1424. AIP, 2000.
- [62] William Emrich, Jr. Practical interplanetary travel using a gasdynamic mirror fusion propulsion system. In *32nd Joint Propulsion Conference and Exhibit*, page 3067, 1996.
- [63] Terry Kammash, Myoung-Jae Lee, and David I Poston. Thrust enhancement of the gasdynamic mirror (gdm) fusion propulsion system. In *AIP Conference Proceedings*, volume 387, pages 1481–1486. AIP, 1997.
- [64] C Choi, L Cox, Jr, and G Nakafuji. Fusion plasma thruster using a dense plasma focus device. In *30th Joint Propulsion Conference and Exhibit*, page 3322, 1995.
- [65] CL Leakeas. Parametric studies of dense plasma focus for fusion space propulsion with d-he3. Technical report, PHILLIPS LAB EDWARDS AFB CA, 1991.
- [66] JW Mather. 15. dense plasma focus. In *Methods in Experimental Physics*, volume 9, pages 187–249. Elsevier, 1971.
- [67] NV Filippov, TI Filippova, and VP Vinogradov. Dense high-temperature plasma in a non-cylindrical z-pinch compression. *Nucl. Fusion, Suppl.*, 1962.
- [68] Thomas James Dolan. *Fusion research. Volume 1 : Principles*. Pergamon Press, 1982.
- [69] H-S Bosch and GM Hale. Improved formulas for fusion cross-sections and thermal reactivities. *Nuclear fusion*, 32(4):611, 1992.
- [70] WM Nevins and R Swain. The thermonuclear fusion rate coefficient for p-11b reactions. *Nuclear fusion*, 40(4):865, 2000.
- [71] Hiromu Momota, Akio Ishida, Yasuji Kohzaki, George H Miley, Shoichi Ohi, Masami Ohnishi, Kunihiro Sato, Loren C Steinhauer, Yukihiro Tomita, and Michel Tuszewski. Conceptual design of the d-3he reactor artemis. *Fusion Technology*, 21(4):2307–2323, 1992.
- [72] John H Scott, Jeffrey A George, and Alfonso G Tarditi. Direct energy conversion for low specific mass in-space power and propulsion. 2013.

- [73] William Emrich. Plasma instabilities in the gasdynamic mirror propulsion experiment. In *40th AIAA/ASME/SAE/ASEE Joint Propulsion Conference and Exhibit*, page 3538, 2004.
- [74] UN General Assembly. Principles relevant to the use of nuclear power sources in outer space. Technical report, A/RES/47/68). Retrieved from <http://www.un.org/documents/ga/res/47/a47r068> , 1992.
- [75] David I Poston, Thomas F Marcille, Richard J Kapernick, Matthew T Hiatt, and Benjamin W Amiri. Evaluation of metal-fueled surface reactor concepts. In *AIP Conference Proceedings*, volume 880, pages 149–156. AIP, 2007.
- [76] *Material Balance Sheet*.
- [77] IAEA InfCirc. 153 (corrected). *The Structure and Content of Agreements between the Agency and States Required in Connection with the Treaty on the Non-Proliferation of Nuclear Weapons, Vienna, 1972*.
- [78] Joseph S Imburgia. Space debris and its threat to national security: a proposal for a binding international agreement to clean up the junk. *Vand. J. Transnat'l L.*, 44:589, 2011.
- [79] Paul W Stockett and Robert S Bean. Nonproliferation in the new space age: Where do we stand? In *INMM 60th Annual Meeting*. Institute of Nuclear Materials Management, 2019.
- [80] Dianna Sue Blair. A global perspective on continuity of knowledge: Concepts and challenges. Technical report, Sandia National Lab.(SNL-NM), Albuquerque, NM (United States), 2014.
- [81] Chris A Pickett, Nathan C Rowe, James R Younkin, Bernard Wishard, Robert Bean, Dianna Blair, Ray Lawson, George Weeks, and Keith Tolk. The importance of establishing and maintaining continuity of knowledge during 21st century nuclear fuel cycle activities. *JNMM*, 40(4):81–87, 2012.
- [82] Robert Bean, Dianna S Blair, and Chris Pickett. Attaining and maintaining a continuity of knowledge to draw safeguards conclusions with confidence. *ESARDA Bulletin*, 51(SAND-2014-19685J), 2014.
- [83] Buzz Aldrin. Cyclic trajectory concepts. In *SAIC presentation to the Interplanetary Rapid Transit Study Meeting, Jet Propulsion Laboratory*, volume 28, 1985.

## APPENDICES

## APPENDIX A

### COMPUTER CODES

Two computer codes/scripts were used for this project. The first is the Dense Plasma Focus Propulsion Code and the second was a script to perform the Gasdynamic Mirror calculations.

#### A.1 GDM-script

The following is the GDM script that was written to perform a paper study of a fission assisted DT fueled GDM where the user could select which of the three cases to run as part of the function.

---

```

function [m_fission,m_total,T_to_W,t_flight] = GDM(Power_system)
%-----
%Title: Gasdynamic Mirror
%Creator: Paul Stockett
%Contributors: None
%Date of Creation: 15-Apr-2019
%Date of Last Modification: 21-Jun-2019
%Purpose: To perform the necessary calculations for a gasdynamic
mirror fusion propulsion system based off the work of Dr. Terry
Kammash, Dr. Myoung-Jae Lee, Dr. David Poston and Dr. David L.
Galbraith at the University of Michigan and Dr. William Emrich at
NASA. The following papers were used to source the data from:
%       1. Performance Optimization of Gasdynamic Mirror
Propulsion System (1998)
%       2. Direct Energy Conversion for Low Specific Mass In-Space
Power and Propulsion (2013)
%       3. A comparison of Brayton and Stirling Space Nuclear
Power Systems for Power Levels from 1 Kilowatt to 10 Megawatts (2001)
%       4. Multi Megawatt Power System Analysis Report (2001)
%-----
warning('off','all')
%-----Fundamental Constants-----
DT_product1=3.54;           % He4 energy in MeV
DT_product2=14.05;        % n energy in MeV
g=9.81;                   % Gravitational Constant on Earth (m/
s^2)

%-----Rocket System Parameters-----
% DT Rocket System Parameters from "Performance Optimization of the
% Gasdynamic Mirror Propulsion System" by Emrich (2000)
Thrust=22100;             % N
ISP=142200;              % s
Q=2.935;                 % Fusion Gain Factor
Pf=14860;                % Fusion Power (MW)
P_inject=5064;           % MW Injector Power (MW)
P_brem=317;              % Bremsstrahlung Loss (MW)
P_sync=103;              % Synchrotron Loss (MW)
P0=1000;                 % Start Up Pulse Energy (MW)
eta_t=0.3;               % Brayton Cycle Efficiency
m_magnet=30;             % Magnet Mass (Mg)
m_radiator=1077;        % Radiator Mass (Mg)
m_TEC=55;                % Thermal Electric Converter Mass (Mg)
m_DEC=53;                % Direct Electric Converter Mass (Mg)
m_injector=23;          % Neutral Beam Injector Mass (Mg)
m_fuelcap=35;           % Fuel Cell/Capacitor System Mass (Mg)
m_breeding=10;          % Tritium Breeding System Mass (Mg)
m_shield=37;            % Lithium Shield Mass (Mg)
m_cooling=19;           % Magnet Cooling System Mass (Mg)
m_struct=36;            % Structure Mass (Mg)
m_hab=65;               % Habitat Mass (Mg)
m_lander=60;            % Lander Mass (Mg)

```

---

---

```

m_fuel=30; % Fuel Masss (Mg) assumed from 1996-
Practical Interplanetary Travel Using a Gasdynamic Mirror Fusion
Propulsion System
m_payload=100; % Payload Mass consistent with DPF
reports
%-----Fission Reactor Parameters-----
%Fission Reactor Scaling from "A comparison of Brayton and Stirling
Space
%Nuclear Power Levels from 1 Kilowatt to 10 Megawatts" by Mason and
%"Multi Megawatt Power System Analysis Report" by Longhurst et al.
alpha_thermionic=1; % kg/kW for 10 MW Reactor with
thermionic conversion
alpha_brayton=2; % kg/kW for 10 MW Reactor with Bryaton
Cycle conversion
alpha_rankine=6.06; % kg/kW for 10 MW Reactor with Rankine
Cycle conversion
alpha_stirling=20.7; % kg/kW for 10 MW Reactor with
Stirling conversion
Reactor_Power=10; % 10 MW Fission Reactor

%-----Begin Code-----

% Power Calculations
Fc_DT=DT_product1/(DT_product1+DT_product2);
Ploss=P_brem+P_sync;
psi_r=(Fc_DT*Pf-Ploss)/Pf;
P_ch=Pf*(1/Q+psi_r);

i=1;
for eta_d=0.1:0.1:0.7
    P_DEC(i)=eta_d*P_ch;
    i=i+1;
end
% Mass Updates
E_cap_old=36; % Specific Energy of
Capacitors in Original Paper (kJ/kg)
m_cap_old=P0*10^3/E_cap_old/10^3; % Original Paper Capacitor
Weight (Mg)
m_fuelcell=m_fuelcap-m_cap_old; % Assumed to remain constant
E_cap_new=828; % Specific Energy of Modern
Capacitors (kJ/kg)
m_cap_new=P0*10^3/E_cap_new/10^3; % New Capacitor Weight (Mg)
m_fuelcap=m_fuelcell+m_cap_new;

% Power System 1-Fusion Only Mass and Performance Calculations
if Power_system==1
    m_fission=0;
end

% Power System 2 - Fission Only Mass and Performance Calculations
if Power_system==2
    N_reactors=ceil(P_inject/Reactor_Power);
    m_DEC=0;
    m_TEC=0;

```

---

---

```

        m_fission=Reactor_Power*alpha_thermionic*N_reactors;
    end

    % Power System 3 - Fission+Fusion Mass and Performance Calculations
    if Power_system==3
        m_TEC=0;
        Conversion_type=1;
        line_color=['b','g','r','m','c'];
        while Conversion_type<5
            if Conversion_type==1
                alpha=alpha_thermionic;
            elseif Conversion_type==2
                alpha=alpha_brayton;
            elseif Conversion_type==3
                alpha=alpha_rankine;
            elseif Conversion_type==4
                alpha=alpha_stirling;
            end
            alpha_DEC=m_DEC/P_DEC(7);
            i=1;
            while i<8
                P_net(i)=P_inject-P_DEC(i)
                if P_net(i)<0
                    P_net(i)=0;
                end
                i=i+1;
            end
            N_reactors=ceil(P_net/Reactor_Power);
            m_fission(Conversion_type,:)=(Reactor_Power*alpha*N_reactors);
            %Mg
            m_dec=alpha_DEC*P_DEC;
            m_total=m_payload+m_DEC+m_TEC+m_magnet+m_radiator+m_fission
+m_DEC+m_injector+m_fuelcap+m_breeding+m_shield+m_cooling+m_struct
+m_hab+m_lander+m_fuel;
            T_to_W=Thrust./(m_total*10^3)/g;
            eta_d=[0.1:0.1:0.7];
            figure(1)
            plot(eta_d,T_to_W(Conversion_type,:))
            ylabel('Thrust to Weight Ratio')
            xlabel('Direct Energy Converter Efficiency, \eta_d (%)')
            Conversion_type=Conversion_type+6;
        end
    end

    % Rocket Performance Calculations
    m_total=m_payload+m_TEC+m_magnet+m_radiator+m_fission+m_DEC+m_injector
+m_fuelcap+m_breeding+m_shield+m_cooling+m_struct+m_hab+m_lander
+m_fuel;
    T_to_W=Thrust./(m_total*10^3)/g;
    fm=(m_total(5)-m_fuel)/m_total(5);
    t_flight=Flight_time(ISP, fm);

```

*Published with MATLAB® R2017b*

### A.1.1 Sample Output

Table A.1.  
GDM Code Sample output for a fission powered Gasdynamic Mirror

$m_{Fission}$ , kg	$m_{total}$ , kg	$\frac{T}{W}$	$t_{flight}$ , days
5070	$6.5654 * 10^3$	$3.4313 * 10^{-4}$	208.85

### A.2 DPF Propulsion Code

The Dense Plasma Focus Propulsion Code was originally written in Fortran by C.L. Leakeas and Mei-Yu Wang, but has been converted to Matlab for the the current work. The code consists of a main script from which multiple functions are called:

- **DPF.m** is the main script where the user decides which fuels,  $\Delta V$ s, number of thrusters and which power system to use.
- the subfunctions include:
  - **DPF\_prop.m** which performs all of the DPF parameter and propulsion calculations as well as the bulk of the mass calculations. This function calls all other functions. This includes many of the system constants such as capacitor specific energy and payload mass which can also be changed by the user.
  - **Fusion\_ov.m** is the function used to calculate the reaction rate parameter for the various fuels using correlations from literature.
  - **Fusion\_power.m** performs the power calculations for the fusion reactions using an iterative method.
  - **DPF\_fission.m** is the function which calculates the mass and power needs of the fission reactor for the DPF system based on specific mass data from literature.

- **TWDEC.m** is the function for the Travelling Wave Direct Energy Converter and the associated mass and power calculations.
- **Flight\_time.m** solves the patched conics problem as demonstrated by Emrich [23] and optimizes it by varying the departure angle to solve for minimum trip time from Earth to Mars.

---

```

%-----
%Title: Dense Plasma Focus
%Created by: C.L. Leakeas
%Modified by: Mei-Yu Wang and Paul Stockett
%Date of Creation: Mar-1991
%Date of Last Modification: 20-Jun-2019
%Purpose: Modified matlab version of the fortran code created
         by C.L. Leakeas found in "Parameteric Studies of Dense Plasma
         Focus for Fusion Space Propulsion with D-He3" Report number: PL-
         TR-91-3014 which was later modified by Mei-Yu Wang for "Engineering
         Considerations for the Self-Energizing Magnetoplasma dynamic (MPD)-
         Type Fusion Plasma Thruster" Report number: PL-TR-91-3087
%-----

clear all
close all
clc

%-----Rocket System
Parameters-----
n_thrusters=[4];           %number of DPF thrusters
DeltaV=[20];              %km/s
% FUEL TYPE SELECTION
% 1 = DD Fuel
% 2 = DT Fuel
% 2.5 = Spin-polarized DT Fuel
% 3 = D-He3 Fuel
% 3.5 = Spin-polarized D-He3 Fuel
% 4 = p-B11 Fuel
% 4.5 = Spin-polarized p-B11 Fuel
Fuel_type=[2,3];

% POWER SYSTEM SELECTION
% 1 = Fusion Only
% 2 = Fission Only
% 3 = Fusion and Fission
Power_system=[1,2,3];

%-----Begin
Code-----

i=1;
j=1;
k=1;
l=1;
m=1;
for i=1:length(Fuel_type)
    for j=1:length(DeltaV)
        for k=1:length(n_thrusters)
            for l=1:length(Power_system)
                a(m,:)=Fuel_type(i);
                b(m,:)=DeltaV(j);
            end
        end
    end
end

```

---

---

```

        c(m,:)=n_thrusters(k);
        d(m,:)=Power_system(l);

    x(m,:)=DPF_prop(n_thrusters(k),DeltaV(j),Fuel_type(i),Power_system(l));
        m=m+1;
    end
end
end
end

Power_system=d;
Fuel_type=a;
DeltaV=b;
n_thrusters=c;
Pf_total=x(:,1);
P_ch=x(:,2);
P_brem_total=x(:,3);
P_cyc_total=x(:,4);
P_loss_total=x(:,5);
m_dot_total=x(:,6);
t_burn=x(:,7);
m_payload=x(:,8);
m_propellant=x(:,9);
m_prop_system=x(:,10);
m_fuel=x(:,11);
m_fuel_system=x(:,12);
m_pmad=x(:,13);
m_capacitors=x(:,14);
m_magnet=x(:,15);
m_shield=x(:,16);
m_DEC=x(:,17);
m_fission=x(:,18);
m_total=x(:,19);
Thrust_total=x(:,20);
T_to_W=x(:,21);
ISP=x(:,22);
t_flight=x(:,23);
T=table(Power_system,Fuel_type,DeltaV,n_thrusters,Pf_total,P_ch,P_brem_total,P_cyc.
Output=[Power_system,Fuel_type,DeltaV,n_thrusters,Pf_total,P_ch,P_brem_total,P_cyc.
save('Sample','Output')

```

*Published with MATLAB® R2018a*

---

## Table of Contents

.....	1
Focus Parameters .....	3
Reaction Rate Calculations .....	4
Propulsion Calculations .....	5
Mass Calculations .....	7

```
function [output] =
    DPF_prop(n_thrusters,DeltaV,Fuel_type,Power_system)

%-----
%Title: DPF Propulsion Code
%Created by: C.L. Leakeas
%Modified by: Mei-Yu Wang and Paul Stockett
%Date of Creation: Mar-1991
%Date of Last Modification: 20-Jun-2019
%Purpose: Modified matlab version of the fortran code created by C.L.
%Leakeas found in "Parameteric Studies of Dense Plasma Focus for
    Fusion
%Space Propulsion with D-He3" Report number: PL-TR-91-3014 which was
    later
%modified by Mei-Yu Wang for "Engineering Considerations for the
%Self-energizing Magnetoplasmadynamic (MPD)-Type Fusion Plasma
    Thruster"
%Report number: PL-TR-91-3087
%-----

%-----Fundamental Constants-----
g=9.81; %m/s
mu0=4*pi*10^-7; %Tm/A
rho_cu=1.673*10^-8; %resitivity of copper in
    ohm-m
rho_LiH=725; %Density of LiH shield in
    kg/m^3
Cp_H2=4157; %J/kg/K
Cp_electron=1.517*10^7; %J/kg/K
Cp_Hion=8267; %J/kg/K
DHe=[0.35715,-3.32451,10.11363,-25.66533]; %Reaction rate
    coefficients for D-He3 reaction
DDN=[0.29811,-2.08296,5.70135,-22.0878]; %Reaction rate
    coefficients for DDN reaction
DDP=[0.30795,-2.12009,5.68718,-22.03746]; %Reaction rate
    coefficients for DDP reaction

%-----System Constants-----
alpha_pmad=1; %kg/kW from "Direct Energy
    Conversion for Low Specific Mass In-Space Power and Propulsion" by
    Scott et al.
cycrefl=0.6; %Percent of cycltron
    radiation retained by plasma
```

---

```

C0=3.55*10^-4; %Initial capacitance of
  capacitor bank in Farads
E_specific=828; %Specific energy of
  capacitors in kJ/kg (NAC supercapacitor from Li et al 2016)
Efficiency_pinch=0.25; %Percent of particles
  trapped in the pinch
Efficiency_snowplow=0.70; %Percent of particles
  trapped in the rundown phase
f=100; %Frequency of firing in Hz
F1_fraction=0.5; %Percent of Fuel 1 in the
  fill gas
F2_fraction=0.5; %Percent of Fuel 2 in the
  fill gas
iterations=1000; %number of iterations
I_magnet=3.18*10^5; %Current necessary to
  produce 2T magnetic field in Amperes
I_optimum=20*10^6; %Optimum maximum current
  achievable in Amperes
L_pinch=0.0254; %Length of the Pinch in
  meters
L_anode=0.382; %Length of the anode in
  meters
K_c=0.2; %Percent of cyclotron
  radiation absorbed in walls and electrodes
L0=2.5*10^-8; %Initial inductance in H
m_dot_extra=30; %Extra propellant mass
  that is mixed in kg/s
m_payload=10^5; %Mass of the payload in kg
n_shield=0.125; %Assumed 12.5% of neutrons
  from DDN reaction contacting the shield
r_anode=0.0508; %Radius of the anode in
  meters
r_cathode=0.080; %Radius of the cathode in
  meters
rho0=2.2*10^-4; %Initial fill gas density
  in kg/m^3
r_pinch=0.0015; %Radius of the pinch in
  meters
t_discharge=10^-7; %Time for fill gas to be
  discharged in seconds
t_firing=30; %Number of days the DPF is
  firing for
t_pinch=10^-4; %Pinch lifetime in seconds
T_ionization=5000; %Assumed full ionization
  temperature in Kelvin
T_limit=2000; %Wall temperature maximum
  limit in K
T_turbine_exit=700; %Assumed exit temp of the
  turbine
T_hydrogen_flow=20; %Hydrogen flow
Voltage=27*10^3; %Voltage in volts

%-----Fuel Parameters-----
Fuel_type;

```

---

---

```

if Fuel_type==1
    m_f1=3.344495*10^-27;           %Mass of Deuterium in
    kg                               %Mass of Deuterium in
    m_f2=3.344495*10^-27;           %Mass of Deuterium in
    kg                               %Mass of Deuterium in
elseif Fuel_type==2
    m_f1=3.344495*10^-27;           %Mass of Deuterium in
    kg                               %Mass of Deuterium in
    m_f2=5.008268*10^-27;           %Mass of Tritium in kg
elseif Fuel_type==2.5
    m_f1=3.344495*10^-27;           %Mass of Deuterium in
    kg                               %Mass of Deuterium in
    m_f2=5.008268*10^-27;           %Mass of Tritium in kg
elseif Fuel_type==3
    m_f1=3.344495*10^-27;           %Mass of Deuterium in
    kg                               %Mass of Deuterium in
    m_f2=5.008234*10^-27;           %Mass of Helium-3 in
    kg                               %Mass of Helium-3 in
elseif Fuel_type==3.5
    m_f1=3.344495*10^-27;           %Mass of Deuterium in
    kg                               %Mass of Deuterium in
    m_f2=5.008234*10^-27;           %Mass of Helium-3 in
    kg                               %Mass of Helium-3 in
else
    m_f1=1.672622*10^-27;           %Mass of a proton in
    kg                               %Mass of a proton in
    m_f2=1.828138*10^-26;           %Mass of Boron-11 in
    kg                               %Mass of Boron-11 in
end

%-----Converter Parameters-----
eta_T=0.2;                          %Turbine efficiency
% DPF ENERGY CONVERTOR SYSTEM
% 1 = Thermal Only
% 2 = DEC Only
% 3 = Thermal and DEC
Energy_conversion=1;

%-----Begin Code-----

Not enough input arguments.

Error in DPF_prop (line 63)
Fuel_type;

```

## Focus Parameters

```

A_cross_DPF=pi*(r_cathode^2-r_anode^2);
V_pinch=pi*r_pinch^2*L_pinch;
V0=A_cross_DPF*L_anode;
Efficiency_total=Efficiency_snowplow*Efficiency_pinch;
m_ave=F1_fraction*m_f1+F2_fraction*m_f2;

```

---

```

%Current
I_max=sqrt(2.704*sqrt((C0*Voltage^3)/(mu0*L0*log(r_cathode/
r_anode)))*(r_anode^2*rho0/mu0)^0.25));

%Plasma Temperature
KT_max=mu0*I_max^(2)*m_ave*L_pinch/
(78.96*Efficiency_total*rho0*L_anode*(r_cathode^2-
r_anode^2)*1.6*10^-16);
K=KT_max/I_max^(2);
KT_optimum=K*I_optimum^(2);           %Assuming plasma
temperature scales as current^2

%Run-down Velocity
v_run=sqrt(mu0*I_optimum^2/(78.96*r_anode^2*rho0));

%Pinch Number Density
N_pinch=Efficiency_total*rho0*L_anode*(r_cathode^2-r_anode^2)/
(m_ave*r_pinch^2*L_pinch);
if Fuel_type==1
    F1_fraction=1;
    F2_fraction=1;
end
N_F1_pinch=F1_fraction*N_pinch;
N_F2_pinch=F2_fraction*N_pinch;

%Electrode Characteristics
Voltage_max=Voltage*(I_optimum+I_magnet)/I_max;
P0=Voltage_max*I_optimum*f*t_discharge*10^-6;
B_pinch=mu0*Efficiency_total*I_optimum/(2*pi*r_pinch);

%Non-Fusion Thrust
Thrust_nonfusion=rho0*v_run^2*A_cross_DPF*f*t_discharge;

```

## Reaction Rate Calculations

```

Fuel_type1=floor(Fuel_type);
ov1=Fusion_ov(KT_optimum,Fuel_type1);
if Fuel_type==1
    ov1=0;
    ov=Fusion_ov(KT_optimum,Fuel_type1);
    ov2=ov(1);
    ov3=ov(2);
elseif Fuel_type==2           %Secondary DD Reactions in DT Reactions
    Fuel_type2=1;
    ov=Fusion_ov(KT_optimum,Fuel_type2);
    ov2=ov(1);
    ov3=ov(2);
elseif Fuel_type==2.5         %Secondary DD Reactions in Spin Polarized
    DT Reactions
    ov1=1.5*ov1;
    Fuel_type2=1;
    ov=Fusion_ov(KT_optimum,Fuel_type2);
    ov2=ov(1);

```

---

```

    ov3=ov(2);
elseif Fuel_type==3      %Secondary DD Reactions in D-He3 Reactions
    Fuel_type2=1;
    ov=Fusion_ov(KT_optimum,Fuel_type2);
    ov2=ov(1);
    ov3=ov(2);
elseif Fuel_type==3.5    %Secondary DD Reactions in Spin Polarized D-
He3 Reactions
    ov1=1.5*ov1;
    Fuel_type2=1;
    ov=Fusion_ov(KT_optimum,Fuel_type2);
    ov2=ov(1);
    ov3=ov(2);
elseif Fuel_type==4      %Absence of Secondary DD reactions in p-B11
Reactions
    ov2=0;
    ov3=0;
else                      %Absence of Secondary DD reactions in Spin Polarized p-B11
Reactions
    ov1=1.5*ov1;
    ov2=0;
    ov3=0;
end

%Variable Packaging for passing to Fusion Power
Pinch_parameters=[ov1,ov2,ov3,KT_optimum,I_optimum,N_pinch,N_F1_pinch,N_F2_pinch];
System_parameters=[V_pinch,L_pinch,t_pinch,iterations,cycrefl,f,Efficiency_total,F
[Power,RR_DDN,N_F1_pinch,N_F2_pinch]=Fusion_power(Pinch_parameters,System_paramete
Power;

%Variable Separation and Assignment from Fusion Power
Pf_total=Power(1);
P_loss_total=Power(2);
P_net_total=Power(3);
Pf_Fuel_total=Power(4);
Pf_DDN_total=Power(5);
Pf_DDP_total=Power(6);
P_brem_total=Power(7);
P_cyc_total=Power(8);
ov_DDN=ov3;

```

## Propulsion Calculations

```

P_absorbed=K_c*(1-cycrefl)*P_cyc_total;
P_ohmic=I_optimum^2*rho_cu*L_anode*(1/(pi*r_anode^2)+1/
(pi*(r_cathode^2-r_anode^2)))*10^-6*t_discharge*f; %MW
P_magnet=0.01; %MW
P_waste=P_ohmic+P_absorbed+P_magnet;

m_dot=P_waste*61.14/(T_turbine_exit-T_hydrogen_flow);
m_dot_total=m_dot+m_dot_extra;

```

---

```

Q=Pf_total/P0;
[m_DEC,P_DEC,P_ch]=TWDEC(Fuel_type,Q,P_net_total,P_loss_total);

if Energy_conversion == 1
    m_DEC=0;
    P_DEC=0;
    P_thermal=eta_T*P_waste;
elseif Energy_conversion == 2
    P_thermal=0;
else
    P_thermal=eta_T*P_waste;
end

Fusion_electric=P_thermal+P_DEC;

if Power_system==2
    m_DEC=0;
    P_DEC=0;
    P_thermal=0;
end

P_net_total=P_ch-P_loss_total;

T_ave=(m_dot*T_turbine_exit+m_dot_extra*T_hydrogen_flow)/
(m_dot_total);

Q_dot_removed=(m_dot_total)*Cp_H2*(T_ionization-T_ave);
Q_dot=10^6*P_net_total-Q_dot_removed;
T_stag_electrons=T_ionization+Q_dot/
(m_dot_total*Cp_electron*0.000545);
T_stag_ions=T_ionization+Q_dot/(m_dot_total*Cp_Hion*0.999455);
T_throat_electrons=T_stag_electrons/1.35;
T_throat_ions=T_stag_ions/1.35;

v_ion_throat=sqrt(2*Cp_Hion*(T_stag_ions-T_throat_ions));
v_electron_throat=sqrt(2*Cp_electron*(T_stag_electrons-
T_throat_electrons));
v_ion_exit=2*v_ion_throat;
v_electron_exit=2*v_electron_throat;

Thrust_electron=0.000545*m_dot_total*v_electron_exit;
Thrust_Hion=0.999455*m_dot_total*v_ion_exit;
Thrust_fusion=Thrust_electron+Thrust_Hion;
Thrust_total=n_thrusters*(Thrust_fusion+Thrust_nonfusion);

ISP=Thrust_total/g/(rho0*V0*f+m_dot_total);
v_exit=ISP*g;

%Fuel_burnup=1-N_pinch(iterations+1)/N_pinch(1);

```

---

---

## Mass Calculations

```

E_capacitors=0.5*C0*Voltage^2*((I_optimum+I_magnet)/I_max)^2;
m_capacitors=n_thrusters*E_capacitors/1000/E_specific;

m_magnet=67.55*n_thrusters;

if Power_system==1
    m_pmad=alpha_pmad*Fusion_electric*10^3;
elseif Power_system==2
    m_pmad=0;
elseif Power_system==3
    m_pmad=alpha_pmad*(P0-Fusion_electric)*10^3;
end

m_fission=DPF_fission(Power_system,P0,E_capacitors,Fusion_electric);

% m_propellant=m_dot_total*t_firing*86400
m_propellant=(exp(DeltaV*10^3/v_exit)-1)*(m_payload+m_magnet
+m_capacitors+m_fission+m_DEC+m_pmad);
m_prop_system=0.15*m_propellant;
t_burn=m_propellant/(m_dot_total);
% m_fuel=rho0*V0*f*t_firing*86400
m_fuel=n_thrusters*rho0*V0*f*t_burn;
m_fuel_system=0.1*m_fuel;

if Fuel_type1==4
    m_shield=0;
else
    RR_DDN(iterations+1)=N_Fl_pinch(iterations
+1)*N_Fl_pinch(iterations+1)*ov_DDN;
    %Thickness_shield=0.1*log(n_shield*RR_DDN(iterations
+1)*t_pinch*f*V_pinch*t_firing/(4*pi*1.157*10^12));
    Thickness_shield=0.1*log(n_shield*RR_DDN(iterations
+1)*t_pinch*f*V_pinch*t_burn/(86400*4*pi*1.157*10^12));
    %m_shield=rho_LiH*pi*Thickness_shield;
    m_shield=n_thrusters*rho_LiH*pi*Thickness_shield;
end

m_dry=m_payload+m_magnet+m_prop_system+m_fuel_system+m_capacitors
+m_shield+m_fission+m_DEC+m_pmad;
m_total=m_payload+m_magnet+m_propellant+m_prop_system+m_fuel
+m_fuel_system+m_capacitors+m_shield+m_fission+m_DEC+m_pmad;
fm=m_dry/m_total;

T_to_W=Thrust_total/g/m_total;

t_flight=Flight_time(ISP, fm);

output=[Pf_total,P_ch,P_brem_total,P_cyc_total,P_loss_total,m_dot_total,t_burn,m_p

```

*Published with MATLAB® R2018a*

---

```

function [ov]=Fusion_ov(E_lab,Fuel_type)

%-----
%Title: Fusion Reaction Rates
%Created by: C.L. Leakeas
%Modified by: Mei-Yu Wang and Paul Stockett
%Date of Creation: Mar-1991
%Date of Last Modification: 20-Mar-2019
%Purpose: To utilize the Bosch-Hale formulas from "Improved Formulas
for Fusion Cross-sections and Thermal Reactivities" to calculate the
cross sections and reaction rates for various fusion fuels.
%-----

%-----Fundamental Constants-----
C=299792458; %m/s
e=1.602176634*10^-19; %C
epsilon0=8.854*10^-12; %C^2/N/m^2
g=9.81; %m/s
h=6.62607015*10^-34; %Js
k=1.380649*10^-23; %J/K
K=8.6*10^-5;
mu0=4*pi*10^-7; %Tm/A
Na=6.02214076*10^23; %mol^-1
R=8.314462618; %J/mol/K
DDN=[0.29811,-2.08296,5.70135,-22.0878]; %Reaction rate
coefficients for DDN reaction
DDP=[0.30795,-2.12009,5.68718,-22.03746]; %Reaction rate
coefficients for DDP reaction

%-----Begin Code-----
T=E_lab;

Not enough input arguments.

Error in Fusion_ov (line 26)
T=E_lab;

```

## Reaction Rate Parameters from Bosch-Hale

```

if Fuel_type==1 %D(d,p)T
    Bg=31.3970; %sqrt(keV)
    MrC2=937814; %keV
    C1=5.65718*10^-12;
    C2=3.41267*10^-3;
    C3=1.99167*10^-3;
    C4=0.00;
    C5=1.05060*10^-5;
    C6=0.00;
    C7=0.00;

    denominator=1-(T*(C2+T*(C4+T*C6)))/(1+T*(C3+T*(C5+T*C7)));
    theta=T/denominator;

```

---

```

    xi=(Bg^2/(4*theta))^(1/3);
    ov_DDP=C1*theta*sqrt(xi/(MrC2*T^3))*exp(-3*xi)*10^-6;
%D(d,n)He3
    Bg=31.3970;           %sqrt(keV)
    MrC2=937814;         %keV
    C1=5.43360*10^-12;
    C2=5.85778*10^-3;
    C3=7.68222*10^-3;
    C4=0.00;
    C5=-2.96400*10^-6;
    C6=0.00;
    C7=0.00;

    denominator=1-(T*(C2+T*(C4+T*C6)))/(1+T*(C3+T*(C5+T*C7)));
    theta=T/denominator;
    xi=(Bg^2/(4*theta))^(1/3);
    ov_DDN=C1*theta*sqrt(xi/(MrC2*T^3))*exp(-3*xi)*10^-6;
    ov=[ov_DDP,ov_DDN];
%
% X=log10(E_lab);
% exponent_DDN=DDN(1)*X^3+DDN(2)*X^2+DDN(3)*X+DDN(4);
% ov_DDN=10^-6*10^exponent_DDN
% exponent_DDP=DDP(1)*X^3+DDP(2)*X^2+DDP(3)*X+DDP(4);
% ov_DDP=10^-6*10^exponent_DDP
%
elseif Fuel_type==2           %T(d,n)He4
    Bg=34.3827;           %sqrt(keV)
    MrC2=1124656;         %keV
    C1=1.17302*10^-9;
    C2=1.51361*10^-2;
    C3=7.51886*10^-2;
    C4=4.60643*10^-3;
    C5=1.35000*10^-2;
    C6=-1.06750*10^-4;
    C7=1.36600*10^-5;

    denominator=1-(T*(C2+T*(C4+T*C6)))/(1+T*(C3+T*(C5+T*C7)));
    theta=T/denominator;
    xi=(Bg^2/(4*theta))^(1/3);
    ov=C1*theta*sqrt(xi/(MrC2*T^3))*exp(-3*xi)*10^-6;
elseif Fuel_type==3           %He3(d,p)He4
    Bg=68.7508;           %sqrt(keV)
    MrC2=1124572;         %keV
    C1=5.51036*10^-10;
    C2=6.41918*10^-3;
    C3=-2.02896*10^-3;
    C4=-1.91080*10^-5;
    C5=1.35776*10^-4;
    C6=0.00;
    C7=0.00;

    denominator=1-(T*(C2+T*(C4+T*C6)))/(1+T*(C3+T*(C5+T*C7)));
    theta=T/denominator;
    xi=(Bg^2/(4*theta))^(1/3);
    ov=C1*theta*sqrt(xi/(MrC2*T^3))*exp(-3*xi)*10^-6;

```

---

---

end

## Reaction Rate Parameters for P-B11 Reactions from Nevins and Swain (2000)

```

if Fuel_type==4           % B11(p,alpha)2alpha
    Eg=22.589*10^3;       %keV
    MrC2=859526;         %keV
    P1=4.4467*10^-14;    %keV*m^3/s
    P2=-5.9357*10^-2;    %keV^-1
    P3=2.0165*10^-1;     %keV^-1
    P4=1.0404*10^-3;     %keV^-2
    P5=2.7621*10^-3;     %keV^-2
    P6=-9.1653*10^-6;    %keV^-3
    P7=9.8305*10^-7;     %keV^-3

    fraction=(P2+T*(P4+T*P6))/(1+T*(P3+T*(P5+T*P7)));
    denominator=1-T*fraction;
    theta=T/denominator;
    xi=(Eg/4/theta)^(1/3);
    ov=P1*theta*sqrt(xi/MrC2/T^3)*exp(-3*xi);

    if T<=130
        ov_resonance=5.41*10^-21*(1/T)^(3/2)*exp(-148/T);
        ov=ov+ov_resonance;
    end
end

```

*Published with MATLAB® R2018a*

---

```

function [Power,RR_DDN,N_F1_pinch,N_F2_pinch] =
    Fusion_power(Pinch_parameters,System_parameters)

%-----
%Title: Fusion Power
%Created by: C.L. Leakeas
%Modified by: Mei-Yu Wang and Paul Stockett
%Date of Creation: Mar-1991
%Date of Last Modification: 21-Mar-2019
%Purpose: To perform the fusion power calculations for various fuel
types for a Dense Plasma Focus Device
%-----

%-----Fundamental Constants-----
C=299792458; %m/s
e=1.602176634*10^-19; %C
epsilon0=8.854*10^-12; %C^2/N/m^2
g=9.81; %m/s
h=6.62607015*10^-34; %Js
k=1.380649*10^-23; %J/K
mu0=4*pi*10^-7; %Tm/A
Na=6.02214076*10^23; %mol^-1
R=8.314462618; %J/mol/K
WDHe=2.93*10^-12; %Energy released per D-He3
    reaction in Joules
WDDN=5.24*10^-13; %Energy released per DDN
    reaction in Joules
WDDP=6.46*10^-13; %Energy released per DDP
    reaction in Joules
WDT=2.82*10^-12; %Energy released per DT
    reaction in Joules
WPB11=1.39*10^-12; %Energy released per DT
    reaction in Joules

%-----Begin Code-----

%Variable Separation and Assignment
ov1=Pinch_parameters(1); %Reaction Rate
    Parameter of Primary Fuel Reaction
ov2=Pinch_parameters(2); %DDp Reaction Rate
    Parameter for Secondary Fuel Reaction
ov3=Pinch_parameters(3); %DDn reaction Rate
    Parameter for Secondary Fuel Reaction
KT_optimum=Pinch_parameters(4); %Temperature of the
    Plasma
I_optimum=Pinch_parameters(5); %Optimal current
N_pinch=Pinch_parameters(6); %Total Pinch Number
    density (m^-3)
N_F1_pinch=Pinch_parameters(7); %Pinch Density of Fuel
    1 (m^-3)
N_F2_pinch=Pinch_parameters(8); %Pinch Density of Fuel
    2(m^-3)

```

---

---

```

V_pinch=System_parameters(1);           %Volume of the Pinch
(m^3)
L_pinch=System_parameters(2);           %Length of the Pinch
(m)
t_pinch=System_parameters(3);           %Pinch Time (s)
iterations=System_parameters(4);        %Number of iterations
cycrefl=System_parameters(5);           %Fraction of Cyclotron
Radiation Retained by the Plasma
f=System_parameters(6);                 %Frequency in hz
Efficiency_total=System_parameters(7);  %System efficiency of
the DPF
Fuel_type=System_parameters(8);         %Fuel Type Selection

Not enough input arguments.

Error in Fusion_power (line 30)
ovl=Pinch_parameters(1);                %Reaction Rate
Parameter of Primary Fuel Reaction

```

## Power Calculations

```

Fuel_type=floor(Fuel_type);
i=1;
Pf_total=0;
P_loss_total=0;
P_net_total=0;
Pf_fuel_total=0;
Pf_DDN_total=0;
Pf_DDP_total=0;
P_brem_total=0;
P_cyc_total=0;
if Fuel_type==1           %DD Reaction
    for i=1:iterations
        RR_DDN(i)=0.5*N_F1_pinch(i)*N_F1_pinch(i)*ov3;
        RR_DDP(i)=0.5*N_F1_pinch(i)*N_F1_pinch(i)*ov2;
        %Determine Fusion Power
        Pf_DDN(i)=0.25*RR_DDN(i)*WDDN*V_pinch*f*t_pinch/
iterations*10^-6;
        Pf_DDP(i)=0.25*RR_DDP(i)*WDDP*V_pinch*f*t_pinch/
iterations*10^-6;
        Pf_t(i)=Pf_DDN(i)+Pf_DDP(i);
        %Determine Net Power Change
        P_cyc(i)=(6.21*10^-17)/
(8*pi)*mu0^2*(Efficiency_total*I_optimum)^2*L_pinch*N_pinch(i)*KT_optimum*(1+KT_op
iterations*10^-6;

        P_brem(i)=5.35*10^-37*Efficiency_total^2*N_pinch(i)*(N_F1_pinch(i)+N_F2_pinch(i))
iterations*10^-6;
        P_loss(i)=P_brem(i)+(1-cycrefl)*P_cyc(i);
        P_net(i)=Pf_t(i)-P_loss(i);
        %Thrust Calculations
        N_F1_pinch(i+1)=N_F1_pinch(i)-
(2*RR_DDN(i)+2*RR_DDP(i))*t_pinch/iterations;

```

---

```

        N_F2_pinch(i+1)=N_F2_pinch(i)-
(2*RR_DDN(i)+2*RR_DDP(i))*t_pinch/iterations;
        N_pinch(i+1)=N_F1_pinch(i+1)+N_F2_pinch(i+1);

        Pf_total=Pf_total+Pf_t(i); %MW
        P_loss_total=P_loss_total+P_loss(i); %MW
        P_net_total=P_net_total+P_net(i); %MW
        Pf_fuel_total=Pf_fuel_total+Pf_DDN(i)+Pf_DDP(i); %MW
        Pf_DDN_total=Pf_DDN_total+Pf_DDN(i); %MW
        Pf_DDP_total=Pf_DDP_total+Pf_DDP(i); %MW
        P_brem_total=P_brem_total+P_brem(i); %MW
        P_cyc_total=P_cyc_total+P_cyc(i); %MW
    end
elseif Fuel_type==2 %DT Reaction
    for i=1:iterations
        RR_DT(i)=N_F1_pinch(i)*N_F2_pinch(i)*ov1;
        RR_DDN(i)=0.5*N_F1_pinch(i)*N_F1_pinch(i)*ov3;
        RR_DDP(i)=0.5*N_F1_pinch(i)*N_F1_pinch(i)*ov2;
        %Determine Fusion Power
        Pf_DT(i)=RR_DT(i)*WDT*V_pinch*f*t_pinch/iterations*10^-6;
        Pf_DDN(i)=0.25*RR_DDN(i)*WDDN*V_pinch*f*t_pinch/
iterations*10^-6;
        Pf_DDP(i)=0.25*RR_DDP(i)*WDDP*V_pinch*f*t_pinch/
iterations*10^-6;
        Pf_t(i)=Pf_DT(i)+Pf_DDN(i)+Pf_DDP(i);
        %Determine Net Power Change
        P_cyc(i)=(6.21*10^-17)/
(8*pi)*mu0^2*(Efficiency_total*I_optimum)^2*L_pinch*N_pinch(i)*KT_optimum*(1+KT_op
iterations*10^-6;

        P_brem(i)=5.35*10^-37*Efficiency_total^2*N_pinch(i)*(N_F1_pinch(i)+N_F2_pinch(i))
iterations*10^-6;
        P_loss(i)=P_brem(i)+(1-cycrefl)*P_cyc(i);
        P_net(i)=Pf_t(i)-P_loss(i);
        %Thrust Calculations
        N_F1_pinch(i+1)=N_F1_pinch(i)-
(RR_DT(i)+2*RR_DDN(i)+2*RR_DDP(i))*t_pinch/iterations;
        N_F2_pinch(i+1)=N_F2_pinch(i)-RR_DT(i)*t_pinch/iterations;
        N_pinch(i+1)=N_F1_pinch(i+1)+N_F2_pinch(i+1);

        Pf_total=Pf_total+Pf_t(i); %MW
        P_loss_total=P_loss_total+P_loss(i); %MW
        P_net_total=P_net_total+P_net(i); %MW
        Pf_fuel_total=Pf_fuel_total+Pf_DT(i); %MW
        Pf_DDN_total=Pf_DDN_total+Pf_DDN(i); %MW
        Pf_DDP_total=Pf_DDP_total+Pf_DDP(i); %MW
        P_brem_total=P_brem_total+P_brem(i); %MW
        P_cyc_total=P_cyc_total+P_cyc(i); %MW
    end
elseif Fuel_type==3 %D-He3 Reaction
    for i=1:iterations
        RR_DHe(i)=N_F1_pinch(i)*N_F2_pinch(i)*ov1;
        RR_DDN(i)=0.5*N_F1_pinch(i)*N_F1_pinch(i)*ov3;
        RR_DDP(i)=0.5*N_F1_pinch(i)*N_F1_pinch(i)*ov2;

```

---

---

```

        %Determine Fusion Power
        Pf_DHe(i)=RR_DHe(i)*WDHe*V_pinch*f*t_pinch/iterations*10^-6;
        Pf_DDN(i)=0.25*RR_DDN(i)*WDDN*V_pinch*f*t_pinch/
iterations*10^-6;
        Pf_DDP(i)=0.25*RR_DDP(i)*WDDP*V_pinch*f*t_pinch/
iterations*10^-6;
        Pf_t(i)=Pf_DHe(i)+Pf_DDN(i)+Pf_DDP(i);
        %Determine Net Power Change
        P_cyc(i)=(6.21*10^-17)/
(8*pi)*mu0^2*(Efficiency_total*I_optimum)^2*L_pinch*N_pinch(i)*KT_optimum*(1+KT_op
iterations*10^-6;

        P_brem(i)=5.35*10^-37*Efficiency_total^2*N_pinch(i)*(N_F1_pinch(i)+2*N_F2_pinch(i
iterations*10^-6;
        P_loss(i)=P_brem(i)+(1-cycrefl)*P_cyc(i);
        P_net(i)=Pf_t(i)-P_loss(i);
        %Thrust Calculations
        N_F1_pinch(i+1)=N_F1_pinch(i)-
(RR_DHe(i)+2*RR_DDN(i)+2*RR_DDP(i))*t_pinch/iterations;
        N_F2_pinch(i+1)=N_F2_pinch(i)-RR_DHe(i)*t_pinch/iterations;
        N_pinch(i+1)=N_F1_pinch(i+1)+N_F2_pinch(i+1);

        Pf_total=Pf_total+Pf_t(i);           %MW
        P_loss_total=P_loss_total+P_loss(i); %MW
        P_net_total=P_net_total+P_net(i);    %MW
        Pf_fuel_total=Pf_fuel_total+Pf_DHe(i); %MW
        Pf_DDN_total=Pf_DDN_total+Pf_DDN(i); %MW
        Pf_DDP_total=Pf_DDP_total+Pf_DDP(i); %MW
        P_brem_total=P_brem_total+P_brem(i); %MW
        P_cyc_total=P_cyc_total+P_cyc(i);    %MW
    end
elseif Fuel_type==4 %p-B11 Reaction
    for i=1:iterations
        RR_PB11(i)=N_F1_pinch(i)*N_F2_pinch(i)*ov1;
        %Determine Fusion Power
        Pf_PB11(i)=RR_PB11(i)*WPB11*V_pinch*f*t_pinch/
iterations*10^-6;
        Pf_t(i)=Pf_PB11(i);
        %Determine Net Power Change
        P_cyc(i)=(6.21*10^-17)/
(8*pi)*mu0^2*(Efficiency_total*I_optimum)^2*L_pinch*N_pinch(i)*KT_optimum*(1+KT_op
iterations*10^-6;

        P_brem(i)=5.35*10^-37*Efficiency_total^2*N_pinch(i)*(N_F1_pinch(i)+5*N_F2_pinch(i
iterations*10^-6;
        P_loss(i)=P_brem(i)+(1-cycrefl)*P_cyc(i);
        P_net(i)=Pf_t(i)-P_loss(i);
        %Thrust Calculations
        N_F1_pinch(i+1)=N_F1_pinch(i)-(RR_PB11(i))*t_pinch/iterations;
        N_F2_pinch(i+1)=N_F2_pinch(i)-RR_PB11(i)*t_pinch/iterations;
        N_pinch(i+1)=N_F1_pinch(i+1)+N_F2_pinch(i+1);

        Pf_total=Pf_total+Pf_t(i);           %MW
        P_loss_total=P_loss_total+P_loss(i); %MW

```

---

---

```
    P_net_total=P_net_total+P_net(i);           %MW
    Pf_fuel_total=Pf_fuel_total+Pf_PB11(i);     %MW
    P_brem_total=P_brem_total+P_brem(i);       %MW
    P_cyc_total=P_cyc_total+P_cyc(i);          %MW
end
RR_DDN=0;
end
```

## Variable packaging

```
Power=[Pf_total,P_loss_total,P_net_total,Pf_fuel_total,Pf_DDN_total,Pf_DDP_total,P
```

*Published with MATLAB® R2018a*

## Table of Contents

.....	1
Case 1 (Power_system = 1), Fusion Only .....	1
Case 2 (Power_system = 2), Fission Only .....	2
Case 3 (Power_system = 3), Fusion + Fission .....	2

```
function [m_fission] =
    DPF_fission(Power_system,P0,E_capacitors,Fusion_electric)

%-----
%Title: DPF Fission Assisted Code
%Creator: Paul Stockett
%Contributors: None
%Date of Creation: 28-May-2019
%Date of Last Modification: 17$-June-2019
%Purpose: To perform the necessary calculations for a fission assisted
    DPF
%device in terms of necessary reactor power and mass calculations.
%-----

%-----Fundamental Constants-----
g=9.81;                                %m/s
mu0=4*pi*10^-7;                         %Tm/A

%-----Reactor Parameters-----
% High Voltage Brayton Cycle-2000K,1.5kg/m^2,5000Vac from
% "A Comparison of Brayton and Stirling Space Nuclear Power for Power
% Levels from 1 Kilowatt to 10 Megawatts"-Lee S. Mason 2006
reactor_power10=10*10^3;                %kW
alpha10=2;                               %kg/kWe (Varies
    depening on Power Conversion System used)
alpha_shield=1;                          %kg/kW from
    "Direct Energy Conversion for Low Specific Mass In-Space Power and
    Propulsion" by Scott et al.
eta_pmad=0.95;                            %PMAD efficiency from
    "Direct Energy Conversion for Low Specific Mass In-Space Power and
    Propulsion" by Scott et al.
reactor_voltage10=2000;                   %V
reactor_power1=1*10^3;                    %kW

%-----Begin Code-----
Fusion_electric=Fusion_electric*10^3;    %kW
P0=P0*10^3 ;                              %kW
m_shadow_shield=P0*alpha_shield;
```

## Case 1 (Power\_system = 1), Fusion Only

```
if Power_system==1
```

---

```

    m_fission=0;
end

```

## Case 2 (Power\_system = 2), Fission Only

```

if Power_system==2
    N_reactors10=ceil(P0/reactor_power10);
    %number of reactors
    m_reactor10=reactor_power10*alpha10;
    %Weight of one fission reactor in kilograms
    %N_reactor1=rem(P0,reactor_power10)/reactor_power1
    %m_reactor1=reactor_power1*alpha1
    m_fission=m_reactor10*N_reactors10+m_shadow_shield;%
+m_reactor1*N_reactor1;      %Total Fission Weight
end

```

## Case 3 (Power\_system = 3), Fusion + Fission

```

if Power_system==3
    Power_level=P0-Fusion_electric;
    N_reactors10=floor(Power_level/reactor_power10);
    %number of reactors
    m_reactor10=reactor_power10*alpha10;
    %Weight of one fission reactor in kilograms
    m_fission=m_reactor10*N_reactors10+m_shadow_shield;
    %Total Fission Weight
    if Power_level<0
        m_fission=0;
    end
end

```

*Published with MATLAB® R2017b*

---

```

function [m_DEC,P_DEC,P_ch] = TWDEC(Fuel_type,Q,Pf,P_loss_total)
%-----
%Title: Flight Time
%Creator: Paul Stockett
%Contributors: None
%Date of Creation: 19-Jun-2019
%Date of Last Modification: 20-Jun-2019
%Purpose: To calculate the minimum flight time between Earth and Mars
         using
%the patched conic method as described by Emrich in Principles of
         Nuclear
%Rocket Propulsion
%-----

%-----Fundamental Constants-----
DT_product1=3.54;           % He4 energy in MeV
DT_product2=14.05;        % n energy in MeV
DDn_product1=0.82;        % He3 energy in MeV
DDn_product2=2.45;        % n energy in MeV
DDp_product1=1.01;        % T energy in MeV
DDp_product2=3.02;        % p energy in MeV
DHe3_product1=3.66;       % He4 energy in MeV
DHe3_product2=14.6;       % p energy in MeV
pB11_product=8.68;        % 3(He4) energy in MeV

%-----System Parameters-----
alpha_twdec=0.14;         % Specific mass in kg/kW_in of
         Traveling Wave Direct Energy Converter from "Direct Energy Conversion
         for Low Specific Mass In-Space Power and Propulsion" by Scott et al.
eta_twdec=0.76;          % DEC efficiency from "Direct Energy
         Conversion for Low Specific Mass In-Space Power and Propulsion" by
         Scott et al.

%-----Begin Code-----
Fuel_type=floor(Fuel_type);
% Fc calculation
Fc_DT=DT_product1/(DT_product1+DT_product2);
Fc_DD=(DDn_product1+DDp_product2)/
(DDn_product1+DDn_product2+DDp_product1+DDp_product2);
Fc_DHe3=1;
Fc_pB11=1;

% Charged Particle Power Calculation
if Fuel_type == 1
    psi_r=(Fc_DD*Pf-P_loss_total)/Pf;
    P_ch=Pf*(1/Q+psi_r);
elseif Fuel_type == 2
    psi_r=(Fc_DT*Pf-P_loss_total)/Pf;
    P_ch=Pf*(1/Q+psi_r);
elseif Fuel_type == 3
    psi_r=(Fc_DHe3*Pf-P_loss_total)/Pf;
    P_ch=Pf*(1/Q+psi_r);

```

---

---

```
elseif Fuel_type == 4
    psi_r=(Fc_pB11*Pf-P_loss_total)/Pf;
    P_ch=Pf*(1/Q+psi_r);
end

% Mass and Electric Power Calculations
P_DEC=eta_twdec*P_ch;
Pf=Pf*10^3;
m_DEC=alpha_twdec*P_ch;

if P_ch<0
    m_DEC=0;
    P_DEC=0;
end
```

*Published with MATLAB® R2017b*

---

```

function [t_flight,epsilon] = Flight_time(Isp,fm)
%-----
%Title: Flight Time
%Creator: Paul Stockett
%Contributors: None
%Date of Creation: 19-Jun-2019
%Date of Last Modification: 20-Jun-2019
%Purpose: To calculate the minimum flight time between Earth and Mars
using
%the patched conic method as described by Emrich in Principles of
Nuclear
%Rocket Propulsion
%-----

%-----Fundamental Constants-----
d_earth=149700000; %km
d_mars=228000000; %km
r_earth=6378; %km
r_mars=3393; %km
mu_earth=398600; %km^3/s^2
mu_sun=1.327*10^11; %km^3/s^2
mu_mars=42830; %km^3/s^2

%-----Initial Guesses-----
epsilon=0;
alpha_earth=0;
beta_earth=0;
theta_earth=0;
H_earth=200; %Altitude of parking orbit
around earth in km
H_mars=100; %Altitude of parking orbit
around mars in km
Delta_difference=1;
a=d_earth*(1+epsilon*cosd(theta_earth))/(1-epsilon^2);

%-----Begin Code-----
i=1;
DeltaV_vehicle=-0.0098*Isp*log(fm);

for alpha_earth=0:0.01:180
while Delta_difference>0.1

%Earth Velocity Calculations
V_helio_earth=sqrt(mu_sun*(2/d_earth-1/a));
V_earth=sqrt(mu_sun/d_earth);

V_hyper_earth=sqrt(V_helio_earth^2+V_earth^2-2*V_helio_earth*V_earth*cosd(alpha_e
V_cutoff_earth=sqrt(2*mu_earth/(r_earth
+H_earth)+V_hyper_earth^2);
V_orbit_earth=sqrt(mu_earth/(r_earth+H_earth));
DeltaV_earth=V_cutoff_earth-V_orbit_earth;

```

---

---

```

    %Mars Velocity Calculations
    V_helio_mars=sqrt(V_helio_earth^2-2*mu_sun*(1/d_earth-1/
d_mars));
    alpha_mars=acosd(d_earth*V_helio_earth*cosd(alpha_earth)/
(d_mars*V_helio_mars));
    V_mars=sqrt(mu_sun/d_mars);

    V_hyper_mars=sqrt(V_helio_mars^2+V_mars^2-2*V_helio_mars*V_mars*cosd(alpha_mars))
    V_fire_mars=sqrt(V_hyper_mars^2+(2*mu_mars/(r_mars+H_mars)));
    V_orbit_mars=sqrt(mu_mars/(r_mars+H_mars));
    DeltaV_mars=V_fire_mars-V_orbit_mars;

    %Total Delta V
    DeltaV_mission=DeltaV_earth+DeltaV_mars;

    %Epsilon Guess Check
    Delta_difference=abs(DeltaV_vehicle-DeltaV_mission);
    if Delta_difference>0.1
        epsilon=epsilon+0.00001;
        a=d_earth*(1+epsilon*cosd(theta_earth))/(1-epsilon^2);
    end

    end
    theta_mars=real(acosd((a*(1-epsilon^2)-d_mars)/(epsilon*d_mars)));
    E_mars=acosd((epsilon*cosd(theta_mars))/
(1+epsilon*cosd(theta_mars)));
    t=sqrt(a^3/mu_sun)*(acos(cosd(E_mars))-
epsilon*sind(E_mars))/86400;
    time(i)=t;
    i=i+1;
end
time;
t_flight=min(time);

```

*Published with MATLAB® R2017b*

### A.2.1 Sample Output

Table A.2.

Sample Output of DPF Propulsion Code. For 4 thrusters with a  $\Delta V$  of 20 km/s for all three cases as established for both DT and  $D - He^3$  fuel types (2 and 3 respectively). No direct energy conversion was used in this sample run.

Power System	Fuel Type	$\Delta V$ , km/s	$n_{thrusters}$	$P_{f,total}$ , MW	$P_{ch}$ , MW	$P_{brem,total}$ , MW	$P_{cyc,total}$ , MW	$P_{loss,total}$ , MW
1	2	20	4	5345.914	1125.96	1.212163	74.97278	31.20128
2	2	20	4	5345.914	1125.96	1.212163	74.97278	31.20128
3	2	20	4	5345.914	1125.96	1.212163	74.97278	31.20128
1	3	20	4	3381.157	3295.267	8.299186	193.926	85.86959
2	3	20	4	3381.157	3295.267	8.299186	193.926	85.86959
3	3	20	4	3381.157	3295.267	8.299186	193.926	85.86959

Power System	Fuel Type	$m_{total}$ , kg/s	$t_{burn}$ , sec	$Thrust_{total}$ , kN	$\frac{T}{W}$	$I_{SP}$ , sec	$t_{flight}$ , days
1	2	30.54065	1896.804	1354218	0.794252	4520.016	90.94729
2	2	30.54065	6877.417	1354218	0.223811	4520.016	89.25599
3	2	30.54065	8125.603	1354218	0.189709	4520.016	89.14122
1	3	31.39627	1179.967	2052994	1.358794	6665.599	90.89454
2	3	31.39627	4199.676	2052994	0.39547	6665.599	88.31982
3	3	31.39627	4940.187	2052994	0.336972	6665.599	88.15287

Table A.3.

Sample Output of the mass calculations from the DPF Propulsion code. For 4 thrusters with a  $\Delta V$  of 20 km/s for all three cases as established for both DT and  $D - He^3$  fuel types (2 and 3 respectively). No direct energy conversion was used in this sample run.

Power System	Fuel Type	$m_{payload}$ , kg	$m_{propellant}$ , kg	$m_{propsystem}$ , kg	$m_{fuel}$ , kg	$m_{fuelsystem}$ , kg	$m_{pmad}$ , kg
1	2	100000	57929.63	8689.444	0.765084	0.076508	1202.621
2	2	100000	210040.8	31506.12	2.774035	0.277403	0
3	2	100000	248161.2	37224.18	3.277495	0.32775	86883.3
1	3	100000	37046.58	5556.987	0.475945	0.047594	3105.873
2	3	100000	131854.2	19778.12	1.693956	0.169396	0
3	3	100000	155103.5	23265.52	1.992645	0.199264	84980.05
Power System	Fuel Type	$m_{capacitors}$ , kg	$m_{magnet}$ , kg	$m_{shield}$ , kg	$m_{DEC}$ , kg	$m_{fission}$ , kg	$m_{total}$ , kg
1	2	166.334	270.2	5545.618	0	0	173804.7
2	2	166.334	270.2	6719.132	0	268085.9	616791.6
3	2	166.334	270.2	6871.075	0	248085.9	727665.8
1	3	166.334	270.2	7869.251	0	0	154015.8
2	3	166.334	270.2	9025.863	0	268085.9	529182.5
3	3	166.334	270.2	9173.816	0	248085.9	621047.5